Congenital and Ethanol-induced Disorders of N-linked Protein Glycosylation

---

Dissertation

zur

Erlangung der naturwissenschaftlichen Doktorwürde (Dr. sc. nat.)

vorgelegt der

Mathematisch-naturwissenschaftlichen Fakultät

der

Universität Zürich

von

Michael Andreas Welti

von

Berikon AG

Promotionskomitee

Prof. Dr. Thierry Hennet (Vorsitz)

Dr. Andreas Hülsmeier

PD Dr. Lubor Borsig

Prof. Dr. Matthias Baumgartner

Zürich, 2013

TABLE OF CONTENTS

SUMMARY

Protein glycosylation is an essential protein modification existing in all domains of life. About 2% of the human genome is involved in the glycosylation machinery and 50% of the human proteins are modified with glycans. In the endoplasmic reticulum, N-linked protein glycosylation begins with the assembly of an oligosaccharide precursor by step-wise transfer of sugar building blocks to a membrane-embedded, reduced polyprenol anchor called dolichol-phosphate. The fully assembled N-linked glycan precursor is then transferred co- or post-translationally to defined asparagine residues of target proteins.

Considering the abundance of N-glycosylated proteins throughout all human cell types, inherited glycosylation defects called congenital disorders of glycosylation (CDG) show multi-systemic involvement due to developmental defects in children. Most CDG involve a neurological component resulting in psychomotor retardation. Among the most common symptoms are epilepsy, hypotonia, hyporeflexia, strabismus, retinitis pigmentosa, polyneuropathy, myopathy, and cerebellar hypotrophy/hypoplasia. A common marker for CDG is the underglycosylation of blood serum proteins such as transferrin. Depending on the type of CDG, the N-linked glycans differ in their structure and can be detected in carbohydrate-deficient transferrin (CDT). Interestingly, alcoholic liver disease (ALD) is accompanied by a N-glycosylation defect as well. Besides a similar pattern of CDT, certain forms of CDG and ALD share another common symptom: liver fibrosis. Chronic alcoholism is estimated to be responsible for 4% of global death and the liver being the primary site of ethanol metabolism is particularly affected. Despite the long history of CDT in ALD, glycosylation deficiency in ALD has not yet been characterized at the molecular level.

So far, treatment of CDG is very restricted. In MPI-CDG, the mannose-phosphate isomerase is defective, an enzyme responsible for the conversion of fructose-6-phosphate to mannose-6-phosphate, thereby providing mannose for the glycosylation machinery. A simple supplementation of nutrition with mannose was shown to attenuate the manifestations of MPI-CDG.

In the first part of this thesis, we tested the potential of a cholesterol-lowering drug, Zaragozic acid A, to improve N-glycosylation in DPM1-CDG. DPM1 is a subunit of the dolichol-phosphate-mannose synthase which produces dolichol-phosphate-mannose, an important mannose donor for N-linked glycosylation. Zaragozic acid A inhibits an

enzyme at a bifurcation of the anabolic pathway common to dolichol and cholesterol synthesis. At this bifurcation, the metabolic flux either goes towards cholesterol or dolichol synthesis. By blocking the enzyme for cholesterol synthesis, N-linked protein glycosylation improved as observed by increased dolichol-phosphate-mannose levels, increased dolichol-phosphate levels, normalized dolichol- and N-linked oligosaccharide distribution. The restored dolichol-phosphate-mannose pool also resulted in better GPI-anchor availability. We could compensate the lower dolichol-phopshate-mannose synthase activity by increasing substrate availability. Thus Zaragozic acid represents a possibility for drug treatment of DPM1-CDG.

The second part of the thesis is focusing on ethanol-induced N-glycosylation deficiency. We studied the effect of ethanol on N-glycosylation in two hepatoma cell lines. The two cell lines VA-13 and HepaRG are distinct because they express alcohol dehydrogenase and cytochrome P450 2E1, respectively, which confers ethanol-metabolizing properties usually lost in cultured hepatocytes. We found lower dolichol levels in ethanol-treated cells. Moreover, the dolichol-linked oligosaccharide pattern was disturbed with a lower fraction of the final N-glycan precursor. The changes in glycosylation were accompanied by transcriptional changes. DPM1 was downregulated while RPN2 was upregulated. The transcriptional changes could be regulatory responses since we observed an increased DPM synthase activity despite the lower DPM1 transcription.

In conclusion, we explored CDG and acquired deficiency in N-linked protein glycosylation by using a therapeutic approach to treat DPM1-CDG and by the characterization of N-glycosylation in an ethanol-induced glycosylation deficiency model. With this work we contributed to the search for treatment possibilities for CDG and promoted the understanding of ethanol-induced N-glycosylation deficiency.

ZUSAMMENFASSUNG

Die Glykosylierung von Proteinen ist eine essentielle Proteinmodifikation, die in allen Domänen des Lebens vorkommt. Etwa 2% des humanen Genoms kodiert Proteine, die Teil der Glykosylierungsmaschinerie sind, und 50% der humanen Proteine sind glykosyliert. Die N-Glykosylierung von Proteinen beginnt im endoplasmatischen Retikulum, wo zuerst der N-Glykan Precursor schrittweise aufgebaut wird, indem einzelne Zuckerbausteine auf einem membran-gebundenen, reduzierten Polyprenolanker, dem Dolichol-phosphat, zusammengefügt werden. Der angefertigte N-Glykan Precursor wird dann co- oder posttranslational vom Dolichol-phosphat auf spezifische Asparaginseitenketten von Zielproteinen übertragen.

Aufgrund der Abundanz der N-Glykosylierung von menschlichen Proteinen in allen Zelltypen weisen vererbte N-Glykosylierungsdefekte ein multi-systemisches Krankheitsbild auf. Vererbte Glykosylierungsdefekte (CDG) beeinträchtigen meist die pränatale Entwicklung des Menschen. Die häufigsten CDG-Symptome sind Epilepsie, Hypotonie, Hyporeflexie, Strabismus, Retinitis pigmentosa, Polyneuropathie, Myopathie und Hypotrophie/Hypoplasie des Kleinhirns. Die Unterglykosylierung von Serumproteinen, wie z.B. Transferrin, wird als Marker für CDG benutzt. Abhängig vom CDG-Typ unterscheiden sich die N-Glykane auf Transferrin, weshalb verschiedene Formen von Desialotransferrin (CDT) detektiert werden können. Die alkoholische Leberkrankheit (ALD) wird interessanterweise von einem N-Glykosylierungsdefekt begleitet. Neben einem ähnlichen CDT-Bild zeigen gewisse CDG-Typen und ALD auch ein anderes gemeinsames Symptom: die Leberfibrose. Die Leber als primärer Ort des Ethanolabbaus ist besonders den Effekten des Alkoholismus betroffen. Obwohl der Zusammenhang zwischen CDT und ALD schon lange bekannt ist, wurde die Glykosylierungsdefizienz in ALD noch nicht vollständig auf molekularer Ebene charakterisiert.

Die medikamentöse Behandlung von CDG ist sehr beschränkt. Ein Beispiel ist MPI-CDG, in der das Enzym, das für die Konversion von Fruktose-6-phosphat zu Mannose-6-phosphat, defekt ist. Diese Reaktion ist wichtig, um Mannose für die Glykosylierungsreaktionen zur Verfügung zu stellen. Eine einfache Supplementierung der Nahrung mit Mannose ist in diesem Fall genug, um die Krankheitserscheinungen zu mildern.

Im ersten Teil dieser Dissertation untersuchten wir das Potenzial eines cholesterin-senkenden Stoffs, Zaragozic acid A, die N-Glykosylierung in DPM1-CDG zu verbessern. DPM1 ist eine Untereinheit der Dolichol-phosphate-mannose Synthase, die als Komplex Dolichol-phosphate-mannose, einen wichtigen Mannose-donor für die N-Glykosylierung, produziert. Zaragozic acid A inhibiert ein Enzym an einer Verzweigung eines Synthesewegs, über den sowohl die Dolichol- als auch Cholesterinproduktion stattfindet. Bei der genannten Verzweigung geht der metabolische Fluss entweder in Richtung Dolichol- oder Cholesterinsynthese. Mit der Blockade des Enzyms, das die abzweigende Reaktion zur Cholesterinsynthese katalysiert, wurde die N-Glykosylierung verbessert, so dass erhöhtes Dolichol-phosphate und eine verbesserte Verteilung der dolichol- und N-assozierten Oligosaccharide gemessen werden konnte. Ausserdem hatte die auf Normwerte erhöhte Dolichol-phosphat-mannose zur Folge, dass die Verfügbarkeit von GPI-Ankern verbessert wurde. Wir konnten also die reduzierte Aktivität der Dolichol-phosphate-mannose Synthase mittels verbesserter Substratverfügbarkeit kompensieren. Daher stellt Zaragozic acid A ein potenzielles Medikament zur Behandlung von DPM1-CDG dar.

Der zweite Teil der Dissertation fokussiert auf die ethanol-induzierte N-Glykosylierungsdefizienz. Dazu haben wir den Effekt von Ethanol auf die N-Glykosylierung in zwei Leberkrebszelllinien untersucht. Die VA-13 und die HepaRG Zelllinien sind gut dazu geeignet, weil sie im Gegensatz zu anderen kultivierten Leberzellen die Alkoholdehydrogenase und das Zytochrom P450 2E1 exprimieren, was die Metabolisierung von Ethanol ermöglicht. Wir konnten nach der Behandlung mit Ethanol niedrigeres Dolichol-phosphat sowie eine niedrigere Verfügbarkeit des N-Glykan Precursors feststellen. Diese Glykosylierungsstörung wurde von transkriptionalen Veränderungen begleitet. DPM1 war runterreguliert während RPN2 hochreguliert wurde. Diese Veränderungen der Transkription könnten regulatorische Mechanismen darstellen, da die DPM Synthase Aktivität erhöht war, obwohl die DPM1-Untereinheit transkriptional runterreguliert war.

Zusammenfassend haben wir uns mit einem vererbten wie auch einem erworbenen N-Glykosylierungsdefekt befasst. Wie haben einen therapeutischen Ansatz zur Milderung des N-Glykosylierungsdefekts in DPM1-CDG Fibroblasten erfoglsversprechend getestet und den ethanol-induzierten N-Glykosylierungsdefekt in zwei Leberzelllinien charakterisiert.

ABBREVIATIONS

9-ADM	9-anthryldiazomethane
ADH	Alcohol dehydrogenase
ALD	Alcoholic liver disease
ALG	Asparagine-linked glycosylation
CDG	Congenital Disorders of Glycosylation
CDT	Carbohydrate-deficient transferrin
CYP2E1	Cytochrome P450 2E1
DLO	Dolichol-linked oligosaccharide
DMSO	Dimethyl sulfoxide
DNA	Desoxyribonucleic acid
Dol	Dolichol
Dol-P	Dolichol-phosphate
Dol-PP	Dolichol-pyrophosphate
DPM	Dolichol-phosphate mannose (synthase)
ER	Endoplasmic Reticulum
ERAD	Endoplasmic reticulum-associated degradation
FBS	Fetal bovine serum
Gal	Galactose
GDP	Guanosine diphosphate
Glc	Glucose
GlcNAc	N-acetlyglucosamine
GPI	Glycophosphatidylinositol
HMG-CoA	3-hydroxy-3-methyl-glutaryl-coenzyme A
HPLC	High performance liquid chromatography
IEF	Isoelectric focusing
LLO	Lipid-linked oligosaccharide
Man	Mannose
MPI	Mannose-phosphate isomerase

mRNA	Messenger RNA
NAD(H)	β-Nicotineamide adenine dinucleotide (reduced)
NLO	N-linked oligosaccharide
OST	Oligosaccharyltransferase
PCR	Polymerase chain reaction
PMM	Phosphomannomutase
RNA	Ribonucleic acid
UDP	Uridine disphosphate
ZGA	Zaragozic acid A
Fuc	Fucose

INTRODUCTION

Post-translational modifications of proteins are crucial for maintaining proper functioning of cells and whole organisms. Among the most important protein modifications in animals are phosphorylation, lipid conjugation, ubiquitination, and glycosylation. Phosphorylation is essential in many cellular processes and mostly regulates activity of the modified proteins (Hunter, 2000) while ubiquitination marks proteins for the major pathway of proteasomal protein degradation (Hochstrasser, 2009). Lipid modifications serve as membrane anchors to restrict proteins to the ER, Golgi apparatus, or the plasma membrane (Nadolski and Linder, 2007). Glycosylation is the most frequent protein and lipid modification which is apparent when looking at the complex and dense layer of glycans that covers the surface of all living organisms including viruses (Larkin and Imperiali, 2011; Spiro, 2002). About 2% of the human genes are involved in glycan formation as enzymes, transporters, or cofactors (Freeze et al., 2012; Varki et al., 2008). Glycans are the most diverse and versatile biomolecules in terms of target substrates, chemical linkages, and non-linear branching. In humans, 50% of all proteins are glycosylated underlining the significance of protein glycosylation. However, defining functions of glycosylation is difficult due to its inherent complexity and requirement for advanced technology and methodology. The process of glycosylation describes the attachment of a single saccharide or polysaccharide from a donor substrate to an acceptor substrate. The donor substrate consists of a sugar building block activated by a carrier via phospho-diester or phospho-ester bond. Donor as well as the acceptor substrates are recognized by enzymes termed glycosyltransferases which attach the sugar building block to the acceptor substrate in a linkage-specific manner.

Monosaccharides: Building blocks of glycosylation

Nine different monosaccharides are used to produce glycoconjugates in mammals (Figure 1). Despite the close to infinite number of possibilities to combine these monosaccharides due to linkage and branching features of sugars, relatively few combinations do actually exist. This can be explained by the specificity of the known glycosyltransferases which function with donor and acceptor substrate specificity as

well as linkage specificity. Therefore, unlimited and functional glycan diversity would require a huge number of glycosyltransferases which themselves would need regulation.

Another level of complexity is added by modifications of glycans. Sulfation, acetylation, and methylation and epimerization of GlcA to iduronic acid can occur on the conjugated glycan (Silbert and Sugumaran, 2002; Varki et al., 2009). These glycan modifications require activated substrates, i.e. 3′-phosphoadenyl-5′-phosphosulfate for sulfation, acetyl-CoA for acetylation, and S-adenosylmethionine for methylation. Activated substrates are produced in the cytoplasm and therefore depend on membrane transporters to reach the ER-Golgi pathway.

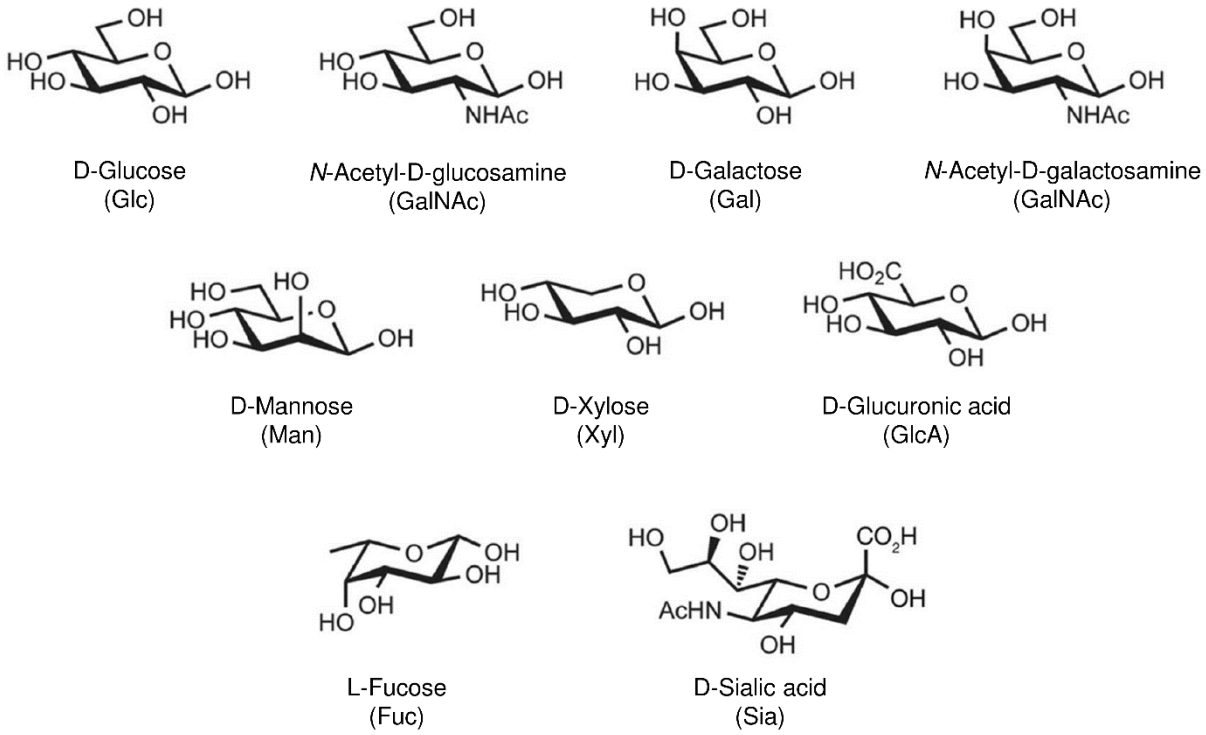

Figure 1 Structural representations of the nine monosaccharides used in mammalian glycosylation. The names of the sugars are indicated below the structure including the abbreviations used in this thesis. (adapted from (Varki et al., 2008))

The complexity of glycans is major challenge for structural elucidation even with the most advanced approaches using mass spectrometry (Kolarich et al., 2013; Mechref et al., 2012; Zaia, 2010; Zaia, 2013).

Major glycan classes in eukaryotic cells

The major classes of glycosylation in animal cells take place in the ER and the Golgi apparatus (Figure 2). O-GlcNAc (Comer and Hart, 2000; Guinez et al., 2005; Hart and Akimoto, 2009), O-Glc (Whitworth et al., 2010), and O-Fuc (Moloney et al., 2000; Panin et al., 2002) modifications can occur in the ER as well as in the nucleus and cytoplasm representing exceptions and are not within the scope of this thesis. Every glycan class features an individual glycan core that can be elongated and modified.

N-glycans, O-glycans, and glycosaminoglycans (GAG) are protein-linked whereas GPI anchors and glycosphingolipids represent lipid-linked modes of glycosylation. GPI anchors themselves are protein modifications and are conjugated to the C-terminus of target proteins in the ER.

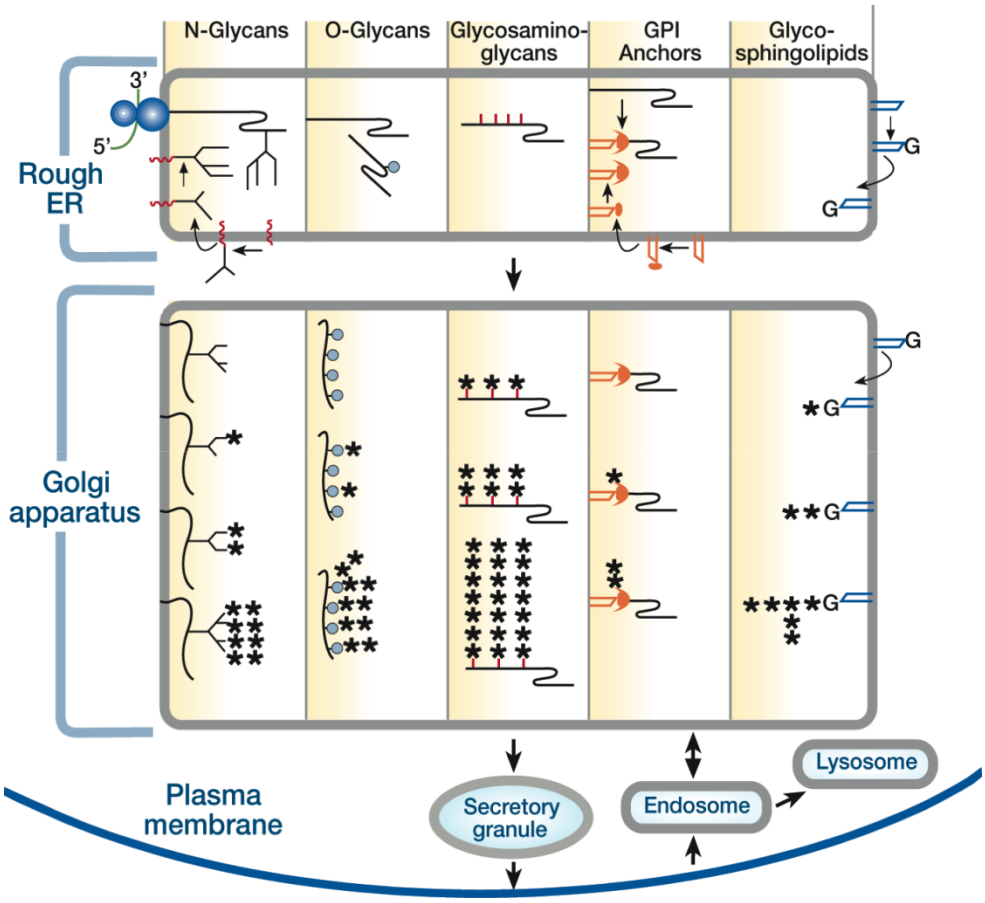

Figure 2 Glycan classes and their maturation in the ER-Golgi pathway. The initial steps of N-glycosylation, O-glycosylation, glycosaminoglycan synthesis, GPI anchor formation, and glycosphingolipid synthesis occur in the ER. Elongation and maturation processes take place in the Golgi complex. (from (Varki et al., 2008))

N-linked protein glycosylation

The N-linked glycan core originates from an N-glycan precursor in the ER (Aebi, 2013). There, N-linked protein glycosylation occurs on Asn residues co- or post-translationally. When a protein with an N-glycan consensus sequence Asn-X-Ser/Thr (X can be any amino acid except Pro) is translated into the ER, an oligosaccharide structure termed N-glycan precursor is transferred from dolichol-pyrophosphate (Dol-PP) to the Asn of the consensus site (Marshall, 1974). The N-glycan thereafter can assist in the folding of the modified protein in the ER. After trimming the original N-glycan, the N-glycosylated protein follows the secretory pathway to the Golgi apparatus where further trimming and subsequent addition of various monosaccharides can occur. Furthermore, glycans can undergo a maturation process involving chemical modifications. Finally, the glycosylated protein is secreted or transported to its target membrane.

Types of N-linked glycans

Three types of N-linked glycans are distinguished: High mannose type, complex type, and hybrid type (Figure 3). They all originate from the N-glycan precursor after passing through the glycosylation machinery in the ER and Golgi complex.

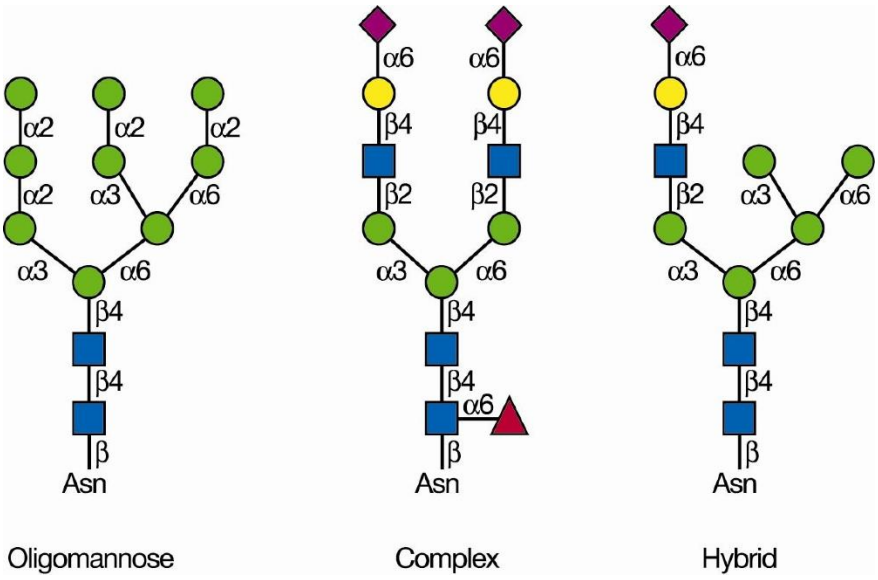

Figure 3 N-glycan classes. The three N-glycan classes share a common core ($Man_3GlcNAc_2$). Blue squares represent GlcNAc, green circles Man, yellow circles Gal, purple diamonds sialic acid, and red triangle Fuc. (from (Varki et al., 2008))

Biosynthesis of the N-linked glycan precursor in the Endoplasmic Reticulum

The first part of N-linked protein glycosylation requires the assembly of the N-glycan precursor $Glc_3Man_9GlcNAc_2$ on Dol-PP, a lipid carrier residing in the ER membrane (Figure 4). The formation of dolichol (Dol) occurs in the mevalonate pathway and is described and discussed in detail in the section "Regulation of Dolichol-linked glycosylation" (Ramachandran and Melnykovych, 1986). The substrate for the initial glycosyltransferases is dolichol-P (Dol-P) that is supplied by dolichol kinase (DK) phosphorylating Dol (red rectangle in Fig. 4). The precursor is built by the addition of single sugar blocks in a sequence-, linkage-, and conformation-specific manner. The first seven steps occur at the outer leaflet of the ER. Two GlcNAc (blue squares) are sequentially added to Dol-P by DPGAT1 and ALG13/14, respectively. Both enzymes require UDP-GlcNAc as a substrate but DPGAT1 links P-GlcNAc to Dol-P resulting in GlcNAc-PP-Dol and UMP. ALG13/14 produces $GlcNAc_2$-PP-Dol and UDP. ALG1 catalyzes the addition of the first Man residues (green circles) from GDP-Man to $GlcNAc_2$-PP-Dol. Thereafter, ALG2 adds two Man from GDP-Man to $ManGlcNAc_2$-PP-Dol. The last two steps at the outer leaflet of the ER are catalyzed by ALG11 which adds two Man to -$Man_3GlcNAc_2$-PP-Dol resulting in the intermediate Dol-linked oligosaccharide (DLO) $Man_5GlcNAc_2$-PP-Dol. RFT1 flips this DLO across the ER membrane into the lumen by a yet unresolved mechanism. Four further Man are added by the indicated enzymes using Dol-P-Man as source of Man. Notably, ALG9 recognizes both $Man_6GlcNAc_2$-PP-Dol as well as $Man_8GlcNAc_2$-PP-Dol as substrates for mannosylation. Three Glc sugars are transferred from Dol-P-Glc to the DLO by the sequential action of ALG6, ALG8, and ALG10. Finally, the completed N-glycan precursor $Glc_3Man_9GlcNAc_2$ (Figure 4) is transferred *en bloc* from Dol-PP to the amide group of Asn side chains in the consensus sequence Asn-X-Ser/Thr by the oligosaccharyl-transferase complex (OST). Site occupancy analyses of different glycoproteins revealed a preference for N-X-T over N-X-S sites (Gavel and von Heijne, 1990). Dol-PP is recycled by dephosophorylation to Dol-P and subsequent flipping to the cytosolic leaflet (Cantagrel and Lefeber, 2011; Ramachandran and Melnykovych, 1986; Rush et al., 2008). Recycling critically contributes to Dol-P availability but the molecular details of Dol-P recycling remain elusive.

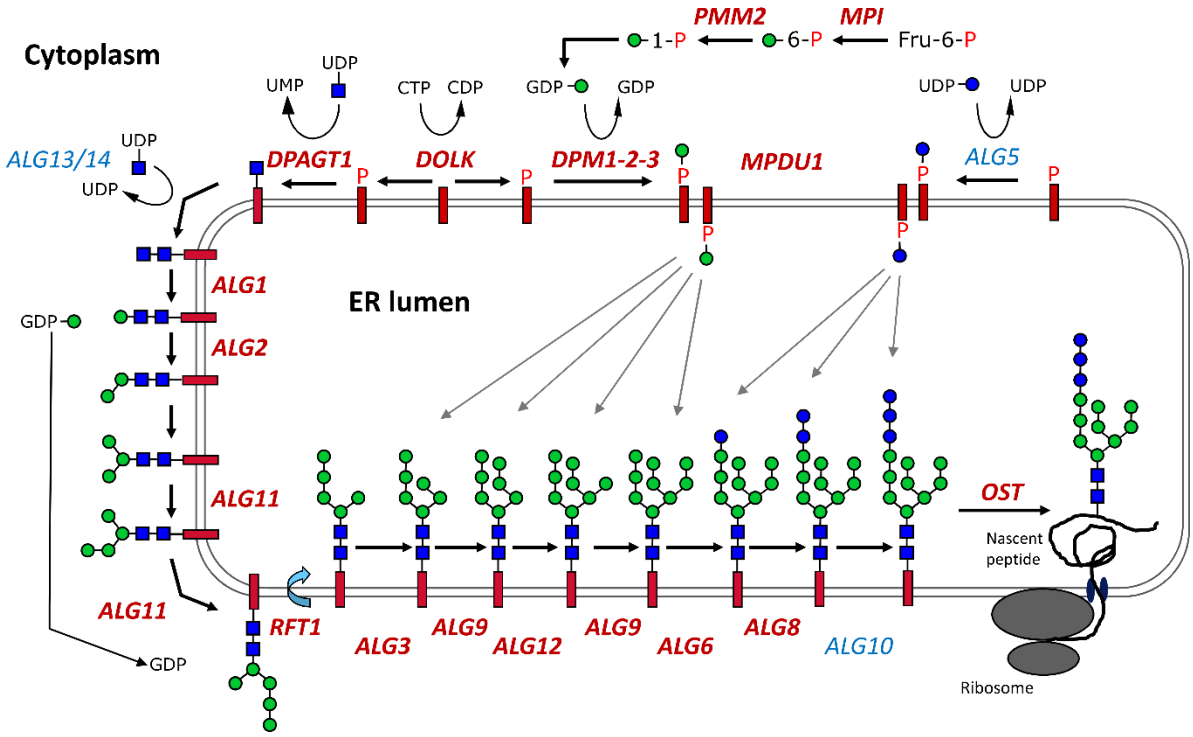

Figure 4 Biosynthesis of dolichol-linked oligosaccharides (DLO) dolichol-activated monosaccharides. The N-glycan precursor is assembled by the stepwise addition of monosaccharides. On the cytosolic leaflet of the ER, two GlcNAc and five Man are transferred to Dol-P using nucleotide-activated monosaccharides as substrates. Dol-PP-$GlcNAc_2Man_5$ is flipped into the ER lumen where the DLO is extended with four Man and three Glc by glycosyl-transferases using Dol-P-activated monosaccharides as substrates. The finished Dol-PP-linked N-glycan precursor can then be transferred to a target protein. Red labels indicate proteins associated with congenital disorders of glycosylation. Blue labels indicate proteins that have not been found in congenital disorders of glycosylation so far. (adapted from (Haeuptle and Hennet, 2009))

Processing of the N-linked glycan

After transfer to target proteins, the N-linked glycan can assist the protein in folding properly. This cyclic process is termed ER quality control and involves the chaperone proteins calnexin and calreticulin which can recognize N-glycans on unfolded proteins (Williams, 2006). Immediately after the glycan transfer, α-glucosidase I removes the terminal α1–2-linked Glc and glucosidase II then removes the two α1-3-linked Glc sugars. The resulting oligosaccharide is taking part in the ER folding quality control. Iterative reglucosylation by UGGT1 and deglucosylation during the folding process

ensure retention of improperly folded proteins in the so-called calnexin/calreticulin cycle (see section "ER quality control of protein folding" and (Helenius and Aebi, 2004)). Many de-glucosylated glycans on properly folded proteins are processed by ER α-mannosidase I before exiting the ER which removes the α1-2-linked Man from the central branch of the glycan resulting in a $Man_8GlcNAc_2$-Asn isomer. Most glycans exit the ER with eight or nine Man residues but some escape the quality control processing and can carry a terminal Glc when entering the Golgi apparatus.

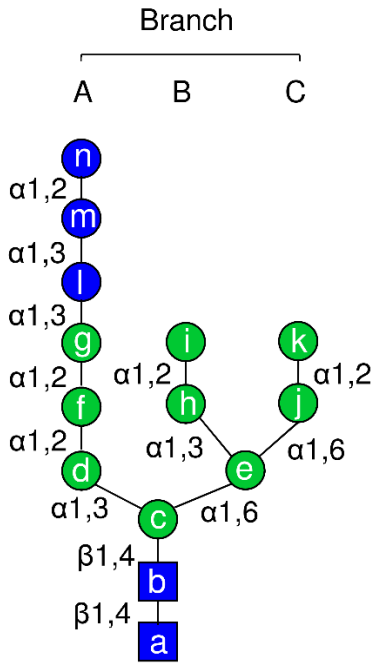

Figure 5 Schematic structure of the N-linked glycan precursor. It consists of two GlcNAc (blue squares), nine Man (green circles), and three Glc (blue circles). The residues are labeled alphabetically for cross-referencing. Linkage specificities are indicated at the connections between linked sugars.

In the Golgi, incompletely processed $GlcMan_8GlcNAc_2$-Asn is acted on by endo-α-mannosidase which cleaves the disaccharide Glcα1-3Man off the glycan resulting in a $Man_8GlcNAc_2$-Asn different from the one produced by ER α-mannosidase I. Further trimming occurs by α1-2 mannosidases IA, IB, and IC in the *cis*-Golgi resulting the important intermediate glycan $Man_5GlcNAc_2$-Asn. From $Man_5GlcNAc_2$-Asn, hybrid and complex N-glycans can arise from remodeling but some of these structures escape remodeling. Glycans that evade these early de-mannosylation steps will not be further processed and together with un-processed $GlcNAc_2Man_5$-Asn represent oligomannose glycans of the type $Man_{5-9}GlcNAc_2$-Asn on mature glycoproteins. Most glycoproteins carry some unprocessed, oligomannose glycans.

The initial step in hybrid and complex glycan formation occurs in the *medial*-Golgi and is catalyzed by the β1-2 N-acetylglucosaminyltransferase GnT-I which adds an GlcNAc to position C2 of the α1-3-linked Man in the core of $Man_5GlcNAc_2$-Asn (cp. Figure 4). Only

after GnT-I action, the glycan is recognized by α-mannosidase II which removes terminally attached α1-3 and α1-6 Man. The resulting $GlcNAcMan_3GlcNAc_2$-Asn is further modified by GnT-II giving rise to the precursor of all biantennary, complex N-glycans. If α-mannosidase II is not acting on the glycan, the result are hybrid N-glycans still carrying the unmodified terminal α1-3 and α1-6 Man in the mature glycoprotein. From glycans that are incompletely processed by α-mannosidase II, another hybrid of the type $GlcNAcMan_4GlcNAc_2$-Asn emerges. Another enzyme, α-mannosidase IIx, also cleaves $GlcNAcMan_5GlcNAc_2$-Asn generated by GlcNAcT-I. Mouse double knockouts missing α-mannosidase II and IIx totally lack complex N-glycans (Moremen, 2002). Branching of complex N-glycans starts with GlcNAcylation of Man giving rise to complex glycans with up to four branches in mammals and five branches in fish and birds.

In the *trans*-Golgi, hybrid and branched N-glycans undergo further modifications which is referred to as maturation. Three types of maturation can occur: sugar additions to the core glycan, sugar additions to elongate branching GlcNAc, and capping of the elongated branches. In vertebrates, fucosylation by FucT-VIII is the most common core modification. Very rarely, modification of the core with GlcNAc can occur. Elongation typically takes place by initial addition of β-linked N-acetyllactosamine to the initiating GlcNAc. If lactose is added to the C4 position of the initiating GlcNAc, the most frequent -Galβ1-4GlcNAc- repeat termed type-2 N-acetyllactosamine is produced. If lactose is linked to position C3, the less frequent type-1 N-acetyllactosamine, -Galβ1-3GlcNAc-, arises. Further alternate elongation by GlcNAc and Gal yield a type-2 or type-1 "LacNAc" sequence. The last and most important modification is the "capping" or "decorating" of glycan branches. Capping encompasses the addition of terminal sialic acid, fucose, galactose, GlcNAc, and sulfate. Interestingly, such capping structures are shared by N- and O-glycans as well as glycolipids. The α-linkage of the terminal sugars contrasts with the common β-linkages within the branches and confers better accessibility for lectins or antibodies due to the protrusion away from the β-linked ribbon-like branches.

Functions of N-linked protein glycosylation

The most prominent and obvious functions of N-linked protein glycosylation are linked to the early steps of protein glycosylation. Early functions of N-linked glycans encompass recruitment of molecular chaperones for facilitated protein folding, proper

processing and targeting of the N-glycosylated protein, and enhancing solubility and protein stability (Hebert et al., 1997; Hurtley and Helenius, 1989; Klausner and Sitia, 1990; Olden et al., 1982). In addition to structural and regulatory properties, glycans are involved in more specific recognition events which are dependent on carbohydrate-binding proteins, so-called lectins. With increasing complexity of the N-glycans in the elongation and maturation process, less global but more specific functions of the glycan unfold. Functions of glycans which require specific recognition involve carbohydrate-binding proteins termed lectins. Moreover, glycosaminoglycan-binding proteins and carbohydrate-binding antibodies are defined classes of glycan-binding proteins. Different types of lectins are defined based on their sequence and structural homology. Generally, a function of a specific glycan for a specific glycoprotein is difficult to assess. Moreover, the same glycan structure can have different functions depending on the protein it is attached to, on the location within an organism, and on the developmental state of an organism or life cycle of a single cell (Varki, 1993; Varki et al., 2008). Functions of glycans are difficult to address especially since an introduced defect in isolated cells often may or may not show a marked phenotype but still may have catastrophic consequences on the whole, functional organism. Below, some functions of N-glycans are presented. More extensive discussion of N-glyan functions are described elsewhere (Varki, 1993; Varki et al., 2008).

Quality control of protein folding in the Endoplasmic Reticulum

Folding and subsequent processing and secretion of some proteins is highly dependent on N-linked glycans. Notably, blocked N-glycosylation can result in different outcomes ranging from partial loss of folding and impaired secretion efficiency to temperature sensitivity of the affected proteins (Helenius, 1994). The importance of N-glycosylation for folding usually correlates with the number of N-glycosylation sites in a protein (Helenius and Aebi, 2004). The effects of a glycan on protein folding can be of biophysical nature by restricting the conformational space of the polypeptide chain, by promoting the formation of β-turns through the interaction of the N-acetyl groups of the first GlcNAc residues with the polypeptide chain, or by just globally enhancing solubility of folding peptide chains (Imberty and Perez, 1995; Imperiali and O'Connor, 1999; O'Connor and Imperiali, 1996; Wormald and Dwek, 1999). The indirect effects of N-glycans on protein folding are dependent on a complex machinery of

glucosyltransferase, glucosidase, lectins (carbohydrate-binding proteins), and associated factors as for instance thiol-disulfide oxidoreductases.

The central enzyme of protein folding quality control is the glucosyl-transferase UGGT1. It can recognize and bind hydrophobic patches of unfolded proteins and re-glucosylate $Man_9GlcNAc_2$-Asn. As long as an N-glycosylated protein remains unfolded, the oligosaccharide is subjected to iterative de- and re-glucosylation by glucosidase and UGGT1, respectively (Suh et al., 1989). Unfolded proteins carrying monoglucosylated glycans enter the so-called calnexin/calreticulin cycle and are bound by calnexin (membrane bound) or calreticulin (soluble ER protein) which retain the protein in the ER (Hammond and Helenius, 1993; Hammond and Helenius, 1994; Peterson et al., 1995). Binding to calcium-dependent lectins calnexin or calreticulin prevents unfolded proteins from aggregation or premature degradation thereby assisting in folding together with other chaperones and protein disulfide isomerases (e.g. BiP, Grp94, ERp57, PDI). Monoglucosylated Man structures on unfolded proteins also interacts with degradation enhancing α-mannosidase-like protein (EDEM) targeting terminally misfolded proteins to proteasomal degradation.

Endoplasmic Reticulum-associated degradation (ERAD)

Degradation of proteins from the ER require translocation to the cytosol due to the cytoplasmic location of the proteasomal degradation machinery. Terminally misfolded proteins from the ER are recognized, targeted to the ER membrane, and retrotranslocated to the cytosol in a multi-step process. Numerous ERAD factors act on target peptides which function in substrate recognition, targeting, extraction from the ER, ubiquitination, and finally degradation (Helenius and Aebi, 2004; Nakatsukasa and Brodsky, 2008).

The basis of ERAD is given by the competition for unfolded, N-glycosylated proteins by calnexin/calreticulin and binding of EDEM. This competition depends on N-glycan trimming and is time-dependent. Immediate removal of the terminal Glc sugars after the transfer of the glycan precursor on a target protein ensures entering into the calnexin/calreticulin cycle for assisted folding. The longer the time an unfolded protein spends in the ER, the more likely it will be degraded via ERAD. This mechanism is possible through the trimming enzyme mannosidase I which removes the terminal Man

from the mid branch of the N-linked glycan to yield $Man_8GlcNAc_2$-Asn. Mannosidase I seems to act as a timer due to its relative inefficiency to act on N-glycans. Once mannosidase I action is complete, unfolded target proteins are recognized by EDEM 30-90 minutes after translation. The recognition by EDEM depends on a bipartite signal consisting of an N-glycan trimmed by mannosidase I and an unfolded peptide (Xie et al., 2009). Interestingly, Man removal slows down the calnexin/calreticulin cycle because of decreased efficiency of glucosidase II and UGGT1 upon mannosidase I action. Other mannosidases cleaving the terminal Man from the other two branches have been found but their roles in ERAD are not yet fully understood.

Intracellular transport and targeting to lysosomes

Protein sorting and targeting is often based on signals within the amino acid sequence of a protein. Specific glycan structures can target proteins to different compartments of a cell as well. Targeting to the Golgi complex for instance is achieved by P-type lectins that bind mannose-6-phosphate (M6P). Two different M6P receptors exist and both bind to M6P with high affinity (Ghosh et al., 2003; Munier-Lehmann et al., 1996).

Lysosomal enzymes carry oligomannose N-glycans with one or two phosphate modifications on the C6 position of various Man. Selected Man are not directly phosphorylated by kinases but are acted on by UDP-GlcNAc-dependent GlcNAc-1-phosphotransferase (GlcNAc-P-T) (Gelfman et al., 2007; Ghosh and Kornfeld, 2004). The resulting GlcNAcα1-P-6-Manα1-(N-glycan)-Asn is then processed by a Golgi-resident enzyme removing GlcNAc and uncovering the M6P recognition marker. The generation of the M6P recognition marker must be very specific in order to deliver lysosomal enzymes reliably to the lysosome. Since GlcNAc-P-T target proteins do not share any amino acid sequence similarity, substrate specificity is given by secondary and tertiary structures of target proteins. As few as two lysine residues in proper orientation towards each other and towards the oligomannose N-glycan are sufficient to be recognized by GlcNAc-P-T. Additional amino acid residues or recognition domains can enhance interaction with GlcNAc-P-T (Braulke et al., 2008).

The M6P receptors mainly localize to the *trans*-Golgi network and late endosomes from where they cycle between early sorting endosomes, recycling endosomes, and the cell membrane. M6P receptor trafficking is achieved by sorting signals in their cytoplasmic

tails. Once a lysosomal protein is recognized by a receptor in the *trans*-Golgi network, the receptor-protein complex is recruited to clathrin-coated pits. Arrival at the early endosomes triggers the release of the lysosomal protein from the M6P receptors due to the decrease in pH. Interestingly, accidentally secreted lysosomal proteins can be captured by one of the two receptors at the cell surface and internalized by clathrin-mediated endocytosis.

Hepatic asialoglycoprotein receptor

The hepatic asialoglycoprotein receptor, ASGPR, was the first C-type (Ca^{2+} dependent) lectin to be discovered (Irie and Tavassoli, 1986; Tavassoli, 1985). ASPGR assists in the clearance of blood proteins by binding desialylated blood proteins. Studies demonstrated a preference of ASPGR for terminal GalNAc residues but also binding to Gal. Many pituitary protein hormones and parasite-derived proteins contain terminal GalNAc residues potentially recognized by ASPGR. Protein stability mediated by glycans is therefore not only a direct effect of enhanced solubility or protection against proteases but also by regulatory possibilities by marking desialylated proteins for clearance. This mechanism can also be observed in immune cells that recognize glycans as virulent factors and mediate endocytosis.

N-glycans and integrin functions

Integrins are plasma membrane proteins with a lectin portion in the extracellular space and function as adhesion proteins binding the extracellular matrix as well as in transducing signals from the extracellular space into the cell (Gu et al., 2012; Hynes, 2002). As a consequence, aberrant integrin function has been associated with tumor invasion (Bellis, 2004; Dennis et al., 2002). Changes in N-glycosylation of integrins were shown to potentially regulate cell adhesion (Isaji et al., 2010). The *N*-acetylglucosaminyltransferase III (GnT-III) adds the "bi-secting" GlcNAc to the core Man (c, Figure 4) of the N-linked glycan thereby suppressing further branching of the glycan. Overexpression of GnT-III resulted in decreased branching of integrin N-glycans and inhibition of integrin-mediated spreading and migration of cancer cells. Conversely, GnT-III knockdown resulted in more N-glycan branching and increased cell migration. Accordingly, diverse cancer cell lines were reported to have increased glycan branching

(Blomme et al., 2012a; Blomme et al., 2012b; Blomme et al., 2013; Blomme et al., 2009; Dennis, 1991).

Congenital disorders in N-linked glycosylation

Congenital disorders of glycosylation (CDG) are a rapidly growing family of diseases affecting different glycosylation pathways (Eklund and Freeze, 2006; Freeze, 2007; Grunewald, 2007; Jaeken, 2013). Genetic defects can affect all classes of glycosylation presently adding up to more than 80 affected genes. The most frequently affected pathway in CDG is N-linked glycosylation (Freeze and Aebi, 2005; Haeuptle and Hennet, 2009). Among these CDG, defects in the assembly of the N-glycan precursor in the ER (Figure 4) and defects in N-glycan maturation and processing in the Golgi complex are distinguished.

Individuals with CDG typically show diverse dysfunctions in several organ systems reflecting the importance and abundance of functions of glycosylation. Most prominently, patients show strong neurological defects or at least a neurological component among the symptoms. The most frequent symptoms are psychomotor retardation, epilepsy, hypotonia, hyporeflexia, strabismus, retinitis pigmentosa, polyneuropathy, myopathy, and cerebellar hypotrophy/hypoplasia. This broad range of symptoms hampers recognition of CDG and likely lead to under-diagnosis. Additionally, the severity of CDG often leads to death in early infancy making diagnosis more difficult (Funke et al., 2013). Decreased occupancy of N-glycosylation sites are a common feature of most CDG. Therefore, diagnosis of CDG is done by carbohydrate-deficient transferrin (CDT) analysis using isoelectric focusing or mass spectrometry-based approaches. Transferrin is a blood serum protein with two Fe(III) binding sites produced and secreted by the liver. Serum transferrin takes part in iron homeostasis by binding Fe(III) in the blood and transporting it to target sites where it is absorbed by receptor-mediated endocytosis. Reaching early endosomes, the drop in pH triggers the release of iron without breaking the association of transferrin to its receptor. After iron release, receptor-bound transferrin is recycled into the blood stream where it can again bind iron. Transferrin normally carries two bi-antennary N-glycans and therefore has four capping sialic acids in total. Besides this so-called tetrasialo-transferrin, 10-15% of transferrin carry one or two tri-antennary N-glycans giving rise to pentasialo- and

hexasialo-transferrin. CDG can be distinguished from other metabolic diseases with similar manifestations by assessing the glycoform distribution of transferrin. Blood plasma from CDG patients contains hypoglycosylated transferrin. Deficiencies in the early steps of the glycan precursor assembly (former CDG-I type) on Dol result in increased occurrence of disialo- and asialo-transferrin while defects in later stage of N-glycosylation (former CDG-II type) result in a higher proportion of trisialo- and monosialo-transferrin. Notably, a missing hypoglycosylation phenotype of transferrin does not rule out CDG. In adults, a hypoglycosylation phenotype can arise from alcohol abuse that results in perturbed N-glycosylation in the liver leading to CDT. With the discovery of vesicular transport defects impairing glycosylation, the former distinction between CDG-I and CDG-II types was replaced by the name of the deficient gene instead, e.g. CDG-ALG6 (Jaeken et al., 2008).

The identification and characterization of CDG of N-linked glycosylation has shown that basically every single gene along the pathway can be affected (Figure 4). However, the severity of a given CDG at the systemic level is difficult to predict. A totally dysfunctional enzyme is likely to lead to embryonic death and observed gene defects in CDG seem to retain residual enzyme activity of the affected protein. Yeast models have played a pivotal role in identifying gene defects in CDG (Aebi and Hennet, 2001). Typically, a patient diagnosed with CDG based on CDT analysis has an aberrant DLO pattern that can be defined from skin fibroblasts. Comparison of a specific accumulation of DLO with yeast mutants is used to identify affected genes. Cloning of the human gene and complementation analysis in the yeast mutant can confirm the putative CDG. The development of whole-exome sequencing methods has enabled screening of patients with psychomotor retardation for mutated genes and recently has led to the identification of new forms of CDG (Freeze et al., 2012; Hennet, 2012; Matthijs et al., 2013).

Recently, a novel type of CDG affecting the biosynthesis of Dol-P has emerged. Dol is not only involved in N-glycosylation but also in O-mannosylation, C-mannosylation and GPI-anchor biosynthesis. This group of CDG is discussed in the section “Regulation of Dol-linked glycosylation” (Welti, 2013).

Alcoholic liver disease and N-linked glycosylation deficiency

Alcoholic liver disease (ALD) is a consequence of chronic and excessive alcohol intake. Since the liver is the primary site of ethanol degradation, side-effects of ethanol and its degradation products acetaldehyde and acetate along with "by-products" like excess NADH and reactive oxygen species have considerable impact on liver function. An estimated 50% of liver cirrhosis with lethal outcome is attributable to alcohol consumption (WHO, 2011).

A major cause of ethanol-induced liver injury is oxidative stress exerted by the products of ethanol degradation. Many symptoms of liver injury have been described involving disruption of various liver functions. Transcription factors are activated (NF-κB, Nrf-2, AP-1) and the expression of antioxidant enzymes (glutathione S-transferase, catalase, heme oxigenase-1) is upregulated (Dey and Cederbaum, 2006). Moreover, ethanol impairs the ubiquitin-proteasome system, leading to the promotion of apoptosis through pathways depending on the degradation of inhibitory factors (Donohue et al., 2007). Degradation of ethanol occurs in two major pathways. Alcohol dehydrogenase (ADH) is constitutively expressed in hepatocytes and converts ethanol to acetaldehyde under expenditure of NAD. The second pathway depends on the inducible cytochrome P450 system, originally discovered as microsomal ethanol-oxidizing system and occurs in the smooth ER. Many isoforms of these microsomal cytochromes exist but only cytochrome P450 II E1 (CYP2E1) is induced upon ethanol consumption (Koivisto et al., 1996; Oneta et al., 2002; Salmela et al., 1998; Takahashi et al., 1993). Acetaldehyde produced by ADH and CYP2E1 is further oxidized by acetaldehyde dehydrogenase to yield acetate. Acetate can be fueled into the citric acid cycle or used for the biosynthesis of a variety of carbohydrate-based molecules (Berg et al., 2007).

Initial effects of chronic alcohol abuse are of metabolic nature and result in inhibition of glycolysis due to excess reductive compound NADH. Glycolysis is a major pathway for energy production in which Glc yields 2 molecules of ATP, 2 molecules of NADH, and 2 molecules of pyruvate. Pyruvate can then be fueled into the citric acid cycle which produces 15 ATP molecules per Glc. The conversion of ethanol to acetaldehyde and eventually acetate produces 2 molecules of NADH. Acetate is used as a substrate for the citric acid cycle. Excess NADH from ethanol metabolism from chronic alcohol abuse induces a negative feedback loop and disrupts the chemical equilibrium of reactions in

glycolysis and the citric acid cycle. Additionally, NADH accumulation inhibits β-oxidation of lipids thus inhibiting lipid breakdown. As a consequence, fatty acid synthesis is prompted and lipid storage marks the beginning of fatty liver disease (Sozio and Crabb, 2008). Sustained ethanol abuse leads to chronic inflammation of the liver eventually leading to fibrosis and cirrhosis.

Protein glycosylation deficiency in the context of ALD is a poorly investigated area despite the fact that ethanol uptake correlates with carbohydrate-deficient blood proteins (Stibler, 1991). The blood serum protein transferrin for instance is carbohydrate-deficient in both, CDG and alcoholism. Interestingly, liver fibrosis is not only frequent in ALD but also in some forms of CDG (Jaeken et al., 1998; Pelletier et al., 1986). The detection of carbohydrate-deficient transferrin has been widely used as a tool to detect alcoholism and CDG (Jaeken and Matthijs, 2007). The detection of carbohydrate-deficient transferrin is based on the detection of the different glycoforms. Transferrin contains two consensus sequences for N-linked glycosylation. Potentially each N-linked glycan can carry three sialic acids, each conferring a negative charge to the protein. Isoelectric focusing separates the distinct glycoforms according to their isoelectric point that is dependent on the number of carboxyl functional groups. In healthy individuals, the tetrasialo-transferrin is predominant. Pentasialo-, trisialo-, and disialo-transferrin can be detected to a lower extent. The glycoform distribution is shifted in individuals suffering from chronic alcoholism. Still, the tetrasialo-transferrin is the predominant form but more disialo-transferrin can be detected. In addition, monosialo- and asialo-transferrin are present (Helander et al., 2004; Stibler, 1991). A commonly used model is the human hepatocellular carcinoma cell line HepG2 which was isolated from a child and shows active plasma protein secretion (Knowles et al., 1980). HepG2 cells treated with 50-100 mM ethanol were shown to have a decreased transcription of the alpha-2,6-sialyltransferase (2,6-ST). This transferase is responsible for the sialylation of transferrin at the ends of the attached sugar chains. Lower 2,6-ST and increased activity of plasma and plasma membrane sialidases were observed in the liver from chronically ethanol-fed rats and humans (Cottalasso et al., 1996; Ghosh et al., 1993; Xin et al., 1995). Additionally, the 2,6-ST mRNA is destabilized by a 3'-untranslated region-specific binding protein as could be demonstrated by depletion experiments (Garige et al., 2006; Garige et al., 2005; Rao and Lakshman, 1997; Rao and Lakshman, 1999). Notably, the downregulation of 2,6-ST does not necessarily need to be

the only cause of carbohydrate-deficient transferrin. Furthermore, lower GlcNAc transferase activity was found in livers of ethanol-fed rats (Xin et al., 1995). As illustrated in Figure 4, several intermediates might be affected as well, potentially leading to asialo-transferrin or a shift in glycoforms. In CDG patients suffering from very severe forms the disorder, the occupancy of the second N-glycosylation site can be reduced to 41%. In contrast, the occupancy of the first site was maximally reduced to 71%. CDT from chronic alcohol abuse exhibits a site occupancy of more than 90% for both N-glycosylation sites (Hülsmeier et al., 2007). The presence of sialic acid-deficient transferrin was mainly attributed to the loss of an entire oligosaccharide in another study (Peter et al., 1998). Another defect induced by chronic alcohol treatment is an impaired synthesis of Dol and Dol-P (Cottalasso et al., 1998; Cottalasso et al., 1996).

References

Aebi, M. 2013. N-linked protein glycosylation in the ER. *Biochimica et biophysica acta*

Aebi, M., and T. Hennet. 2001. Congenital disorders of glycosylation: genetic model systems lead the way. *Trends Cell Biol* 11:136-141.

Bellis, S.L. 2004. Variant glycosylation: an underappreciated regulatory mechanism for beta1 integrins. *Biochimica et biophysica acta* 1663:52-60.

Berg, J.M., J.L. Tymoczko, and L. Stryer. 2007. Biochemistry. Freeman, New York. 1026 pp.

Blomme, B., E. Fitzpatrick, A. Quaglia, R. De Bruyne, A. Dhawan, and H. Van Vlierberghe. 2012a. Serum protein N-glycosylation in paediatric non-alcoholic fatty liver disease. *Pediatr Obes* 7:165-173.

Blomme, B., S. Francque, E. Trepo, L. Libbrecht, D. Vanderschaeghe, A. Verrijken, P. Pattyn, Y.V. Nieuwenhove, D.V. Putte, A. Geerts, I. Colle, J. Delanghe, C. Moreno, L.V. Gaal, N. Callewaert, and H.V. Vlierberghe. 2012b. N-glycan based biomarker distinguishing non-alcoholic steatohepatitis from steatosis independently of fibrosis. *Dig Liver Dis* 44:315-322.

Blomme, B., F. Heindryckx, J.M. Stassen, A. Geerts, I. Colle, and H. Van Vlierberghe. 2013. Serum protein N-glycan alterations of diethylnitrosamine-induced hepatocellular carcinoma mice and their evolution after inhibition of the placental growth factor. *Mol Cell Biochem* 372:199-210.

Blomme, B., C. Van Steenkiste, N. Callewaert, and H. Van Vlierberghe. 2009. Alteration of protein glycosylation in liver diseases. *J Hepatol* 50:592-603.

Braulke, T., S. Pohl, and S. Storch. 2008. Molecular analysis of the GlcNac-1-phosphotransferase. *J Inherit Metab Dis* 31:253-257.

Cantagrel, V., and D.J. Lefeber. 2011. From glycosylation disorders to dolichol biosynthesis defects: a new class of metabolic diseases. *J Inherit Metab Dis* 34:859-867.

Comer, F.I., and G.W. Hart. 2000. O-Glycosylation of nuclear and cytosolic proteins. Dynamic interplay between O-GlcNAc and O-phosphate. *J Biol Chem* 275:29179-29182.

Cottalasso, D., A. Bellocchio, M.A. Pronzato, C. Domenicotti, N. Traverso, M.V. Gianelli, U.M. Marinari, and G. Nanni. 1998. Effect of ethanol administration on the level of dolichol in rat liver microsomes and Golgi apparatus. *Alcoholism, clinical and experimental research* 22:730-737.

Cottalasso, D., P. Gazzo, D. Dapino, C. Domenicotti, M.A. Pronzato, N. Traverso, A. Bellocchio, G. Nanni, and U.M. Marinari. 1996. Effect of chronic ethanol consumption on glycosylation processes in rat liver microsomes and Golgi apparatus. *Alcohol and alcoholism (Oxford, Oxfordshire)* 31:51-59.

Dennis, J.W. 1991. N-linked oligosaccharide processing and tumor cell biology. *Semin Cancer Biol* 2:411-420.

Dennis, J.W., J. Pawling, P. Cheung, E. Partridge, and M. Demetriou. 2002. UDP-N-acetylglucosamine:alpha-6-D-mannoside beta1,6 N-acetylglucosaminyltransferase V (Mgat5) deficient mice. *Biochimica et biophysica acta* 1573:414-422.

Dey, A., and A.I. Cederbaum. 2006. Alcohol and oxidative liver injury. *Hepatology (Baltimore, Md* 43:S63-74.

Donohue, T.M., Jr., A.I. Cederbaum, S.W. French, S. Barve, B. Gao, and N.A. Osna. 2007. Role of the proteasome in ethanol-induced liver pathology. *Alcoholism, clinical and experimental research* 31:1446-1459.

Eklund, E.A., and H.H. Freeze. 2006. The congenital disorders of glycosylation: a multifaceted group of syndromes. *NeuroRx* 3:254-263.

Freeze, H.H. 2007. Congenital Disorders of Glycosylation: CDG-I, CDG-II, and beyond. *Curr Mol Med* 7:389-396.

Freeze, H.H., and M. Aebi. 2005. Altered glycan structures: the molecular basis of congenital disorders of glycosylation. *Curr Opin Struct Biol* 15:490-498.

Freeze, H.H., E.A. Eklund, B.G. Ng, and M.C. Patterson. 2012. Neurology of inherited glycosylation disorders. *Lancet Neurol* 11:453-466.

Funke, S., T. Gardeitchik, D. Kouwenberg, M. Mohamed, S.B. Wortmann, E. Korsch, M. Adamowicz, L. Al-Gazali, R.A. Wevers, A. Horvath, D.J. Lefeber, and E. Morava. 2013. Perinatal and early infantile symptoms in congenital disorders of glycosylation. *Am J Med Genet A* 3:578-584.

Garige, M., M. Gong, and M.R. Lakshman. 2006. Ethanol destabilizes liver Gal beta l, 4GlcNAc alpha2,6-sialyltransferase, mRNA by depleting a 3'-untranslated region-specific binding protein. *The Journal of pharmacology and experimental therapeutics* 318:1076-1082.

Garige, M., M. Gong, M.N. Rao, Y. Zhang, and M.R. Lakshman. 2005. Mechanism of action of ethanol in the down-regulation of Gal(beta)1, 4GlcNAc alpha2,6-sialyltransferase messenger RNA in human liver cell lines. *Metabolism: clinical and experimental* 54:729-734.

Gavel, Y., and G. von Heijne. 1990. Sequence differences between glycosylated and non-glycosylated Asn-X-Thr/Ser acceptor sites: implications for protein engineering. *Protein Eng* 3:433-442.

Gelfman, C.M., P. Vogel, T.M. Issa, C.A. Turner, W.S. Lee, S. Kornfeld, and D.S. Rice. 2007. Mice lacking alpha/beta subunits of GlcNAc-1-phosphotransferase exhibit growth retardation, retinal degeneration, and secretory cell lesions. *Invest Ophthalmol Vis Sci* 48:5221-5228.

Ghosh, P., N.M. Dahms, and S. Kornfeld. 2003. Mannose 6-phosphate receptors: new twists in the tale. *Nat Rev Mol Cell Biol* 4:202-212.

Ghosh, P., and S. Kornfeld. 2004. The GGA proteins: key players in protein sorting at the trans-Golgi network. *Eur J Cell Biol* 83:257-262.

Ghosh, P., C. Okoh, Q.H. Liu, and M.R. Lakshman. 1993. Effects of chronic ethanol on enzymes regulating sialylation and desialylation of transferrin in rats. *Alcoholism, clinical and experimental research* 17:576-579.

Grunewald, S. 2007. Congenital disorders of glycosylation: rapidly enlarging group of (neuro)metabolic disorders. *Early Hum Dev* 83:825-830.

Gu, J., T. Isaji, Q. Xu, Y. Kariya, W. Gu, T. Fukuda, and Y. Du. 2012. Potential roles of N-glycosylation in cell adhesion. *Glycoconjugate journal* 29:599-607.

Guinez, C., W. Morelle, J.C. Michalski, and T. Lefebvre. 2005. O-GlcNAc glycosylation: a signal for the nuclear transport of cytosolic proteins? *The international journal of biochemistry & cell biology* 37:765-774.

Haeuptle, M.A., and T. Hennet. 2009. Congenital disorders of glycosylation: an update on defects affecting the biosynthesis of dolichol-linked oligosaccharides. *Hum Mutat* 30:1628-1641.

Hammond, C., and A. Helenius. 1993. A chaperone with a sweet tooth. *Curr Biol* 3:884-886.

Hammond, C., and A. Helenius. 1994. Folding of VSV G protein: sequential interaction with BiP and calnexin. *Science* 266:456-458.

Hart, G.W., and Y. Akimoto. 2009. The O-GlcNAc Modification.

Hebert, D.N., J.X. Zhang, W. Chen, B. Foellmer, and A. Helenius. 1997. The number and location of glycans on influenza hemagglutinin determine folding and association with calnexin and calreticulin. *J Cell Biol* 139:613-623.

Helander, A., J. Bergstrom, and H.H. Freeze. 2004. Testing for congenital disorders of glycosylation by HPLC measurement of serum transferrin glycoforms. *Clinical chemistry* 50:954-958.

Helenius, A. 1994. How N-linked oligosaccharides affect glycoprotein folding in the endoplasmic reticulum. *Mol Biol Cell* 5:253-265.

Helenius, A., and M. Aebi. 2004. Roles of N-linked glycans in the endoplasmic reticulum. *Annual review of biochemistry* 73:1019-1049.

Hennet, T. 2012. Diseases of glycosylation beyond classical congenital disorders of glycosylation. *Biochimica et biophysica acta* 9:9.

Hochstrasser, M. 2009. Origin and function of ubiquitin-like proteins. *Nature* 458:422-429.

Hülsmeier, A.J., P. Paesold-Burda, and T. Hennet. 2007. N-glycosylation site occupancy in serum glycoproteins using multiple reaction monitoring liquid chromatography-mass spectrometry. *Mol Cell Proteomics* 6:2132-2138.

Hunter, T. 2000. Signaling--2000 and beyond. *Cell* 100:113-127.

Hurtley, S.M., and A. Helenius. 1989. Protein oligomerization in the endoplasmic reticulum. *Annu Rev Cell Biol* 5:277-307.

Hynes, R.O. 2002. Integrins: bidirectional, allosteric signaling machines. *Cell* 110:673-687.

Imberty, A., and S. Perez. 1995. Stereochemistry of the N-glycosylation sites in glycoproteins. *Protein Eng* 8:699-709.

Imperiali, B., and S.E. O'Connor. 1999. Effect of N-linked glycosylation on glycopeptide and glycoprotein structure. *Curr Opin Chem Biol* 3:643-649.

Irie, S., and M. Tavassoli. 1986. Liver endothelium desialates ceruloplasmin. *Biochem Biophys Res Commun* 140:94-100.

Isaji, T., Y. Kariya, Q. Xu, T. Fukuda, N. Taniguchi, and J. Gu. 2010. Functional roles of the bisecting GlcNAc in integrin-mediated cell adhesion. *Methods Enzymol* 480:445-459.

Jaeken, J. 2013. Congenital disorders of glycosylation. *Handb Clin Neurol* 113:1737-1743.

Jaeken, J., T. Hennet, H.H. Freeze, and G. Matthijs. 2008. On the nomenclature of congenital disorders of glycosylation (CDG). *J Inherit Metab Dis* 31:669-672.

Jaeken, J., and G. Matthijs. 2007. Congenital disorders of glycosylation: a rapidly expanding disease family. *Annual review of genomics and human genetics* 8:261-278.

Jaeken, J., G. Matthijs, J.M. Saudubray, C. Dionisi-Vici, E. Bertini, P. de Lonlay, H. Henri, H. Carchon, E. Schollen, and E. Van Schaftingen. 1998. Phosphomannose isomerase deficiency: a carbohydrate-deficient glycoprotein syndrome with hepatic-intestinal presentation. *Am J Hum Genet* 62:1535-1539.

Klausner, R.D., and R. Sitia. 1990. Protein degradation in the endoplasmic reticulum. *Cell* 62:611-614.

Knowles, B.B., C.C. Howe, and D.P. Aden. 1980. Human hepatocellular carcinoma cell lines secrete the major plasma proteins and hepatitis B surface antigen. *Science* 209:497-499.

Koivisto, T., V.M. Mishin, K.M. Mak, P.A. Cohen, and C.S. Lieber. 1996. Induction of cytochrome P-4502E1 by ethanol in rat Kupffer cells. *Alcoholism, clinical and experimental research* 20:207-212.

Kolarich, D., E. Rapp, W.B. Struwe, S.M. Haslam, J. Zaia, R. McBride, S. Agravat, M.P. Campbell, M. Kato, R. Ranzinger, C. Kettner, and W.S. York. 2013. The minimum information required for a glycomics experiment (MIRAGE) project: improving the standards for reporting mass-spectrometry-based glycoanalytic data. *Mol Cell Proteomics* 12:991-995.

Larkin, A., and B. Imperiali. 2011. The expanding horizons of asparagine-linked glycosylation. *Biochemistry* 50:4411-4426.

Marshall, R.D. 1974. The nature and metabolism of the carbohydrate-peptide linkages of glycoproteins. *Biochem Soc Symp* 17-26.

Matthijs, G., D. Rymen, M.B. Millon, E. Souche, and V. Race. 2013. Approaches to homozygosity mapping and exome sequencing for the identification of novel types of CDG. *Glycoconjugate journal* 30:67-76.

Mechref, Y., Y. Hu, A. Garcia, and A. Hussein. 2012. Identifying cancer biomarkers by mass spectrometry-based glycomics. *Electrophoresis* 33:1755-1767.

Moloney, D.J., V.M. Panin, S.H. Johnston, J. Chen, L. Shao, R. Wilson, Y. Wang, P. Stanley, K.D. Irvine, R.S. Haltiwanger, and T.F. Vogt. 2000. Fringe is a glycosyltransferase that modifies Notch. *Nature* 406:369-375.

Moremen, K.W. 2002. Golgi alpha-mannosidase II deficiency in vertebrate systems: implications for asparagine-linked oligosaccharide processing in mammals. *Biochimica et biophysica acta* 1573:225-235.

Munier-Lehmann, H., F. Mauxion, and B. Hoflack. 1996. Function of the two mannose 6-phosphate receptors in lysosomal enzyme transport. *Biochem Soc Trans* 24:133-136.

Nadolski, M.J., and M.E. Linder. 2007. Protein lipidation. *FEBS J* 274:5202-5210.

Nakatsukasa, K., and J.L. Brodsky. 2008. The recognition and retrotranslocation of misfolded proteins from the endoplasmic reticulum. *Traffic* 9:861-870.

O'Connor, S.E., and B. Imperiali. 1996. Modulation of protein structure and function by asparagine-linked glycosylation. *Chem Biol* 3:803-812.

Olden, K., J.B. Parent, and S.L. White. 1982. Carbohydrate moieties of glycoproteins. A re-evaluation of their function. *Biochimica et biophysica acta* 650:209-232.

Oneta, C.M., C.S. Lieber, J. Li, S. Ruttimann, B. Schmid, J. Lattmann, A.S. Rosman, and H.K. Seitz. 2002. Dynamics of cytochrome P4502E1 activity in man: induction by ethanol and disappearance during withdrawal phase. *J Hepatol* 36:47-52.

Panin, V.M., L. Shao, L. Lei, D.J. Moloney, K.D. Irvine, and R.S. Haltiwanger. 2002. Notch ligands are substrates for protein O-fucosyltransferase-1 and Fringe. *J Biol Chem* 277:29945-29952.

Pelletier, V.A., N. Galeano, P. Brochu, C.L. Morin, A.M. Weber, and C.C. Roy. 1986. Secretory diarrhea with protein-losing enteropathy, enterocolitis cystica superficialis, intestinal lymphangiectasia, and congenital hepatic fibrosis: a new syndrome. *J Pediatr* 108:61-65.

Peter, J., C. Unverzagt, W.D. Engel, D. Renauer, C. Seidel, and W. Hosel. 1998. Identification of carbohydrate deficient transferrin forms by MALDI-TOF mass spectrometry and lectin ELISABiochim Biophys Acta 1998 Aug 24;1381(3):356. *Biochimica et biophysica acta* 1380:93-101.

Peterson, J.R., A. Ora, P.N. Van, and A. Helenius. 1995. Transient, lectin-like association of calreticulin with folding intermediates of cellular and viral glycoproteins. *Mol Biol Cell* 6:1173-1184.

Ramachandran, C.K., and G. Melnykovych. 1986. Differential regulation of the synthesis of mannosylphosphoryl derivatives of dolichol and retinol in HeLa cells. *Biochimica et biophysica acta* 877:96-103.

Rao, M.N., and M.R. Lakshman. 1997. Chronic ethanol downregulates Gal-beta-1,4GlcNAc alpha 2,6-sialyltransferase and Gal-beta-1,3GlcNAc alpha 2,3-sialyltransferase mRNAs in rat liver. *Alcoholism, clinical and experimental research* 21:348-351.

Rao, M.N., and M.R. Lakshman. 1999. Chronic ethanol consumption leads to destabilization of rat liver beta-galactoside alpha2,6-sialyltransferase mRNA. *Metabolism: clinical and experimental* 48:797-803.

Rush, J.S., N. Gao, M.A. Lehrman, and C.J. Waechter. 2008. Recycling of dolichyl monophosphate to the cytoplasmic leaflet of the endoplasmic reticulum after the cleavage of dolichyl pyrophosphate on the lumenal monolayer. *J Biol Chem* 283:4087-4093.

Salmela, K.S., I.G. Kessova, I.B. Tsyrlov, and C.S. Lieber. 1998. Respective roles of human cytochrome P-4502E1, 1A2, and 3A4 in the hepatic microsomal ethanol oxidizing system. *Alcoholism, clinical and experimental research* 22:2125-2132.

Silbert, J.E., and G. Sugumaran. 2002. Biosynthesis of chondroitin/dermatan sulfate. *IUBMB Life* 54:177-186.

Sozio, M., and D.W. Crabb. 2008. Alcohol and lipid metabolism. *Am J Physiol Endocrinol Metab* 295:E10-16.

Spiro, R.G. 2002. Protein glycosylation: nature, distribution, enzymatic formation, and disease implications of glycopeptide bonds. *Glycobiology* 12:43R-56R.

Stibler, H. 1991. Carbohydrate-deficient transferrin in serum: a new marker of potentially harmful alcohol consumption reviewed. *Clinical chemistry* 37:2029-2037.

Suh, K., J.E. Bergmann, and C.A. Gabel. 1989. Selective retention of monoglucosylated high mannose oligosaccharides by a class of mutant vesicular stomatitis virus G proteins. *J Cell Biol* 108:811-819.

Takahashi, T., J.M. Lasker, A.S. Rosman, and C.S. Lieber. 1993. Induction of cytochrome P-4502E1 in the human liver by ethanol is caused by a corresponding increase in encoding messenger RNA. *Hepatology (Baltimore, Md* 17:236-245.

Tavassoli, M. 1985. Liver endothelium binds, transports, and desialates ceruloplasmin which is then recognized by galactosyl receptors of hepatocytes. *Trans Assoc Am Physicians* 98:370-377.

Varki, A. 1993. Biological roles of oligosaccharides: all of the theories are correct. *Glycobiology* 3:97-130.

Varki, A., R. Cummings, J. Esko, H.H. Freeze, P. Stanley, C.R. Bertozzi, G.W. Hart, and M.E. Etzler. 2009. Essentials of Glycobiology, 2nd edition. *Cold Spring Harbor Laboratory Press*

Varki, A., R.D. Cummings, J. Esko, H.H. Freeze, P. Stanley, C.R. Bertozzi, G.W. Hart, and M.E. Etzler. 2008. Essentials of glycobiology, 2nd ed. *Cold Spring Harb Laboratory Press*

Welti, M. 2013. Regulation of dolichol-linked glycosylation. *Glycoconjugate journal* 30:51-56.

Whitworth, G.E., W.F. Zandberg, T. Clark, and D.J. Vocadlo. 2010. Mammalian Notch is modified by D-Xyl-alpha1-3-D-Xyl-alpha1-3-D-Glc-beta1-O-Ser: implementation of a method to study O-glucosylation. *Glycobiology* 20:287-299.

WHO, W.H.O. 2011. Global status report on alcohol and health.

Williams, D.B. 2006. Beyond lectins: the calnexin/calreticulin chaperone system of the endoplasmic reticulum. *J Cell Sci* 119:615-623.

Wormald, M.R., and R.A. Dwek. 1999. Glycoproteins: glycan presentation and protein-fold stability. *Structure* 7:R155-160.

Xie, W., K. Kanehara, A. Sayeed, and D.T. Ng. 2009. Intrinsic conformational determinants signal protein misfolding to the Hrd1/Htm1 endoplasmic reticulum-associated degradation system. *Mol Biol Cell* 20:3317-3329.

Xin, Y., J.M. Lasker, and C.S. Lieber. 1995. Serum carbohydrate-deficient transferrin: mechanism of increase after chronic alcohol intake. *Hepatology (Baltimore, Md* 22:1462-1468.

Zaia, J. 2010. Mass spectrometry and glycomics. *OMICS* 14:401-418.

Zaia, J. 2013. Glycosaminoglycan glycomics using mass spectrometry. *Mol Cell Proteomics* 12:885-892.

PUBLICATIONS

Improvement of dolichol-linked oligosaccharide biosynthesis by the squalene synthase inhibitor Zaragozic acid

Micha A. Haeuptle[1,3], Michael Welti[1,3], Heinz Troxler[2], Andreas J. Hülsmeier[1], Timo Imbach[1], and Thierry Hennet[1]

[1]Institute of Physiology, University of Zürich, Zürich, Switzerland; [2]Division of Clinical Chemistry and Biochemistry, Children Hospital Zurich, Switzerland

[3]These authors contributed equally

Running head: Zaragozic acid improves N-glycosylation

The Journal of Biological Chemistry. 2011 Feb 25;286(8):6085-91.

Corresponding author:

Thierry Hennet

Institute of Physiology

University of Zürich

Winterthurerstrasse 190

CH-8057 Zürich

Phone: +41-44-635-5080

Fax: +41-44-635-6814

E-mail: thennet@access.uzh.ch

Abstract

The majority of Congenital Disorders of Glycosylation (CDG) are caused by defects of dolichol (Dol)-linked oligosaccharide assembly, which lead to under-occupancy of N-glycosylation sites. Most mutations encountered in CDG are hypomorphic, thus leaving residual activity to the affected biosynthetic enzymes. We hypothesized that increased cellular levels of Dol-linked substrates might compensate for the low biosynthetic activity and thereby improve the output of protein N-glycosylation in CDG. To this end, we have investigated the potential of the squalene synthase inhibitor zaragozic acid to redirect the flow of the poly-isoprene pathway towards Dol by lowering cholesterol biosynthesis. The addition of zaragozic acid to CDG fibroblasts with a Dol-P-Man synthase defect led to the formation of longer Dol-P species and to increased Dol-P-Man levels. This treatment was shown to decrease the pathologic accumulation of incomplete Dol-PP-$GlcNAc_2Man_5$ in Dol-P-Man synthase deficient fibroblasts. Zaragozic acid treatment also decreased the amount of truncated protein N-linked oligosaccharides in these CDG fibroblasts. The increased cellular levels of Dol-P-Man in zaragozic acid-treated cells also led to increased availability of the glycosylphosphatidylinositol-anchor as shown by the elevated cell surface expression of the CD59 protein. The present study shows that manipulation of the cellular Dol pool, as achieved by zaragozic acid addition, may represent a valuable approach aimed at improving N-linked glycosylation in CDG cells.

Introduction

Congenital Disorders of Glycosylation (CDG)[a] are a group of inherited defects of protein glycosylation (Freeze, 2006). Mutations in genes encoding either proteins involved in biosynthesis of lipid-linked oligosaccharide (LLO) required for N-glycosylation (Jaeken and Matthijs, 2007) or proteins involved in glycan processing (De Praeter et al., 2000; Hansske et al., 2002) or transport of N-glycoproteins (Foulquier, 2008) form the molecular basis of CDG. The majority of CDG encompass disorders affecting the assembly of the LLO precursor dolichol-pyrophosphate (Dol-PP)-$GlcNAc_2Man_9Glc_3$, which leads to under-occupancy of N-glycosylation sites (Haeuptle and Hennet, 2009). The stepwise biosynthesis of the LLO precursor begins at the cytosolic side of the endoplasmic reticulum (ER) membrane by transfer of GlcNAc-P to dolichol-P (Dol-P) and completes at the luminal side of the ER membrane. Dol-P does not only serve as carrier of maturing LLO, but also as lipid component of Dol-P-Man and Dol-P-Glc, both donor substrates for luminally acting mannosyl- and glucosyltransferases (Kornfeld and Kornfeld, 1985).

The symptoms associated to CDG are principally of neurologic nature, such as psychomotor retardation, ataxia and hypotonia but also include hormonal alterations and coagulopathies (Leroy, 2006). The clinical severity of CDG mainly depends on the degree of N-glycosylation site under-occupancy (Hülsmeier et al., 2007), which itself depends on the available pool of complete LLO Dol-PP-$GlcNAc_2Man_9Glc_3$. To date, only two forms of CDG can be successfully treated by oral carbohydrate supplementation. The glycosylation defects resulting from deficiency of Man-P isomerase (MPI) can be corrected by Man supplementation (Niehues et al., 1998; Westphal et al., 2001), whereas Fuc uptake has been shown to rescue the deficiency of GDP-Fuc transport (Marquardt et al., 1999). Considering the involvement of Dol throughout the LLO biosynthetic pathway, we made the hypothesis that increased cellular levels of Dol and Dol-P based substrates may increase the formation of Dol-PP-$GlcNAc_2Man_9Glc_3$ in CDG.

Dol biosynthesis follows the sterol pathway up to the formation of the C_{15}-intermediate farnesyl-PP (Swiezewska and Danikiewicz, 2005) (Fig. 1A). Instead of squalene formation by head to head assembly of two farnesyl-PP molecules (Muscio et al., 1974), the consecutive condensation of isopentenyl-PP units leads to the diverging synthesis of polyprenyl-PP, a pre-stage of Dol-P. The enzyme squalene synthase catalyzes the first

reaction leading exclusively to the formation of sterol compounds, such as cholesterol and steroid hormones (Fig. 1A). Inhibition of squalene synthase, for example by zaragozic acid A (ZGA), leads to the stimulation of prior diverging pathways, and hence to increased formation of Dol and Dol-P (Keller, 1996). ZGA, also known as

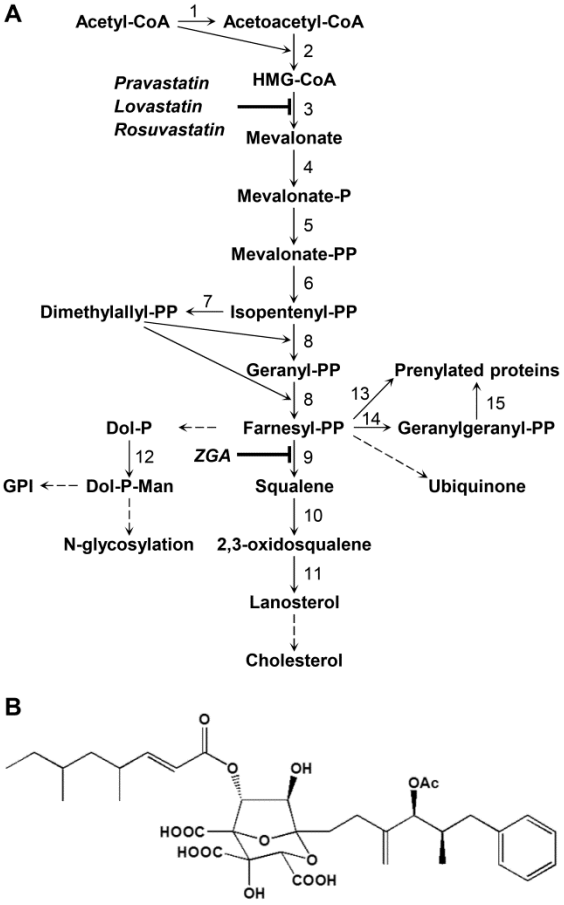

Figure 1: Statins acting on the sterol biosynthesis pathway. **(A)** The biosynthetic formation of sterols, such as cholesterol, starts from acetyl-CoA and leads via the C_{15}-intermediate farnesyl-PP to its various endproducts. The involved enzymes are numbered as follows: (1) acetoacetyl-CoA thiolase, (2) HMG-CoA synthase, (3) HMG-CoA reductase, (4) mevalonate kinase, (5) phosphomevalonate kinase, (6) mevalonate-PP decarboxylase, (7) isopentenyl-PP isomerase, (8) farnesyl-PP synthase, (9) squalene synthase, (10) squalene monooxygenase, (11) squalene epoxydase, (12) Dol-P-Man synthase, (13) protein farnesyltransferase, (14) geranylgeranyl-PP synthase, (15) protein geranylgeranyltransferase. At the point of farnesyl-PP, the pathway diverges to the formation of prenylated proteins, ubiquinone or Dol. The polyisoprene Dol-P is incorporated into Dol-P-Man, a key intermediate in protein glycosylation and GPI-anchor formation. While pravastatin, lovastatin and rosuvastatin lower cellular cholesterol levels by

inhibiting the pathway at the stage of the HMG-CoA reductase, ZGA achieves this by inhibiting the squalene synthase. The chemical structure of ZGA is depicted in **(B)**.

squalestatin I, was discovered by screening metabolites of filamentous fungi for cholesterol lowering activity (Bergstrom et al., 1995). Detailed analysis disclosed that ZGA acts as a competitive inhibitor of the squalene synthase by mimicking the farnesyl-PP substrate or the stable intermediate presqualene-PP with its bicyclic, highly acidic core (Fig. 1B). In contrast to statins acting on common steps of both Dol and cholesterol biosynthesis, such as the 3-hydroxy-3-methyl-glutaryl coenzyme A (HMG-CoA) reductase inhibitors pravastatin (Koga et al., 1990), lovastatin (Alberts et al., 1980) or rosuvastatin (McTaggart et al., 2001), ZGA does not negatively affect the diverging pathways generating Dol, ubiquinone or prenylated proteins (Fig. 1A). In the present study, we have investigated the ability of the squalene synthase inhibitor to increase Dol biosynthesis and thereby the output of N-glycosylation in CDG fibroblasts.

Experimental Procedures

Materials **-** ZGA was a gift from Merck & Co., Inc. (Rahway, NJ). The C_{80}-polyprenyl-P standards were purchased from Larodan Fine Chemicals (Sweden), and broad range mammalian Dol-P standards were from Sigma-Aldrich (Switzerland). Acetonitrile (Scharlau, Spain), dichloromethane (Sigma-Aldrich) and water (Sigma-Aldrich) were of HPLC grade, other chemicals were of analytical grade.

Cholesterol analysis **–** Human primary skin fibroblasts (4 x 10^7 cells) cultured in DMEM (Sigma-Aldrich) with 10% fetal calf serum (Bioconcept, Switzerland) at 37°C were treated for 72 h with either 100 µM ZGA or DMSO alone as negative control. Cells were harvested by trypsinization, washed in PBS and centrifuged at 1000 x g for 5 min. To the cell pellet 1 ml of 4 % (w/v) KOH in 90 % ethanol was added. After vortexing, the solution was incubated for 10 min in a ultrasonic bath and transferred to a glass tube. After addition of 80 µl of internal standard (0.1 mg/ml epicoprostanol (Sigma-Aldrich) in pyridine), the solution was saponified for 60 min at 60°C, mixed with 1 ml of water and extracted three times with 2 ml heptane. The pooled heptane extracts were dried under nitrogen and derivatized with 75 µl BSTFA (Machery-Nagel, Oensingen, Switerzland) in 75 µl pyridine at 60°C for 60 min. For GC/MS analysis, the derivative mixture was diluted 5-fold with heptane and 1 µl was injected (injector temperature: 280°C; splitless injection). A Restek RTX-1MS (BGB Analytik AG, Böckten, Switzerland)

column (15 m, ID = 0.25 mm) was used for chromatographic separation of the sterols. The carrier gas was helium at a constant flow of 1.5 ml/min. After a dwell time of 3 min at 90°C, the oven temperature was raised to 200°C at 20°C/min, then to 260°C at 1.5°C/min, and finally held at 260°C for 10 min. Mass spectrometry was performed on a Finnigan PolarisQ ion trap mass spectrometer. Mass spectra were acquired in the mass range of m/z = 50 - 550.

Dol-P analysis – Fibroblasts (4 x 10^7 cells) were harvested and centrifuged at 1000 x g for 5 min. Cell pellets were dissolved in 12 ml of water/methanol (1:1). Prior to alkaline hydrolysis (Elmberger et al., 1989), 15 µg of C_{80}-polyprenyl-P standards were added. The extracted Dol and Dol-P were purified on a C_{18} Sep Pak column (Waters, USA) and subsequently separated on a Silica Sep Pak column (Waters) (Haeuptle et al., 2010). The Dol-P were dimethylated using diazomethane generated in an Aldrich diazomethane generator system (Sigma-Aldrich) according to the manufacturer's instructions. The resulting Dol-P-Me_2 were selectively demethylated by overnight incubation in *tert*-butylamine (Sigma-Aldrich) at 70°C (Yamada et al., 1986). Monomethylated Dol-P samples were dissolved in a saturated solution of 9-anthryldiazomethane (Sigma-Aldrich) in diethylether and incubated for 6 h on ice in the dark. Anthracene labeled Dol-P were separated from non-reacted labeling agent by organic extraction (Yamada et al., 1986). The purified products were dissolved in acetonitrile/dichloromethane (3:2) and subjected to HPLC on an Inertsil ODS-3 column (5 µm, 4.6 x 250 mm; GL Sciences Inc., Japan) equipped with a precolumn. Isocratic elution in acetonitrile/dichloromethane (3:2) and 0.01% diethylamine (Sigma-Aldrich) was performed at a flow rate of 1 ml/min (Yamada et al., 1986). Fluorescent labeled Dol-P were detected by excitation at 365 nm and emission at 412 nm. Defined amounts of internal standard C_{80}-polyprenyl-P were used for quantification.

Determination of Dol-P-Man - Approximately 4 x 10^7 fibroblasts were grown for 72 h in DMEM containing low Glc (5 mM; Sigma-Aldrich), supplemented with 2% fetal calf serum and 100 µM ZGA or DMSO as negative control. Low Glc medium was utilized to achieve improved Man incorporation (Korner et al., 1998). Cellular Dol-P-Man was metabolically labeled, extracted and purified according to the protocol of Körner and co-workers (Korner et al., 1998). Briefly, the fibroblasts were labeled by incubation in DMEM containing 0.5 mM Glc and 125 µCi [^{3}H]-Man (Hartmann Analytic, Germany) for 30 min. Dol-P-Man and short LLO were extracted once with chloroform/methanol (2:1)

and twice with chloroform/methanol (3:2). The combined organic phases were dried and washed. Thin-layer chromatography on Silica gel 60 plates was performed in chloroform/methanol/water (65:25:4). The plates were analyzed by radiography after signal enhancement with an EN^{3}HANCE spray (PerkinElmer, USA) and the area containing Dol-P-Man were scraped and counted in a TRI–CARB 2900 TR liquid scintillation analyzer (Packard, USA).

CD59 flow cytometry - Fibroblasts (2 x 10^5 cells) were harvested by trypsinization, washed once in PBS containing 2% fetal calf serum and incubated with a FITC conjugated mouse anti-human CD59 antibody (BD Pharmingen, USA) diluted 1:100 in PBS containing 2% fetal calf serum for 20 min on ice (Imbach et al., 2000). Fibroblasts were washed and analyzed on a BD FACSCanto II flow cytometer (BD Biosciences, USA) equipped with BD FACSDiva software (BD Biosciences).

LLO and N-linked oligosaccharide (NLO) analysis - The LLO profiles of 1.5 x 10^7 fibroblasts treated for 72 h with either 100 µM ZGA or DMSO were analyzed as described (Haeuptle et al., 2008). The cells were starved for 45 min in fetal calf serum- and Glc-free DMEM (Invitrogen) and metabolically labeled for 60 min by addition of 150 µCi [^{3}H]-Man. LLO were extracted from cell pellets and oligosaccharides were released by mild acid hydrolysis in 0.1 *N* HCl. Glycoproteins recovered from the LLO extraction were denatured and NLO were released by overnight incubation with PNGaseF endoglycosidase (New England BioLabs, USA) (Grubenmann et al., 2002). Oligosaccharides were purified by ion-exchange chromatography on AG1-X2 and AG50W-X8 resins (Bio-Rad, USA) and by hydrophobic chromatography on Supelclean ENVI-Carb 120/400 beads (Supelco, USA) and C_{18} Sep Pak columns and subjected to HPLC analysis.

Statistics - Results were expressed as mean ± SEM. The one-way ANOVA test with Bonferroni's multiple comparison post-test was applied to confirm differences between groups. Significance was accepted for $p<0.05$.

Results

The toxicity of ZGA was first determined by incubating human primary skin fibroblasts for ten days with increasing concentrations from 10 to 500 µM. ZGA was tolerated by fibroblasts up to a concentration of 125 µM. Above that concentration, the rate of cell proliferation slowed down and cell morphology was altered (data not shown). The addition of 100 µM ZGA to healthy control and CDG fibroblasts led to a moderate decrease of cellular cholesterol levels by 15% and 30%, respectively (Fig. 2).

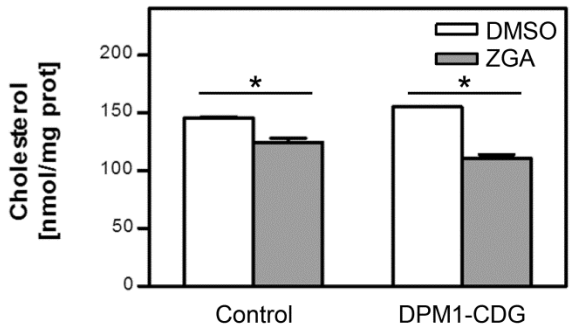

Figure 2: Analysis of cholesterol in healthy control and DPM1-CDG fibroblasts. Steady-state cholesterol levels were determined in fibroblasts by GC/MS after organic extraction. Cholesterol levels relative to the protein amounts of the extracted mock treated cells are shown as white bars and cholesterol levels of ZGA treated fibroblasts are shown as gray bars. Data are represented by mean ± SEM of three independent experiments, * $p<0.05$.

The effect of ZGA on glycosylation was determined by measuring cellular levels of Dol-P, Dol-P-Man, a glycosylphosphatidylinositol (GPI)-anchored model protein, LLO and NLO. The impact of ZGA on Dol-P levels was first addressed on healthy control fibroblasts. After labeling with the fluorochrome 9-anthryldiazomethane, Dol-P levels were quantitated after HPLC separation (Haeuptle et al., 2010). The resulting fluorescent HPLC profiles of untreated cells (Fig. 3A) and of cells treated with 100 µM ZGA for 72 h (Fig. 3B) were compared. The pattern of Dol-P species changed upon ZGA treatment, where the amount of longer C_{100}- and C_{105}-Dol-P increased in ZGA treated fibroblasts (Fig. 3C).

To address the effect of ZGA on various parameters of LLO biosynthesis in CDG, we chose fibroblasts with a deficiency of Dol-P-Man synthase-1 (DPM1) (Imbach et al., 2000), which present low Dol-

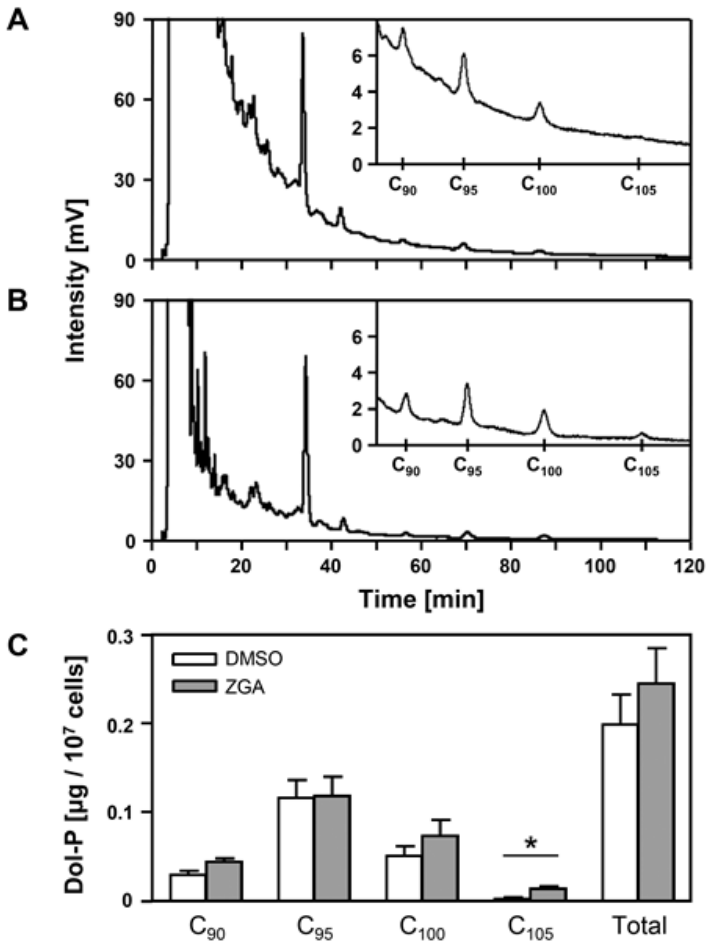

Figure 3: Analysis and quantification of Dol-P levels in mock and ZGA treated control fibroblasts. **(A)** Control cells were grown in the presence of DMSO. Cellular Dol-P were labeled with the fluorophore 9-anthryldiazomethane and separated by HPLC. The enlarged section in the fluorescent profile highlights the separation of the particular Dol-P species. The elution times of mammalian Dol-P standards ranging from C_{90}- to C_{105}-Dol-P are indicated below the section. The internal C_{80}-polyprenol-P standard utilized for quantification eluted at a retention time of 33.5 min. **(B)** The separation of Dol-P from ZGA treated control fibroblasts is presented in the enlarged section, and the respective Dol-P species were assigned like in **(A)**. Quantification was accomplished by comparison with the internal standard hexadecaprenyl-P eluting at 34.2 min. **(C)** The Dol-P levels from four independent HPLC runs were calculated and normalized to 10^7 fibroblasts. White bar represent Dol-P originating from mock treated and gray bars Dol-P from ZGA treated cells. Data are represented by mean ± SEM of four independent experiments, * $p<0.05$.

P-Man levels, an accumulation of the LLO Dol-PP-$GlcNAc_2Man_5$ and the corresponding $GlcNAc_2Man_5$ glycan structure on glycoproteins. Dol-P-Man production was measured after labeling cells with [^{3}H]-Man. The [^{3}H]-Dol-P-Man pool determined in DPM1-

deficient fibroblasts reached 65% of the levels measured in healthy control cells (Fig. 4). When DPM1-deficient fibroblasts were treated with 100 µM ZGA for 72 h, the [^{3}H]-Dol-P-Man levels increased by reaching 120% of normal values. Similarly, when healthy control fibroblasts were incubated with 100 µM ZGA, the levels of [^{3}H]-Dol-P-Man increased by 150% (Fig. 4).

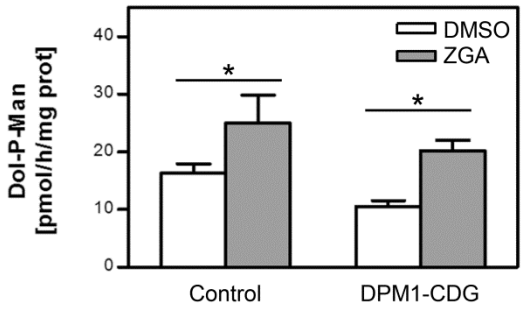

Figure 4: Determination of Dol-P-Man levels in mock and ZGA treated fibroblasts. Dol-P-Man was metabolically labeled in control and DPM1-CDG fibroblasts by incorporation of [^{3}H]-Man and thereafter extracted. The purified lipids were separated by TLC and, on the basis of radiography, the regions corresponding to [^{3}H]-Dol-P-Man were scraped and quantified by liquid scintillation. Normalization of Dol-P-Man levels relative to the protein amounts of the extracted mock treated cells are shown as white bars, while the normalized values of ZGA treated fibroblasts are shown as gray bars. Data are represented by mean ± SEM of four independent experiments, * $p<0.05$.

DPM1 deficiency leads to reduced cell surface expression of GPI-anchored proteins, since Dol-P-Man is required for the assembly of the GPI anchor (Kinoshita et al., 1997). Accordingly, low levels of the GPI-anchored protein CD59 have been detected on the cell surface of DPM1-deficient fibroblasts (Imbach et al., 2000). The addition of ZGA led to increased expression of CD59 in healthy control (Fig. 5A) and DPM1-deficient fibroblasts (Fig. 5B), as monitored by flow cytometry. When DPM1-deficient fibroblasts were treated with 100 µM ZGA for 72 h, the cell surface levels of CD59 returned to the levels observed in untreated control fibroblasts (Fig. 5C). A time course experiment showed that the ZGA effect was maximal by 72 h of treatment, whereas longer periods did not increase CD59 expression further (Fig. 5C). The effect on CD59 expression was also maximal when applying ZGA at 100 µM, but changes were already visible with lower ZGA concentrations (Fig. 5D).

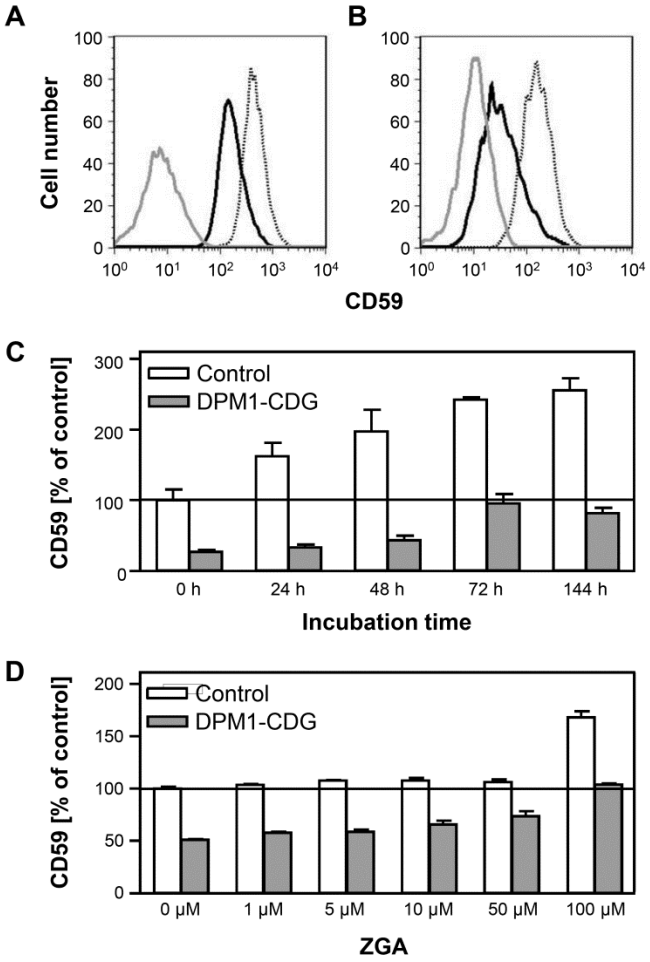

Figure 5: Cell surface expression of GPI-anchored CD59. **(A)** Control fibroblasts were stained with a FITC conjugated α-human CD59 antibody and analysed by flow cytometry. The fluorescent histogram shows unstained cells as gray solid line, mock treated cells as black solid line and ZGA treated cells as black dotted line. **(B)** CD59 expression on DPM1-CDG patient fibroblasts was monitored by flow cytometry. Experimental set up and specimen allocations were like for control cells in **(A)**. **(C)** Control (white bars) and DPM1-CDG fibroblasts (gray bars) were incubated with 100 µM ZGA for varying time periods and the detected CD59 expressions were normalized to CD59 levels of untreated control fibroblasts. **(D)** Different concentrations of ZGA were administered to control (white bars) or DPM1-CDG (gray bars) patient fibroblasts for 72 hours. As in **(C)**, the measured CD59 expressions were normalized to untreated control cells. Data are represented by mean ± SEM of three independent experiments.

The biosynthesis of the LLO Dol-PP-$GlcNAc_2Man_9Glc_3$ requires Dol as carrier of the growing oligosaccharide and as donor substrate for Dol-P-Man and Dol-P-Glc (Kornfeld and Kornfeld, 1985). In normal cells, only the complete LLO Dol-PP-$GlcNAc_2Man_9Glc_3$ can be detected (Fig. 6A). DPM1 deficiency

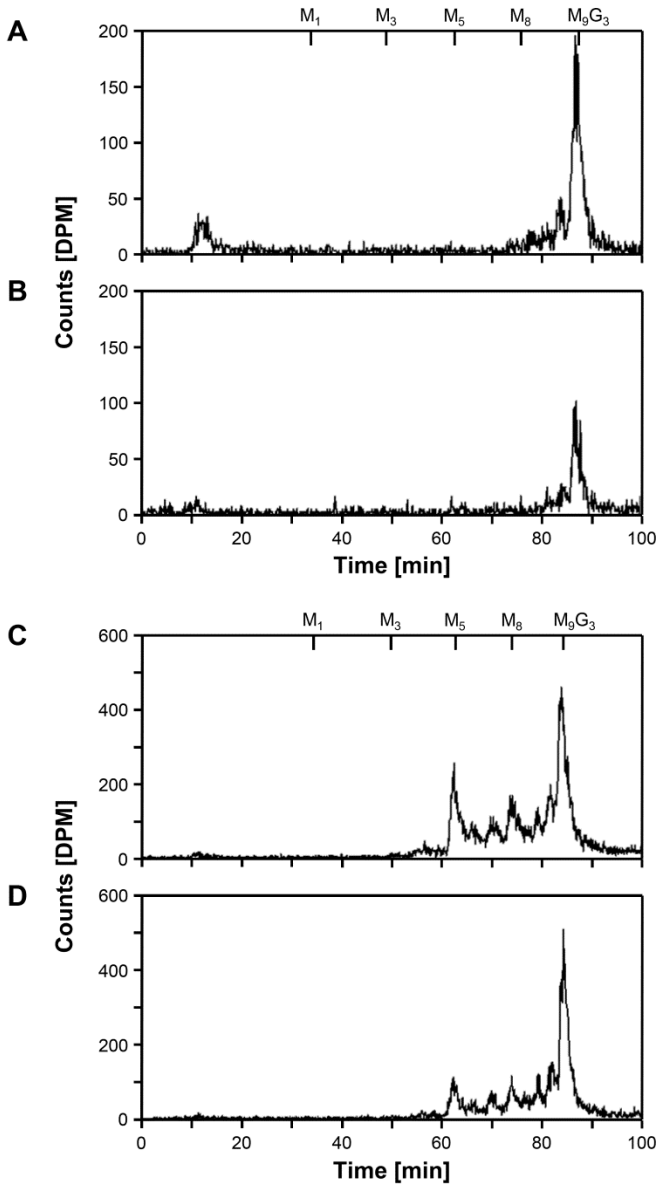

Figure 6: Analysis of ZGA on LLO profiles. Fibroblasts derived from a healthy control **(A** and **B)** or a DPM1-CDG patient **(C** and **D)** were treated for 72 hours either with 100 µM ZGA **(B** and **D)** or DMSO as control **(A** and **C)**. Thereafter, the cells were metabolically labeled with [^{3}H]-Man and the LLO were extracted and hydrolyzed by mild acid treatment. The released oligosaccharides were purified and separated by HPLC. The retention time of standard yeast oligosaccharides ranging from $GlcNAc_2Man_1$ (M_1) to $GlcNAc_2Man_9Glc_3$ (M_9G_3) are indicated at the top of the profiles.

leads to the accumulation of the intermediate LLO Dol-PP-$GlcNAc_2Man_5$ (Fig. 6C) (Imbach et al., 2000; Kim et al., 2000). The amount of this incomplete LLO could be reduced by treatment of DPM1-deficient fibroblasts with 100 µM ZGA. The ratio of the abnormal Dol-PP-$GlcNAc_2Man_5$ peak to the mature Dol-PP-$GlcNAc_2Man_9Glc_3$ peak was decreased from 54% to 17% under ZGA supplementation (Fig. 6D). By comparison, the

addition of 100 µM ZGA to control fibroblasts did not influence the quality of the LLO profile (Fig. 6B).

After transfer from LLO to proteins, the NLO $GlcNAc_2Man_9Glc_3$ is trimmed by glucosidases and mannosidases in the ER (Helenius and Aebi, 2004). The analysis of NLO after [^{3}H]-Man labeling of control fibroblasts showed, as expected, $GlcNAc_2Man_8$, $GlcNAc_2Man_9$ and $GlcNAc_2Man_9Glc_1$ as main oligosaccharide structures (Fig. 7A). In DPM1-deficient fibroblasts, several intermediary oligosaccharide structures ranging from $GlcNAc_2Man_4$ to $GlcNAc_2Man_7$ were found, whereas the normal oligosaccharides $GlcNAc_2Man_8$, $GlcNAc_2Man_9$ and $GlcNAc_2Man_9Glc_1$ were under-represented (Fig. 7C). While ZGA treatment did not affect the NLO profile of control fibroblasts (Fig. 7B), it decreased the occurrence of abnormal N-linked glycans $GlcNAc_2Man_4$ to $GlcNAc_2Man_7$ and increased the amounts of the normal NLO $GlcNAc_2Man_8$, $GlcNAc_2Man_9$ and $GlcNAc_2Man_9Glc_1$ in DPM1-deficient fibroblasts (Fig. 7D). In these cells, the ratio of the pathologic $GlcNAc_2Man_5$ peak to the normal $GlcNAc_2Man_9$ peak was 422% and this ratio was decreased to 143% after addition of ZGA (Fig. 7D). This normalization of the NLO profile demonstrated the beneficial effect of ZGA treatment on N-glycosylation.

Taken together, the present study showed that treatment of human CDG fibroblasts with the squalene synthase inhibitor ZGA stimulated Dol-P biosynthesis and thereby improved the level of N-glycosylation in conditions of limited substrate availability as encountered in DPM1-deficiency. In addition, the supplementation with ZGA resulted in the normalization of the expression of the GPI-anchored protein CD59 on DPM1-deficient fibroblasts.

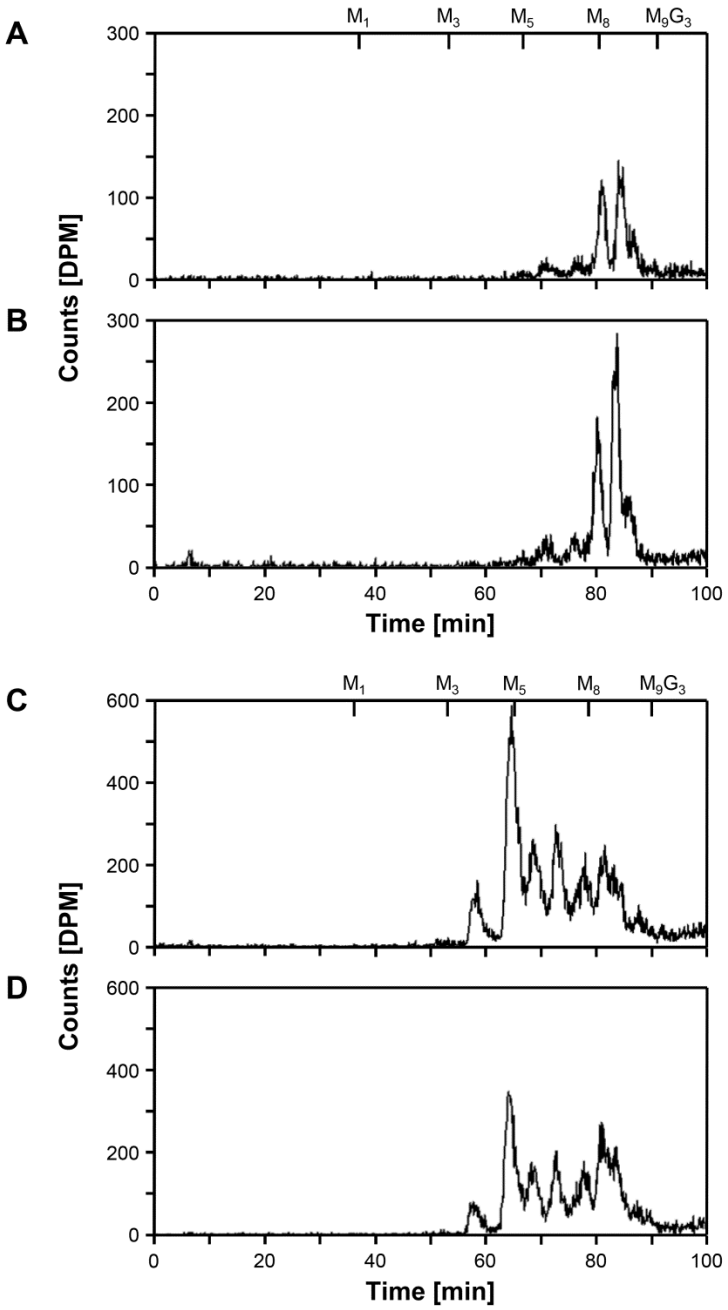

Figure 7: Protein N-glycosylation in ZGA treated fibroblasts. NLO from control **(A** and **B)** and DPM1-CDG patient fibroblasts **(C** and **D)** were separated by HPLC. The protein linked oligosaccharides were prepared by PNGaseF endoglycosidase release from metabolically labeled cells previously treated for 72 hours either with 100 µM ZGA **(B** and **D)** or DMSO as control **(A** and **C)**. The retention times of $GlcNAc_2Man_1$ (M_1) to $GlcNAc_2Man_9Glc_3$ (M_9G_3) are marked at the top of the profiles.

Discussion

Successful treatment of biosynthetic CDG is restricted so far to oral administration of Man to Man-P isomerase deficient (MPI-CDG) patients (Niehues et al., 1998; Westphal et al., 2001). The applied Man could be phosphorylated by hexokinase and allows functional bypassing of the defective isomerization of fructose-6-P to Man-6-P. In the group of Golgi-associated CDG, a deficiency of the Golgi GDP-Fuc transporter (SLC35C1-CDG or leukocyte adhesion deficiency type II) (Lübke et al., 2001) could also be treated by simple supplementation of a monosaccharide. Oral Fuc administration induced the expression of fucosylated glycoproteins and within short terms, the clinical symptoms of a SLC35C1-CDG patient could be relieved (Marquardt et al., 1999). Moreover, a few elementary attempts have been conducted to treat phosphomannomutase-2 deficiency (PMM2-CDG), which forms by far the largest CDG subtype (Freeze, 2009). Mutations in the *PMM2* gene lead to disrupted conversion of Man-6-P to Man-1-P, which acts as precursor of GDP-Man (Matthijs et al., 1997). However, Man-1-P is neither able to diffuse through biological membranes nor does a transport system exist. Thus, it needs chemical modification prior to direct administration to overcome this obstacle (Eklund et al., 2005; Hardre et al., 2007; Rutschow et al., 2002). Membrane permeable Man-1-P analogues were successful in restoring LLO biosynthesis in CDG patient cells, but such prodrugs were toxic, very unstable and had to be applied in high concentrations (Eklund et al., 2005).

Shang and Lehrman discovered a metformin-stimulated Man specific transport activity in human fibroblasts (Shang and Lehrman, 2004). The resulting increased Man uptake was shown to be able to correct artificially induced defects in LLO biosynthesis and protein N-glycosylation in control and PMM2-CDG fibroblasts. However, the observation that the clinical phenotype of PMM2 deficiency could not be treated with dietary Man, which was actually effective in cellular models (Freeze, 2009), renders a therapeutic administration of metformin questionable.

Our approach to increase Dol-P biosynthesis by inhibition of the squalene synthase offers a therapeutic perspective for inherited biosynthetic N-glycosylation defects featuring residual enzymatic activity. Conveniently, ZGA is well tolerated in animal experiments (Baxter et al., 1992; Bergstrom et al., 1993) compared to classical statins, which interfere with various isoprenoid-based biosynthesis pathways and are

associated to adverse effects (Silva et al., 2007). We could show that ZGA decreased cellular cholesterol levels, although only by 15-30%, indicating that membrane properties were likely unaltered due to this treatment. However, we cannot exclude an effect of the lowered cholesterol levels on the formation of glycolipid rafts, in which GPI-anchored proteins partition. Accordingly, the increased expression of the GPI-anchored protein CD59 observed in ZGA-treated cells could be caused by increased Dol-P availability and altered raft distribution. By contrast, the positive effect of ZGA supplementation on Dol-P-Man levels and LLO patterns in DPM1-CDG fibroblasts are unlikely to be related to decreased cholesterol biosynthesis since the ER membrane is low in cholesterol levels (Liscum and Underwood, 1995). Nevertheless, the effects of ZGA on protein modifications, such as farnesylation and geranyl-geranylation, have not been investigated, so that we cannot dismiss an impact of such modifications on the N-glycosylation pathway at this stage.

The present study was based on DPM1-deficient fibroblasts because this form of CDG shows several measurable abnormalities along the biosynthesis of N-glycans and GPI-anchored proteins. By contrast, PMM2-deficiency that represents the largest group of CDG cases (Haeuptle and Hennet, 2009), does not feature accumulating LLO intermediates. Consequently, incomplete oligosaccharides on glycoproteins are usually not encountered in PMM2-deficiency. However, the up-regulation of Dol-P dependent substrates by ZGA may be beneficial in normalizing the glycosylation disorders caused by deficiency of glycosyltransferases catalyzing the attachment of the last four Man and three Glc of the LLO precursor (Kornfeld and Kornfeld, 1985).

Over the last decade, knockout mouse models for PMM2-, MPI- and DPAGT1-deficiency have been generated (DeRossi et al., 2006; Marek et al., 1999; Thiel et al., 2006). These works clearly showed that disruption of LLO biosynthesis lead to early embryonic lethality. In this context, it would be interesting to investigate whether the embryonic lethality of the homozygotes could be lagged to a later stage of development by treating pregnant heterozygous mice with ZGA according to Keller (Keller, 1996). In addition, the generation of viable CDG mouse models, for instance by introduction of selected point mutations, would allow detailed analysis of organ specific effects of ZGA in the context of inherited N-glycosylation deficiencies. This seems to be of particular interest, considering that Keller reported an enormous effect of ZGA on Dol and Dol-P pools in rat livers, but not in other organs such as brain, kidney, intestine or testis (Keller, 1996),

which was similarly observed in different brain cells (Crick et al., 1995). Subcutaneously administered ZGA might preferentially be taken up by mammalian livers via a specific hepatic transport mechanism, which was likewise proposed in other studies (Baxter et al., 1992; Bergstrom et al., 1993). Considering the frequent impairment of liver function in CDG patients (Leroy, 2006), the proposed hepatic transport system for ZGA would suggest that liver N-glycosylation may benefit from treatment with the compound. Along this line, it would be of interest to address the effect of ZGA supplementation in hepatic cell lines, since fibroblasts do not represent suitable cell models to study glycoprotein secretion. The generation of hepatic cell lines with inactivated glycosylation genes will represent an opportunity to study the regulation of N-glycosylation by ZGA and similar compounds.

In conclusion, this study opens new perspectives in developing treatments of glycosylation deficiency by showing that manipulation of the dolichol biosynthesis pathway, as shown here by ZGA administration, represents a valid option.

Footnotes

[a] The abbreviations used are: CDG, Congenital Disorders of Glycosylation; Dol, dolichol; GPI, glycosylphosphatidylinositol; HMG-CoA, 3-hydroxy-3-methyl-glutaryl Coenzyme A; LLO, lipid-linked oligosaccharides; NLO, N-linked oligosaccharides; ZGA, zaragozic acid A

Acknowledgements

We are grateful to Merck & Co., Inc. for the generous providing of zaragozic acid A and to Eric G. Berger for critically reading the manuscript. This work was supported by the Swiss National Science Foundation Grant 31003A-116039 to T. Hennet.

References

Alberts, A.W., J. Chen, G. Kuron, V. Hunt, J. Huff, C. Hoffman, J. Rothrock, M. Lopez, H. Joshua, E. Harris, A. Patchett, R. Monaghan, S. Currie, E. Stapley, G. Albers-Schonberg, O. Hensens, J. Hirshfield, K. Hoogsteen, J. Liesch, and J. Springer. 1980. Mevinolin: a highly potent competitive inhibitor of hydroxymethylglutaryl-coenzyme A reductase and a cholesterol-lowering agent. *Proc. Natl. Acad. Sci. U. S. A.* 77:3957-3961.

Baxter, A., B.J. Fitzgerald, J.L. Hutson, A.D. McCarthy, J.M. Motteram, B.C. Ross, M. Sapra, M.A. Snowden, N.S. Watson, R.J. Williams, and C. Wright. 1992. Squalestatin 1, a potent inhibitor of squalene synthase, which lowers serum cholesterol in vivo. *J. Biol. Chem.* 267:11705-11708.

Bergstrom, J.D., C. Dufresne, G.F. Bills, M. Nallin-Omstead, and K. Byrne. 1995. Discovery, biosynthesis, and mechanism of action of the zaragozic acids: potent inhibitors of squalene synthase. *Annu. Rev. Microbiol.* 49:607-639.

Bergstrom, J.D., M.M. Kurtz, D.J. Rew, A.M. Amend, J.D. Karkas, R.G. Bostedor, V.S. Bansal, C. Dufresne, F.L. VanMiddlesworth, O.D. Hensens, J.M. Liesch, D.L. Zink, K.E. Wilson, J. Onishi, J.A. Milligan, G. Bills, L. Kaplan, M. Nallin-Omstead, R.G. Jenkins, L. Huang, M.S. Meinz, L. Quinn, R.W. Burg, Y.L. Kong, S. Mochales, M. Mojena, I. Martin, F. Pelaez, M.T. Diez, and A.W. Alberts. 1993. Zaragozic acids: a family of fungal metabolites that are picomolar competitive inhibitors of squalene synthase. *Proc. Natl. Acad. Sci. U. S. A.* 90:80-84.

Crick, D.C., J. Suders, C.M. Kluthe, D.A. Andres, and C.J. Waechter. 1995. Selective inhibition of cholesterol biosynthesis in brain cells by squalestatin 1. *J. Neurochem.* 65:1365-1373.

De Praeter, C.M., G.J. Gerwig, E. Bause, L.K. Nuytinck, J.F. Vliegenthart, W. Breuer, J.P. Kamerling, M.F. Espeel, J.J. Martin, A.M. De Paepe, N.W. Chan, G.A. Dacremont, and R.N. Van Coster. 2000. A novel disorder caused by defective biosynthesis of N-linked oligosaccharides due to glucosidase I deficiency. *Am. J. Hum. Genet.* 66:1744-1756.

DeRossi, C., L. Bode, E.A. Eklund, F. Zhang, J.A. Davis, V. Westphal, L. Wang, A.D. Borowsky, and H.H. Freeze. 2006. Ablation of mouse phosphomannose isomerase (Mpi) causes mannose 6-phosphate accumulation, toxicity, and embryonic lethality. *J. Biol. Chem.* 281:5916-5927.

Eklund, E.A., N. Merbouh, M. Ichikawa, A. Nishikawa, J.M. Clima, J.A. Dorman, T. Norberg, and H.H. Freeze. 2005. Hydrophobic Man-1-P derivatives correct abnormal glycosylation in Type I congenital disorder of glycosylation fibroblasts. *Glycobiology* 15:1084-1093.

Elmberger, P.G., I. Eggens, and G. Dallner. 1989. Conditions for quantitation of dolichyl phosphate, dolichol, ubiquinone and cholesterol by HPLC. *Biomed. Chromatogr.* 3:20-28.

Foulquier, F. 2008. COG defects, birth and rise! *Biochim. Biophys. Acta* 1792:896-902.

Freeze, H.H. 2006. Genetic defects in the human glycome. *Nat. Rev. Genet.* 7:537-551.

Freeze, H.H. 2009. Towards a therapy for phosphomannomutase 2 defeciency, the defect in CDG-Ia patients. *Biochim. Biophys. Acta* 1792:835-840.

Grubenmann, C.E., C.G. Frank, S. Kjaergaard, E.G. Berger, M. Aebi, and T. Hennet. 2002. ALG12 mannosyltransferase defect in congenital disorder of glycosylation type lg. *Hum. Mol. Genet.* 11:2331-2339.

Haeuptle, M.A., and T. Hennet. 2009. Congenital Disorders of Glycosylation: an Update on Defects Affecting the Biosynthesis of Dolichol-linked Oligosaccharides. *Hum. Mutat.* 30:1628-1641.

Haeuptle, M.A., A.J. Hülsmeier, and T. Hennet. 2010. HPLC and mass spectrometry analysis of dolichol-phosphates at the cell culture scale. *Anal. Biochem.* 396:133-138.

Haeuptle, M.A., F.M. Pujol, C. Neupert, B. Winchester, A.J. Kastaniotis, M. Aebi, and T. Hennet. 2008. Human RFT1 deficiency leads to a disorder of N-linked glycosylation. *Am. J. Hum. Genet.* 82:600-606.

Hansske, B., C. Thiel, T. Lübke, M. Hasilik, S. Honing, V. Peters, P.H. Heidemann, G.F. Hoffmann, E.G. Berger, K. von Figura, and C. Körner. 2002. Deficiency of UDP-galactose:N-

acetylglucosamine beta-1,4-galactosyltransferase I causes the congenital disorder of glycosylation type IId. *J. Clin. Invest.* 109:725-733.

Hardre, R., A. Khaled, A. Willemetz, T. Dupre, S. Moore, C. Gravier-Pelletier, and Y. Le Merrer. 2007. Mono, di and tri-mannopyranosyl phosphates as mannose-1-phosphate prodrugs for potential CDG-Ia therapy. *Bioorg. Med. Chem. Lett.* 17:152-155.

Helenius, A., and M. Aebi. 2004. Roles of N-linked glycans in the endoplasmic reticulum. *Annu. Rev. Biochem.* 73:1019-1049.

Hülsmeier, A.J., P. Paesold-Burda, and T. Hennet. 2007. N-glycosylation site occupancy in serum glycoproteins using multiple reaction monitoring liquid chromatography-mass spectrometry. *Mol Cell Proteomics* 6:2132-2138.

Imbach, T., B. Schenk, E. Schollen, P. Burda, A. Stutz, S. Grunewald, N.M. Bailie, M.D. King, J. Jaeken, G. Matthijs, E.G. Berger, M. Aebi, and T. Hennet. 2000. Deficiency of dolichol-phosphate-mannose synthase-1 causes congenital disorder of glycosylation type Ie. *J. Clin. Invest.* 105:233-239.

Jaeken, J., and G. Matthijs. 2007. Congenital Disorders of Glycosylation: A Rapidly Expanding Disease Family. *Annu. Rev. Genomics Hum. Genet.* 8:261-278.

Keller, R.K. 1996. Squalene synthase inhibition alters metabolism of nonsterols in rat liver. *Biochim. Biophys. Acta* 1303:169-179.

Kim, S., V. Westphal, G. Srikrishna, D.P. Mehta, S. Peterson, J. Filiano, P.S. Karnes, M.C. Patterson, and H.H. Freeze. 2000. Dolichol phosphate mannose synthase (DPM1) mutations define congenital disorder of glycosylation Ie (CDG-Ie). *J. Clin. Invest.* 105:191-198.

Kinoshita, T., K. Ohishi, and J. Takeda. 1997. GPI-anchor synthesis in mammalian cells: genes, their products, and a deficiency. *J. Biochem.* 122:251-257.

Koga, T., Y. Shimada, M. Kuroda, Y. Tsujita, K. Hasegawa, and M. Yamazaki. 1990. Tissue-selective inhibition of cholesterol synthesis in vivo by pravastatin sodium, a 3-hydroxy-3-methylglutaryl coenzyme A reductase inhibitor. *Biochim. Biophys. Acta* 1045:115-120.

Korner, C., L. Lehle, and K. von Figura. 1998. Abnormal synthesis of mannose 1-phosphate derived carbohydrates in carbohydrate-deficient glycoprotein syndrome type I fibroblasts with phosphomannomutase deficiency. *Glycobiology* 8:165-171.

Kornfeld, R., and S. Kornfeld. 1985. Assembly of asparagine-linked oligosaccharides. *Annu. Rev. Biochem.* 54:631-664.

Leroy, J.G. 2006. Congenital disorders of N-glycosylation including diseases associated with O- as well as N-glycosylation defects. *Pediatr. Res.* 60:643-656.

Liscum, L., and K.W. Underwood. 1995. Intracellular cholesterol transport and compartmentation. *J Biol Chem* 270:15443-15446.

Lübke, T., T. Marquardt, A. Etzioni, E. Hartmann, K. von Figura, and C. Körner. 2001. Complementation cloning identifies CDG-IIc, a new type of congenital disorders of glycosylation, as a GDP-fucose transporter deficiency. *Nat. Genet.* 28:73-76.

Marek, K.W., I.K. Vijay, and J.D. Marth. 1999. A recessive deletion in the GlcNAc-1-phosphotransferase gene results in peri-implantation embryonic lethality. *Glycobiology* 9:1263-1271.

Marquardt, T., K. Luhn, G. Srikrishna, H.H. Freeze, E. Harms, and D. Vestweber. 1999. Correction of leukocyte adhesion deficiency type II with oral fucose. *Blood* 94:3976-3985.

Matthijs, G., E. Schollen, E. Pardon, M. Veiga-Da-Cunha, J. Jaeken, J.J. Cassiman, and E. Van Schaftingen. 1997. Mutations in PMM2, a phosphomannomutase gene on chromosome 16p13, in carbohydrate-deficient glycoprotein type I syndrome (Jaeken syndrome). *Nat. Genet.* 16:88-92.

McTaggart, F., L. Buckett, R. Davidson, G. Holdgate, A. McCormick, D. Schneck, G. Smith, and M. Warwick. 2001. Preclinical and clinical pharmacology of Rosuvastatin, a new 3-hydroxy-3-methylglutaryl coenzyme A reductase inhibitor. *Am. J. Cardiol.* 87:28B-32B.

Muscio, F., J.P. Carlson, L. Kuehl, and H.C. Rilling. 1974. Prequalene pyrophosphate. A normal intermediate in squalene biosynthesis. *J. Biol. Chem.* 249:3746-3749.

Niehues, R., M. Hasilik, G. Alton, C. Körner, M. Schiebe-Sukumar, H.G. Koch, K.P. Zimmer, R. Wu, E. Harms, K. Reiter, K. von Figura, H.H. Freeze, H.K. Harms, and T. Marquardt. 1998.

Carbohydrate-deficient glycoprotein syndrome type Ib. Phosphomannose isomerase deficiency and mannose therapy. *J. Clin. Invest.* 101:1414-1420.

Rutschow, S., J. Thiem, C. Kranz, and T. Marquardt. 2002. Membrane-permeant derivatives of mannose-1-phosphate. *Bioorg. Med. Chem.* 10:4043-4049.

Shang, J., and M.A. Lehrman. 2004. Metformin-stimulated mannose transport in dermal fibroblasts. *J. Biol. Chem.* 279:9703-9712.

Silva, M., M.L. Matthews, C. Jarvis, N.M. Nolan, P. Belliveau, M. Malloy, and P. Gandhi. 2007. Meta-analysis of drug-induced adverse events associated with intensive-dose statin therapy. *Clin. Ther.* 29:253-260.

Swiezewska, E., and W. Danikiewicz. 2005. Polyisoprenoids: structure, biosynthesis and function. *Prog. Lipid Res.* 44:235-258.

Thiel, C., T. Lübke, G. Matthijs, K. von Figura, and C. Körner. 2006. Targeted disruption of the mouse phosphomannomutase 2 gene causes early embryonic lethality. *Mol. Cell. Biol.* 26:5615-5620.

Westphal, V., S. Kjaergaard, J.A. Davis, S.M. Peterson, F. Skovby, and H.H. Freeze. 2001. Genetic and metabolic analysis of the first adult with congenital disorder of glycosylation type Ib: long-term outcome and effects of mannose supplementation. *Mol. Genet. Metab.* 73:77-85.

Yamada, K., S. Abe, T. Suzuki, K. Katayama, and T. Sato. 1986. A high-performance liquid chromatographic method for the determination of dolichyl phosphates in tissues. *Anal. Biochem.* 156:380-385.

Glycoprotein maturation and the UPR

Andreas J. Hülsmeier, Michael Welti and Thierry Hennet

Institute of Physiology, University of Zürich, Winterthurerstrasse 190, CH-8057 Zürich, Switzerland

Running title: N- and O-glycosylation analysis

Methods in Enzymology. 2011;491:163-82.

Corresponding author:

Thierry Hennet

Institute of Physiology

University of Zürich

Winterthurerstrasse 190

CH-8057 Zürich

Tel: +41 44 635 5080

Fax: +41 44 635 6814

E-mail: thennet@access.uzh.ch

Abstract

Glycosylation is a complex form of protein modification occurring in the secretory pathway. The addition of N- and O-glycans affects intracellular processes like the folding and trafficking of most glycoproteins. To better understand the impact of glycosylation in protein folding and maturation, parameters like glycosylation site occupancy and oligosaccharide structure must be measured quantitatively. In the present chapter, we describe current methods enabling the determination of N-glycosylation by assessment of cellular dolichol-phosphate levels, dolichol-linked oligosaccharides and the occupancy of N-glycosylation sites. We also provide detailed methods for the analysis of O-glycosylation, whose role in intracellular protein maturation is often overlooked.

1. Introduction

Glycosylation is a widespread and complex form of modification, which adds signals and specific functions to glycoproteins. N-linked and O-linked glycosylation, which are the main forms of protein glycosylation, are structurally and functionally distinct. N-linked glycosylation is initiated in the endoplasmic reticulum (ER), where the oligosaccharide $GlcNAc_2Man_9Glc_3$ is transferred co-translationally to selected asparagine residues of nascent glycoproteins. While still in the ER, oligosaccharides on glycoproteins are trimmed by glucosidase and mannosidase enzymes to $GlcNAc_2Man_8$. Later in the Golgi apparatus N-linked oligosaccharides undergo further trimming and elongation steps, which contribute to the structural diversity of N-linked glycosylation. In contrast to the co-translational beginning of N-glycosylation, O-linked glycosylation takes place on folded proteins and is initiated by the transfer of monosaccharides to serine and threonine residues. Some forms of O-glycosylation like O-fucosylation (Harris and Spellman, 1993) and O-mannosylation (Lommel and Strahl, 2009) begin in the ER, whereas mucin-type O-glycosylation (Tian and Ten Hagen, 2009) and the biosynthesis of glycosaminoglycan chains (Bishop et al., 2007) begin in the Golgi apparatus.

N-glycosylation is important for the folding and trafficking of many glycoproteins (Helenius and Aebi, 2004). The inhibition of N-linked glycosylation, for example by tunicamycin, results in the accumulation of misfolded proteins in the ER, which is a strong stimulus of the UPR (Shamu et al., 1994). After trimming by glucosidase-I in the ER, N-linked oligosaccharides are bound by the chaperone proteins calnexin and calreticulin, which contribute to the folding of glycoproteins (Ellgaard et al., 1999). Furthermore, N-linked oligosaccharides are also recognized by the EDEM protein, which redirects misfolded proteins from the ER lumen to the cytosol for proteasome-mediated degradation. Another important signal carried by N-linked oligosaccharides is the mannose-6-phosphate epitope, which mediates the recognition and transfer of lysosomal proteins to their target organelle (Dahms et al., 1989).

The most common form of O-glycosylation, i.e. mucin-type glycosylation, does not contribute to glycoprotein folding since it occurs in the Golgi apparatus. However, the trafficking and secretion of some glycoproteins requires proper mucin-type glycosylation, as demonstrated in the case of the hormone FGF23. Deficient initiation of mucin-type O-glycosylation alters the susceptibility of FGF23 to Golgi-localized

proteases, thereby inhibiting the maturation of active FGF23. Mucin-type glycosylation of FGF23 is initiated by the polypeptide N-acetylgalactosaminyltransferase-3 enzyme. Loss of this enzymatic activity leads to the disease tumoral calcinosis, which is also caused by FGF23 deficiency (Chefetz and Sprecher, 2009).

Another example of glycosyltransferase-assisted trafficking is given by the OFUT1 O-fucosyltransferase enzyme. This ER-localized glycosyltransferase adds fucose to the EGF-like repeats of proteins such as Notch and its ligands. Independent from its glycosyltransferase activity, OFUT1 also acts as a chaperone, which is essential for the transfer of Notch from the ER to the Golgi apparatus (Okajima et al., 2005). The contribution of O-linked glycosylation to glycoprotein folding and secretion is much less documented than in the case of N-linked glycosylation. This limited knowledge is certainly related to the technically difficult investigation of O-linked glycan structures. In fact, O-linked glycans are often densely clustered and these glycans cannot be released without significantly altering the polypeptide backbone. The O-glycanase enzyme from *Streptococcus pneumoniae* has a specificity limited to the O-linked disaccharide Gal(β1-3)GalNAc-O. By contrast, N-linked glycans can be conveniently cleaved at the first GlcNAc unit by the N-glycosidase F.

2. N-glycosylation

Proper N-linked glycosylation is required for folding and intracellular trafficking of glycoproteins. Deficiency in the biosynthesis of the precursor of N-glycans or in the processing of N-glycans in the ER can alter glycoprotein folding and induce UPR. The following methods can be applied to identify defects of oligosaccharide assembly and of N-glycosylation site occupancy in target cells.

2.1. Dolichol phosphate analysis

The oligosaccharide core consisting of $GlcNAc_2Man_9Glc_3$ is first assembled on the polyisoprenoid carrier dolichol (Dol). Moreover, dolichol-phosphate (Dol-P) is also part of the glycosylation substrates Dol-P-Man and Dol-P-Glc, which account for the final extension of the oligosaccharide core in the ER. Considering the low levels of Dol-P based structures in cells, a sensitive Dol-P detection can be achieved by labeling with the

fluorescent compound 9-anthryldiazomethane. The procedure was originally described for tissue sample extraction (Elmberger et al., 1989) and we have adapted the method for cultured cells (Haeuptle et al., 2009). Detection of unlabeled Dol-P can also be achieved by negative ion electrospray mass spectrometry (ESI-MS), which, in combination to precursor ion fragmentation, provides detailed information on Dol-P composition and on the saturation state of the α-isoprene unit.

2.1.1. Required materials

Devices and materials

- LaChrom D-7000 HPLC system (Merck), equipped with an Inertsil ODS-3 column (5 µm, 4.6 x 250 mm; GL Sciences Inc., Japan) with a precolumn and a LaChrom 7485 fluorescence detector.

- Nano-flow ESI-ion trap MS (Eksigent nano-LC, 3200 QTRAP-MS, AB/SCIEX)

- C_{18} Sep-Pak and Silica Sep-Pak cartridges (Waters)

Other reagents

- 9-anthryldiazomethane (ADAM) (Sigma-Aldrich)

- C_{80}-polyprenol and C_{95}-Dol-P standards (Larodan Fine Chemicals, Sweden)
- Diazald (Sigma-Aldrich)

- Carbitol (Sigma-Aldrich)

2.1.2. Extraction and purification of Dol and Dol-P

Adherent cells (about 3 x 10^8 cells) are washed in PBS after trypsinization and resuspended in 6 ml of water and then fixed by addition of 6 ml of methanol. The resulting suspension is transferred to a round bottom glass flask and 3 ml of 15 M potassium hydroxide are added for alkaline hydrolysis. An aliquot of the C_{80} polyprenyl-phosphate (e.g. 15 µg) can be added as internal standard for subsequent quantification.

The round bottom flask is attached to a reflux cooler and incubated in a preheated oil bath at 100 °C for 1 h. This alkaline hydrolysis removes carbohydrates from the Dol-P carrier. The resulting lysate is transferred to a glass tube and methanol is added to a total volume of 15 ml. The suspension is mixed with 30 ml of methanol/dichloromethane (1:4, v:v) and incubated at 40 °C for 1 h. Discard the upper phase (methanol) and transfer the lower phase (dichloromethane) containing the extracted lipids to a glass tube suitable for centrifugation. Wash the organic phase with 10 ml of dichloromethane/methanol/water (3:48:47, v:v:v). For phase separation, centrifuge at 6800 x g at room temperature for 10 min and discard the upper phase. Repeat this washing step four times, which ensures the removal of free sugars and salt from the sample. The organic phase is then dried under nitrogen gas.

Dol and Dol-P are purified in two steps using C_{18}- and silica-based chromatography resins. First, equilibrate the C_{18} Sep-Pak cartridge with 5 ml of methanol, followed by 5 ml of chloroform/methanol (2:1, v:v) and 10 ml of methanol/water (98:2, v:v, supplemented with 20 mM phosphoric acid). The dried lipids from the extraction step are dissolved in 400 µl of chloroform/methanol (2:1, v:v) and diluted by adding 10 ml of methanol/water (98:2, v:v) supplemented with 20 mM phosphoric acid. Load the solution onto the C_{18} Sep-Pak cartridge and wash with 20 ml of methanol/water (98:2, v:v, supplemented with 20 mM phosphoric acid). To remove phosphoric acid from the cartridge, wash again with 10 ml of methanol/water (98:2, v:v) devoid of phosphoric acid. Dol and Dol-P can be eluted with 20 ml of chloroform/methanol (2:1, v:v) and collected in a new glass tube. The eluate should be neutralized by adding 100 µl of 25% ammonium hydroxide.

The second purification step through Silica Sep-Pak cartridges allows the separation of Dol from Dol-P. First, equilibrate the cartridge with 10 ml of chloroform/methanol/water (10:10:3, v:v:v) and 40 ml of chloroform/methanol (2:1, v:v, in 0.5% ammoniumhydroxide). Place a new glass tube to collect the dolichol fraction, which will be in the flowthrough of the chromatography. Apply the neutralized eluate from the previous step onto the Silica Sep-Pak cartridge. Rinse the glass tube of the eluate with 10 ml chloroform/methanol (2:1, v:v, in 0.5% ammoniumhydroxide) and load it onto the Silica cartridge. Repeat the process with10 ml chloroform/methanol (2:1, v:v, in 0.5% ammonium hydroxide). Elute Dol-P into another glass tube by applying

30 ml chloroform/methanol/water (10:10:3, v:v:v) onto the Silica cartridge. Dry the Dol and Dol-P fractions under nitrogen gas at 50 °C.

2.1.3. Anthryldiazomethane labeling of Dol-P

Dol-P labeling is made in two steps. First, Dol-P is dimethylated and then selectively demethylated to produce mono methylated <mono-methylated, monomethylated?> Dol-P (Dol-P-Me). The procedure yields an enhanced fluorescence signal when labeling Dol-P-Me with 9-anthryl derivatives (Yamada et al., 1986). The second step is the derivatization of Dol-P-Me with 9-anthryldiazomethane (ADAM). We use the diazomethane generator system (Sigma-Aldrich) for the dimethylation of Dol-P[1]. It consists of two glass tubes: a small internal tube placed inside a larger outer tube. The dried Dol-P fraction is first dissolved in 1 ml of diethylether and transferred into the large outer glass tube of the diazomethane generator. The glass that contained the Dol-P fraction is washed twice with 1 ml of diethylether, which is added to the outer tube of the diazomethane generator. To produce diazomethane, add 0.367 g Diazald (explosive!) to the inner tube of the diazomethane generator system. Dissolve Diazald by addition of 1 ml of Carbitol. Assemble the two parts of the diazomethane generator system and immerse it into an ice bath. Make sure that the generator system is sealed. Using a syringe, carefully add 1.5 ml of 37% potassium hydroxide dropwise to the inner tube of the diazomethane generator system. Add few drops first and wait until the reaction starts, as seen by formation of gaseous diazomethane in the Diazald solution. In this way, the content of the inner tube is prevented from spilling into the outer tube. Then, carefully add the rest of the potassium hydroxide. Gently mix the reactants and incubate the reaction for 1 hour in the ice bath. The diethylether phase containing Dol-P should turn yellow by then, indicating an excess of diazomethane. After disassembly of the diazomethane generator, leftover reactants can be neutralized by addition of 0.15 g of silicic acid to the inner tube.

The outer tube should be sealed with parafilm and left for 2 h at room temperature. The Dol-P-Me_2 solution is transferred to a glass extraction tube and dried under nitrogen gas. To selectively demethylate Dol-P-Me_2, dissolve it in 4 ml of *tert*-butylamine and

[1] Diazomethane is very toxic in contact with eye, skin or by inhalation. Diazomethane may explode in contact with sharp edges and when heated beyond 100 °C.

incubate at 70 °C for 14 h. Make sure to seal the extraction tube completely to prevent the loss of *tert*-butylamine. Then, evaporate *tert*-butylamine under nitrogen gas and dissolve Dol-P-Me in 1.5 ml of 0.1 M hydrochloric acid adjusted to pH 3 with sodium hydroxide. Extract Dol-P-Me twice with 3 ml of diethylether and dry the combined extracts under nitrogen gas. Labeling is performed in 1 ml of diethylether saturated with ADAM. Prepare the ADAM solution in a separate glass tube by gradually adding the reddish ADAM powder to 0.7 ml of diethylether until saturation. Take 600 µl of the yellowish ADAM solution and add it to the dried Dol-P-Me fraction. Incubate the labeling reaction at 4 °C in the dark for 8h. After drying under nitrogen gas, dissolve the reaction products in 2.4 ml of n-hexane. Wash the hexane phase three times with 1.8 ml of acetonitrile. Discard each time the acetonitrile lower phase. Dry the n-hexane phase under nitrogen gas. The ADAM labeled Dol-P-Me fraction can be dissolved in acetonitrile/dichloromethane (3:2, v:v) for HPLC analysis.

2.1.4. HPLC analysis of fluorescently labeled Dol-P

ADAM-derivatized Dol-P are separated by HPLC using an Intertsil ODS-3 column and applying isocratic elution according to Yamada *et al.* (Yamada et al., 1986). The mobile phase consists of acetonitrile/dichloromethan (3:2, v:v) supplemented with 0.01% diethylamine. ADAM fluorescence is detected at 412 nm using an excitatory wavelength of 365 nm.

2.1.5. Negative ion electrospray mass spectrometry of Dol-P

Purified Dol-P can also be directly analyzed by ESI-MS (Haeuptle et al., 2009) without derivatization. The dried Dol-P sample is first dissolved in 90% acetonitrile, 10% n-hexane, containing 0.01% diethylamine, and then vortexed and centrifuged to eliminate any particulate matter. The nano-flow system consists of an injector fitted with a 10 µl fused silica capillary loop, coupled in-line to a nano-flow pump and emitter tip of a nano-electrospray ion source via 20 µm ID fused silica capillary tubing. An aliquot of the sample is loaded into the injector loop and switched in-line to the nano-flow system, introducing the sample directly into the ion source with the dissolution solvent at a flow rate of 400 nl/min. Using a 3200 AB/Sciex QTRAP MS, all mass spectra are acquired manually in the Enhanced MS scan mode (ion trapping mode), scanning from m/z 1000

to m/z 1700 at a scan rate of 1000 amu/sec and a step size of 0.06 amu. The curtain gas flow is maintained at 10 psi, collision gas pressure at 4 x 10e-5 torr (High), interface heater temperature at 150 °C, declustering potential at -200V, entrance potential at -10V, collision energy at -10V and the ion spray voltage is varied between -2400 and -4500 V, depending on the condition of the emitter needle. Fragment ion spectra of selected Dol-P precursor masses are acquired in the Enhanced Product Ion mode (EPI mode, fragmentation in ion trapping mode) with the collision energy set to -100V and linear scanning starting at m/z 100. Extensive rinsing of the nano-flow system in between sample injections is necessary to avoid cross contamination.

2.2. Dolichol-linked oligosaccharide analysis

Defects of Dol-linked oligosaccharide (DLO) assembly decrease the availability of the mature Dol-PP-$GlcNAc_2Man_9Glc_3$ core for glycosylation of acceptor Asn sites on nascent glycoproteins (Hülsmeier et al., 2007). Such a DLO shortage leads to the non-occupancy of N-glycosylation sites, which impacts on protein folding and trafficking (Helenius and Aebi, 2004). DLOs are conveniently analyzed either by metabolic labeling using [^{3}H]-mannose, or by derivatization with the fluorochrome 2-aminobenzamide (2AB). The extraction, hydrolysis, and purification procedure of DLOs is common to both methods.

2.2.1. Required materials

Chemicals

In addition to the solvents mentioned in section 0, you need the reagents listed below.

- ^{3}H-labeled D-mannose, 5 mCi (Hartmann Analytics, Germany)
- 2-Propanol (Sigma-Aldrich)
- Trizma base (Sigma-Aldrich)
- 2-Aminobenzamide (Sigma-Aldrich)

- Sodium cyanoborohydride $NaBH_3CN$, (Sigma-Aldrich)

Devices and other materials

- Dowex AG 1 x 4, Dowex AG 50 x 8 (Bio-Rad)

- ENVI-C_{18} and ENVI-Carb resin (Supelco)

- Ultrafree-MC centrifugal filter devices (Millipore, Cat. No.: UFC30LH25)

- Supelcosil LC-NH2 column, 5 µm particle size, 250 x 4.6 mm (Supelco)

- Scintillation flow monitor FLO-ONE A-525 (Packard)

2.2.2. [^{3}H]-labeling of DLOs

Approximately 2 x 10^8 are washed three times with PBS to remove Glucose from the medium. Cells are then incubated in DMEM without serum and glucose at 37 °C for 45 min. After this starving step, [^{3}H]-mannose (125 µCi / 10^8 cells) is added to the cells, which are incubated further at 37 °C for 1 h.

2.2.3. Extraction of DLOs

The labeling medium is aspirated and cells are washed quickly with 13 ml of ice-cold PBS. Cells are then fixed by adding 11 ml of ice-cold methanol/0.1 M Tris-HCl (8:3, v:v) and collected by scraping when dealing with adherent cells. The cell suspension is transferred to a 50 ml conical tube and 12 ml of chloroform are added. After vigorous mixing using a vortex, the suspension is centrifuged at 6000 x g for 10 min. The upper methanol phase and the lower chloroform phases are discarded, while the interface precipitate is kept for further extraction of DLOs. To this end, add 3 ml of chloroform/methanol/water (10:10:3, v:v:v), vortex for 2 min and spin at 6000 x g for 10 min. Transfer the supernatant to a glass extraction tube. Repeat the extraction three times using 2 ml of chloroform/methanol/water (10:10:3, v:v:v). Then dry the extracted DLOs under nitrogen gas.

2.2.4. Hydrolysis and purification of oligosaccharides

Acid hydrolysis is used to release the oligosaccharide from the lipid carrier. For this, incubate the extracted DLOs in 2 ml of 0.1 M hydrochloric acid (in 50% 2-propanol) at 50 °C for 1 h, then neutralize by adding 1 ml of 0.2 M NaOH. To purify oligosaccharides, prepare a disposable chromatography column with 1ml of Dowex AG 1x4 resin, followed by 0.6 ml of Dowex AG 50x8 resin. Equilibrate the column with 20 ml of 30% 2-propanol and apply the 3 ml hydrolyzate, then wash with 3 ml of 30% 2-propanol. Collect the flowthrough (6 ml total) into a new glass tube and evaporate under nitrogen gas. A second column system is used to further purify the DLOs. Prepare a column with 0.2 ml of ENVI-C_{18} resin and 1 ml of ENVI-Carb 120/400 resin. Place a C_{18} Sep-Pak cartridge on top of the prepared column. Wash the system with 5 ml of 100% methanol, 5 ml of 100% acetonitrile and 5 ml of water/acetonitrile/0.1 M ammonium acetate. Finally, equilibrate with 9 ml of 2% acetonitrile/0.1 M ammonium acetate. Resuspend the dried oligosaccharide sample in 1 ml of acetonitrile/0.1 M ammonium acetate and apply it onto the column. Wash the sample vial with 1 ml of acetonitrile/0.1 M ammonium acetate, which is then loaded onto the column. Make sure that the lower ENVI resin column does not run dry during the loading process. Wash the column system with 9 ml of acetonitrile/0.1 M ammonium acetate. To elute DLOs, add 6 ml of water/acetonitrile (3:1, v:v) and collect the eluate in a new glass tube. The pure oligosaccharides are then dried under nitrogen gas.

2.2.5. HPLC analysis of [^{3}H]-labeled oligosaccharides

A Supelco LC-NH2 normal phase column (including a LC-NH2 guard column) and a two solvent system are used for HPLC separation (Zufferey et al., 1995). Prepare acetonitrile/water (7:3, v:v) and acetonitrile/water (1:1) as mobile phases. Dissolve the purified oligosaccharides in 50-100 µl water for injection. The separation is carried out by running a gradient from acetonitrile/water (7:3, v:v) to acetonitrile/water (1:1) over 75 min at a flow rate of 1 ml/min. The [^{3}H]-labeled oligosaccharides are detected using a flow scintillation detector. When the level of [^{3}H]-incorporation is too low for detection by flow scintillation, fractions of the HPLC run can be collected and measured separately in a scintillation counter (Müller et al., 2005). While more time consuming, the latter detection yields a superior signal to noise ratio.

2.2.6. 2-aminobenzamide labeling of DLOs

The labeling of oligosaccharides with 2-aminobenzamide (2AB) is performed according to Bigge *et al.* (Bigge et al., 1995). For 2AB labeling, DLOs are extracted as described under section 2.2.3 and oligosaccharides are purified as outlined under section 2.2.4. Dried oligosaccharides are resuspended in 200 µl water/acetonitrile (3:1, v:v) and transferred to a 1.5 ml, screw cap Eppendorf tube, where they are dried again. The 2AB labeling reagent is prepared by dissolving 24 mg 2AB in 500 µl acetic acid/DMSO (3:7, v:v) and adding 31 mg sodium cyanoborohydride, thereby achieving a 0.35 M 2AB and 1 M sodium cyanoborohydride solution. Add 20 µl of the labeling reagent to the dried oligosaccharides, mix by vortexing and incubate at 65 °C for 2 h. After cooling, add 380 µl acetonitrile to the sample. Excess labeling reagent is removed using the paper disk clean up procedure (Müller et al., 2005).To this end, punch paper disks from a Whatman 3MM paper using an office hole puncher. Place two paper disks in a centrifugal filter device and wash with 450 µl of water by spinning 30 s at 2000 x g. Wash the filter twice with 450 µl 95% acetonitrile and load the labeled samples. Let the sample pass through the paper disks without spinning the filter device. Wash six times with 450 µl 95% acetonitrile followed by a quick spin at 2000 x g. Elute the labeled oligosaccharides by applying three times 50 µl of water and spinning briefly at 2000 x g.

2.2.7. HPLC analysis of 2AB-labeled oligosaccharides

To separate 2AB-labeled oligosaccharides, we have adapted the procedure of Royle *et al.* (Royle et al., 2002) using a three buffer solvent system (Grubenmann et al., 2004). We use a GlykoSep-N column maintained at 30 °C. Solvent A consists of 80% acetonitrile with 10 mM formic acid (pH 4.4) and solvent B of 40% acetonitrile with 30 mM formic acid (pH 4.4). The 50 mM formic acid stock solution is adjusted to pH 4.4 with ammonium hydroxide. Solvent C is 0.5% formic acid (pH is not adjusted). The gradient is run from 100% solvent A to 100% solvent B over 160 min at a flow rate of 0.4 ml/min. A transition from 100% solvent B to 100% solvent C follows within 2 min at a flow rate of 1 ml/min.

2.3. N-glycosylation Site Occupancy

Most defects of N-glycosylation result in partial occupancy of N-glycosylation sites on proteins. The quantitative analysis of glycosylation site occupancy is not trivial because glycosylated glycosylation sites usually ionize less efficiently than native peptides and it is not feasible to synthesize adequate standard glycopeptides for quantification purposes. Due to the structural microheterogenity of glycopeptides the relatively low sensitivity in detection is further compromised. Therefore, we developed a strategy to simplify the analysis and quantification of glycosylation site occupancy by deglycosylating the N-linked glycopeptides with N-glycosidase F. As an example, we describe here the analysis of human serum transferrin, which carries two N-glycans at Asn_{413} and Asn_{611}. We showed previously that Asn_{611} glycosylation is most sensitive to cellular stress imposed by congenital disorders of glycosylation or alcohol abuse (Hülsmeier et al., 2007). Serum transferrin is immune-affinity purified from 5 µl serum, proteolytically digested and N-glycans are removed by digestion with N-glycosidase F, which converts the corresponding glycosylated Asn to Asp. N-glycosidase F digestion in buffer constituted with isotopic water ($H_2{}^{18}O$) leading to the incorporation of ^{18}O into the respective Asp, which allows to monitor for potential spontaneous deamination of unoccupied Asn prior to digestion with N-glycosidase F. The inclusion of isotopic labeled standard peptide enables sensitive and accurate quantitation of deglycosylated versus unoccupied glycosylation sites. The generated glycosylation sequon peptides are then analyzed by liquid chromatography multiple reaction monitoring mass spectrometry (LC-MRM-MS)[2]. We are using a nanoflow LC (Eksigent) coupled to a hybrid type QTRAP-MS (ABSciex 3200 QTRAP-MS) equipped with a nano-electrospray ionization source. With this instrumentation the triple quadrupole mode MRM-MS can be combined sequentially with product ion scanning in ion trapping mode, or in a MRM signal induced product ion scanning mode. MRM has the advantage that selected fragment transitions are measured resulting in high specificity, sensitivity and reproducible signals for quantitation over a wide range of signal intensities. In our setup, the product ion scanning serves as an additional scanning mode to confirm the sequence of the peptide ion selected in the first quadrupole ion filter.

[2] MRM is also referred to as single reaction monitoring mass spectrometry (SRM MS) and can be considered synonymous to MRM.

2.3.1. Required devices and materials

- Multiple Affinity Removal LC Column, 4.6 x 50 mm, with proprietary buffer system (MARS LC column “Human 6” or custom made “Human 3” for IgG, transferrin and antitrypsin, Agilent Technologies)

- Iodoacetamide (Sigma Ultra grade)

- Endoproteinase Asp-N (Roche Diagnostics GmbH)

- Trypsin (Roche Diagnostics GmbH, proteomics grade)

- N-Glycosidase F (Roche Diagnostics GmbH)

- Aprotenin (Roche Diagnostics GmbH)

- 20 mM ammonium bicarbonate, dissolved in 97 atom % $H_2{}^{18}O$, Cambridge Isotope Laboratories Inc.)

- Custom synthesized, isotope labeled peptides (≥90% purity, HeavyPeptide Basic kit, Thermo Electron Corp.)

- Multiple reaction monitoring- (MRM-) capable nano-LC-MS system

- C_{18} PepMap 100 trap column (300-µm inner diameter × 5 mm, Dionex)

- C_{18} PepMap100 column (75-µm inner diameter × 15 cm, 3 µm, 100 Å, Dionex)

2.3.2. Purification of transferrin

A sample aliquot containing transferrin corresponding to 5 µl human serum is diluted ten times with Agilent buffer A[3] and loaded onto the MARS column according to the manufacturer instructions. Transferrin will be eluted from the column in one step with 100% Agilent buffer B. The chromatography can be monitored by UV absorption at 280 nm and the transferrin containing peak fraction is collected. The eluate is desalted and concentrated by TCA precipitation. The samples are cooled on ice and adjusted to 12% TCA by adding 0.136 volumes of 100% TCA. The samples are kept on ice for 30 min or ideally at -20°C overnight and centrifuged for 30 min at 14000 x g. The supernatants are discarded and the pellet is washed twice with 300 µl ice-cold (-20 °C) acetone. Centrifuge for 15 min at 4 °C and 14000 x g each time after adding the acetone.

2.3.3. Proteolytic digestion and deglycosylation of glycopeptides

The TCA precipitated protein pellet is dissolved by sonication in 250 µl of 0.57 M Tris-HCl, pH 8.5, 50 mM DTT (1M DTT diluted 20-fold with 0.6 M Tris-HCl, pH 8.5). Proteins are incubated for 5 min at 80°C, cooled to room temperature and cysteine residues are alkylated by adding 63 µl of 1M iodoacetamide (5-fold excess over DTT, freshly prepared). The samples are incubated at room temperature in the dark for 40 min and subsequently desalted by TCA precipitation (see section 2.3.2). The alkylated proteins are re-dissolved in 50 µl of 20 mM ammonium bicarbonate, containing 10% acetonitrile. Then 0.5 µg of endoproteinase Asp-N and 0.5 µg of trypsin are added and the sample is incubated at 37°C for 16 h. Proteolysis is minimized by heating the sample for 5 min at 80°C, adding 0.5 µmol EDTA and 100 µg aprotinin. Then 8 pmol of each standard peptide is added and the sample is lyophilized overnight. The sample is re-dissolved in 50 µl of 20 mM ammonium bicarbonate in 95 atom % $H_2{}^{18}O$, 1.5 units of N-Glycosidase F (dissolved in 95 atom % $H_2{}^{18}O$) is added and the sample is digested at 37°C for 8 h. The duration of the N-Glycosidase F digestion was empirically optimized and it is recommended to keep these conditions to avoid sample degradation or incomplete N-Glycosidase F digestion. The reaction is stopped by heat inactivation at 80 °C for 5 min.

[3] Buffers A and B are supplied by Agilent together with the MARS column and their composition is proprietary. Therefore, we name these buffers “Agilent buffer A” and “Agilent buffer B”, respectively.

One tenth of the sample is adjusted to 20 µl of 0.1% formic acid in 2% acetonitrile and filtered through a 0.22 µm centrifugal filter device.

2.3.4. Liquid chromatography multiple reaction monitoring mass spectrometry

The sample is loaded on the trap column and the column is washed with 60 µl of 0.1% formic acid, 2% acetonitrile. After washing, the trap column is switched in line to the PepMap column and a binary gradient at 250 nl/min is applied with Buffer A 0.1% formic acid, and buffer B 80% ACN containing 0.1% formic acid. Buffer B is held at 14% for 3 min, increased to 54% over 102 min and to 100% over 8 min, held at 100% for 12 min, and decreased to 14% over 12 min, and the column is re-equilibrated at 14% buffer B for 16 min. The Asn413 peptides elute between 8 and 14 minutes and the Asn611 peptides elute between 22 and 34 minutes retention time. The transferrin peptides containing N-glycosylation sites can be detected by multiple reaction monitoring mass spectrometry using the parameters listed under table 1.

2.3.5. Calculation of the N-glycosylation site occupancies

The average counts per second (cps) for each MRM transition are calculated by integrating the counts over the time of peak elution with the instrument acquisition software. The molar relative response factor (MRRF) for each peptide sequence is calculated by dividing the cps of the target peptide to the cps of the corresponding standard peptide.

$$MRRF = \frac{cps_{\text{Target peptide}}}{cps_{\text{Standard peptide}}}$$

The percentage of site occupancies is calculated as follows:

$$\%\ at\ Asn_{611} = \frac{MRRF_{DVT}}{MRRF_{DVT} + MRRF_{NVT}} \times 100$$

$$\%\ at\ Asn_{413} = \frac{MRRF_{DK} + MRRF_{DKS}}{MRRF_{DK} + MRRF_{DKS} + MRRF_{NK} + MRRF_{NKS}} \times 100$$

3. O-glycosylation

Mucin-type glycosylation is initiated in the Golgi apparatus and is therefore not directly involved in the UPR. However, mucin-type O-glycosylation is involved in the intracellular processing of glycoproteins and contributes to their stability at the cell surface.

3.1. Release of O-glycans by the β-elimination reaction

O-glycans linked to the hydroxyamino acids Ser or Thr can be released by mild alkali treatment. This mild alkali treatment induces the β-elimination reaction, releasing O-linked carbohydrates from the β-carbon of Ser or Thr and leads to the formation of 2-aminopropenoic acid or 2-amino-2-butenocic acid, respectively (Figure 1). A decrease of Ser or Thr after mild alkali treatment can be monitored by amino acid analysis, providing further information about the presence of O-glycosylation and the hydroxyamino acid involved in the O-glycosyl linkage (Hülsmeier et al., 2010; Hülsmeier et al., 2002). The released O-glycans are unstable under alkaline conditions and undergo stepwise degradation reactions termed "peeling reaction". A second β-elimination reaction occurs at the reducing end GalNAc residue, resulting in the formation of a furanosyl compound, the Morgan Elson chromogen (Figure 1). The "peeling reaction" can be minimized by including sodium borohydride ($NaBH_4$) to the reaction mixture, thereby reducing the aldehydic group of GalNAc to the corresponding primary alcohol N-acetylgalactosaminitol (GalNAc-ol). GalNAc-ol is stable under alkaline conditions. Further GalNAc can be isotopically labeled by using either sodium borodeuterite ($NaBD_4$) or sodium borotritiate as reducing agents. A 2:8(mol:mol) mixture of $NaBH_4$ and $NaBD_4$ can be used, which introduces a "fingerprint" isotope distribution into the O-glycans, facilitating the identification of O-glycans in MALDI-MS and alleviating the assignments of fragmentation ion spectra by marking the reducing end C1 carbohydroxy group (Hülsmeier et al., 2002).

3.1.1. Required devices and materials

- Sodium borohydride, sodium borodeuterite (Sigma)

- Sodium hydroxide, purest available grade (Sigma)

- Clean glass rod and glass tube

- Methyl iodide (ReagentPlus, 99.5%, Sigma-Aldrich)

- sodium thiosulphate (Sigma)

- 2,5-dihydroxybenzoic acid (Fluka)

3.1.2. Reductive β-elimination

The glycoprotein sample (1 mg or less) is lyophilized in a 1.5 ml screw cap polypropylene vial and dissolved in 200 µl freshly prepared 0.1 M sodium hydroxide, containing 0.2 M $NaBH_4$ and 0.8 M $NaBD_4$ (prepared by mixing 1M $NaBH_4$ and 1M $NaBD_4$ solutions 2:8 by volume). The sample is incubated at 37°C for 24 h. Then further 100 µl of 0.1 M sodium hydroxide, containing 0.2 M $NaBH_4$ and 0.8 M $NaBD_4$ are added and incubation continues for further 48 h at 37°C. The reaction is stopped by carefully adding acetic acid until gas development ceases. The sample will be acidified to approximately pH 4.

3.1.3. Purification of the β-eliminated O-glycans

A C18 Sep-Pak cartridge is conditioned with 5 ml methanol, 5 ml propanol and equilibrated with 2 times 5 ml 1% acetic acid. A 0.6 ml Dowex AG50W-X12 column is conditioned with 3 times 5 ml 4 M HCl and washed with water until the flow through becomes neutral. The Sep-Pak cartridge is mounted on top of the Dowex column and both columns are equilibrated with 3 times 5 ml of 1% acetic acid. The β-elimination products are passed through the combined columns and the columns are washed twice with 2 ml of 1% acetic acid. The flow through is collected into a glass vial and dried under vacuum evaporation. Residual boric acid is removed by co-evaporation twice with 250 µl 1% acetic acid in methanol and twice with 250 µl methanol. Residual acetic acid is removed by two evaporations with 50 µl of toluene.

3.1.4. Permethylation

The permethylation derivatization is carried out according to the NaOH method (Ciucanu and Kerel, 1984). The purified O-glycans are dried from 100 µl of 10 mM triethylamine to improve the solubility of negatively charged glycans as triethylamine salts in dimethyl sulfoxide (DMSO). Then, 50 µl DMSO is added and the reaction vial is agitated for 20 min. A 120 mg/ml slurry of NaOH in DMSO is prepared by crushing NaOH pellets with a glass rod in a glass tube. The NaOH will not dissolve completely and precipitate. Mixing of the slurry is required prior application to the derivatization reaction. A 50 µl aliquot of the NaOH/DMSO slurry is added to the reaction vial containing the O-glycans and the vial is shaken for additional 20 min. Then, 10 µl of methyl iodide are added twice, and the vial is agitated for 10 min after each addition, followed by a final addition of 20 µl of methyl iodide and agitation of the vial for further 20 minutes. Permethylated glycans are extracted by adding 250 µl of chloroform and 500 µl of 1 M sodium thiosulphate. The vial is agitated thoroughly and the liquid phases are separated by centrifugation. The aqueous phase is discarded and the chloroform phase, containing the permethylated O-glycans is washed 10 times with 1 ml of water. The chloroform phase is vacuum dried and the permethylated O-glycans are re-dissolved in 50 % acetonitrile for application to MALDI-mass spectrometry (MADLI-MS).

3.1.5. MALDI-MS

The MALDI matrix is prepared by dissolving 10 mg 2,5-dihydroxybenzoic acid (DHB) in 1 ml of 50 % acetonitrile, containing 1 mM sodium chloride (Hülsmeier et al., 2010). Aliquots of the permethylated O-glycans are mixed on the MALDI plate with DHB matrix 1:1 (v:v) and allowed to dry at room temperature. The dried spots are re-crystallized by applying less than 0.1 µl of ethanol. A 10 µl pipette tip is dipped into ethanol and some solvent will be taken up by capillary force. Ethanol outside the tip is evaporated by waving the tip in the air for a few seconds. Then the tip is placed over the dried DHB spot, that the ethanol solvent just touches the MALDI plate surface. The DHB crystals will dissolve quickly and are left to air dry. As a result an even layer of DHB crystals will be formed, permitting sensitive detection of the analytes. The re-crystallization can be repeated, if necessary. Additional DHB matrix can be added, if difficult samples are to be analyzed. MALDI mass spectra are recorded in positive ion mode and glycans are mainly

detected as their sodium ion adducts, due the presence of 1 mM sodium chloride in the DHB matrix.

3.2. Release of O-glycans by hydrazinolysis

Releasing O-glycans by hydrazinolysis has the advantage, that the glycans are liberated with a free reducing end saccharide. This allows subsequent labeling with fluorophores like 2AB or anthranilic acid, facilitating high resolution chromatographic separation combined with unparalleled sensitive fluorescence detection (see section 2.2.6-2.2.7, Figure 2). It is important for this reaction to occur under anhydrous conditions and that the sample is free of salt, metal ions, detergent, dyes and stains. The reaction mechanism during hydrazinolysis has not been elucidated so far. However, an initial formation of a hydrazone derivative with concomitant release of water seems to be likely. After re-N-acetylation of the released glycans, acetohydrazone derivatives are formed and O-glycans in unreduced form can be recovered after passage through cation exchange resin and the addition of Copper-(II)-acetate in mild acid (Patel et al., 1993).

3.2.1. Required devices and materials

- Water and methanol rinsed, oven dried 250 µl glass syringe
- Glass reaction vials
- Lyophilizer
- Pure anhydrous hydrazine (Ludger Ltd, UK)
- Ice cold, saturated sodium bicarbonate solution
- Acetic acid anhydride (Sigma)
- Dowex AG50 [$^{+}$H-form] resin (Bio-Rad)

- Copper-(II)-acetate (Sigma)

- Supelclean™ ENVI-18 resin (Sigma)

3.2.2. Hydrazinolysis

The glycoprotein sample is dialyzed against 0.1% TFA and transferred to a clean glass reaction vial. The sample is lyophilized extensively for one to three days, depending on the amount of protein (up to 5 mg protein). Then, anhydrous hydrazine is added immediately using a glass syringe, pre-rinsed with hydrazine. Hydrazine is added in excess to the sample to give a less than 5 mg protein per ml hydrazine solution. The reaction vessel is capped securely and mixed gently to bring the majority of sample into solution. The sample is transferred in a heating block at 60 °C and incubated for 5 h. The sample is cooled to room temperature and vacuum dried or lyophilized. Residual hydrazine can be removed from the sample by three times re-drying from 100 µl methanol and finally evaporation from 50 µl toluene. The vial is placed on ice and 100 µl of ice-cold saturated sodium-bicarbonate solution is added, followed by the addition of twice 10 µl acetic acid anhydride[4]. The sample is mixed and incubated at room temperature for 10 min. Then, a second aliquot of acetic acid anhydride is added and the incubation proceeds for further 20 min. The sample is passed through a 3 ml Dowex AG50 [$^{+}$H-form] column, followed by 4 ml of water. The eluate is collected, dried and re-dissolved in 2 ml of 1 mM Copper-(II)-acetate in 1 mM acetic acid. The sample is incubated at room temperature for 1 h and the O-glycans are purified by passage through a column of 2 ml ENVI-18 resin over 1 ml Dowex AG50 [$^{+}$H-form] resin, eluted with water. The O-glycans are now ready for 2AB-derivatisation and HPLC analysis (see sections 2.2.6 and 2.2.7). 2AB-labeled glycan can also be subjected to permethylation for analysis by MALDI-MS. In our hands, permethylation of 2AB-glycans leads to significant higher signal intensities in MALDI-MS compared to permethylation of alkaline borohydride reduced glycans.

[4] From our experience, re-N-acetylation with sodium bicarbonate can lead to partial O-acetylation reactions. O-acetylation might are not evident in HPLC analyses, but can be detected in MALDI-MS. Here it can serve as an indicator for the presence of saccharide in precursor ion scanning experiments. Saccharides would be detected in MALDI with a characteristic satellite peak increment of 42 Da.

Acknowledgments

This work was supported by the Swiss National Foundation grant 31003A-116039 to TH.

Table 1: Peptides used for transferrin glycosylation sites Asn_{413} and Asn_{611}. Amino acids containing the isotope label are marked bold: F, +10 Da; L, +7 Da; A, +4 Da. Due to a misscleavage at Lys_{414} two sets of peptides are required. Two Asn_{413} sequon variants are generated at approximately equal abundance in the reaction mixture. The fragmentation conditions for each peptide were optimized empirically for maximum signal intensities. Dwell time, time per transition; DP, declustering potential; EP, entrance potential; CEP, collision cell entrance potential; CE, collision energy; CXP, collision cell exit potential.

Designation	Sequence	m/z value		Q3 ion
		Standard peptide	Target peptide	
Asn413-NK	CGLVPVLAENYNK	749.4	742.4	y_9
Asn413-NKS	CGLVPVLAENYNKS	792.9	785.9	y_{10}
Asn413-DK	CGLVPVLAENYDK	755.9	744.9	y_9
Asn413-DKS	CGLVPVLAENYDKS	799.4	788.4	y_{10}
Asn611-NVT	QQQHLFGSNVT	640.3	633.3	b_5-NH_3
Asn611-DVT	QQQHLFGSDVT	645.3	635.3	b_9

Designation	Dwell time (ms)	DP (V)	EP (V)	CEP (V)	CE (V)	CXP (V)
Asn413-NK	100	40	9.0	40	41	45
Asn413-NKS	100	41	9.5	43	44	48
Asn413-DK	100	41	9.0	40	41	45
Asn413-DKS	100	41	9.5	43	44	48
Asn611-NVT	150	40	9.0	35	37	43
Asn611-DVT	150	40	9.0	35	37	44

References

Bigge, J.C., T.P. Patel, J.A. Bruce, P.N. Goulding, S.M. Charles, and R.B. Parekh. 1995. Nonselective and efficient fluorescent labeling of glycans using 2-amino benzamide and anthranilic acid. *Anal Biochem* 230:229-238.

Bishop, J.R., M. Schuksz, and J.D. Esko. 2007. Heparan sulphate proteoglycans fine-tune mammalian physiology. *Nature* 446:1030-1037.

Chefetz, I., and E. Sprecher. 2009. Familial tumoral calcinosis and the role of O-glycosylation in the maintenance of phosphate homeostasis. *Biochim Biophys Acta* 1792:847-852.

Ciucanu, I., and F. Kerel. 1984. A simple and rapid method for the permethylation of carbohydrates. *Carbohydr. Res.* 131:209-217.

Dahms, N.M., P. Lobel, and S. Kornfeld. 1989. Mannose 6-phosphate receptors and lysosomal enzyme targeting. *J Biol Chem* 264:12115-12118.

Ellgaard, L., M. Molinari, and A. Helenius. 1999. Setting the standards: quality control in the secretory pathway. *Science* 286:1882-1888.

Elmberger, P.G., I. Eggens, and G. Dallner. 1989. Conditions for quantitation of dolichyl phosphate, dolichol, ubiquinone and cholesterol by HPLC. *Biomed Chromatogr* 3:20-28.

Grubenmann, C.E., C.G. Frank, A.J. Hülsmeier, E. Schollen, G. Matthijs, E. Mayatepek, E.G. Berger, M. Aebi, and T. Hennet. 2004. Deficiency of the first mannosylation step in the N-glycosylation pathway causes congenital disorder of glycosylation type Ik. *Human molecular genetics* 13:535-542.

Haeuptle, M.A., A.J. Hülsmeier, and T. Hennet. 2009. HPLC and mass spectrometry analysis of dolichol-phosphates at the cell culture scale. *Analytical biochemistry*

Harris, R.J., and M.W. Spellman. 1993. O-linked fucose and other post-translational modifications unique to EGF modules. *Glycobiology* 3:219-224.

Helenius, A., and M. Aebi. 2004. Roles of N-linked glycans in the endoplasmic reticulum. *Annual review of biochemistry* 73:1019-1049.

Hülsmeier, A.J., P. Deplazes, S. Naem, N. Nonaka, T. Hennet, and P. Köhler. 2010. An *Echinococcus multilocularis* coproantigen is a surface glycoprotein with unique O-glycosylation. *Glycobiology* 20:127-135.

Hülsmeier, A.J., P.M. Gehrig, R. Geyer, R. Sack, B. Gottstein, P. Deplazes, and P. Kohler. 2002. A major Echinococcus multilocularis antigen is a mucin-type glycoprotein. *J Biol Chem* 277:5742-5748.

Hülsmeier, A.J., P. Paesold-Burda, and T. Hennet. 2007. N-glycosylation site occupancy in serum glycoproteins using multiple reaction monitoring liquid chromatography-mass spectrometry. *Mol Cell Proteomics* 6:2132-2138.

Lommel, M., and S. Strahl. 2009. Protein O-mannosylation: conserved from bacteria to humans. *Glycobiology* 19:816-828.

Müller, R., A.J. Hülsmeier, F. Altmann, K. Ten Hagen, M. Tiemeyer, and T. Hennet. 2005. Characterization of mucin-type core-1 beta1-3 galactosyltransferase homologous enzymes in *Drosophila melanogaster*. *FEBS J* 272:4295-4305.

Okajima, T., A. Xu, L. Lei, and K.D. Irvine. 2005. Chaperone activity of protein O-fucosyltransferase 1 promotes notch receptor folding. *Science* 307:1599-1603.

Patel, T., J. Bruce, A. Merry, C. Bigge, M. Wormald, A. Jaques, and R. Parekh. 1993. Use of hydrazine to release in intact and unreduced form both N- and O-linked oligosaccharides from glycoproteins. *Biochemistry* 32:679-693.

Royle, L., T.S. Mattu, E. Hart, J.I. Langridge, A.H. Merry, N. Murphy, D.J. Harvey, R.A. Dwek, and P.M. Rudd. 2002. An analytical and structural database provides a strategy for sequencing O-glycans from microgram quantities of glycoproteins. *Anal Biochem* 304:70-90.

Shamu, C.E., J.S. Cox, and P. Walter. 1994. The unfolded-protein-response pathway in yeast. *Trends Cell Biol* 4:56-60.

Tian, E., and K.G. Ten Hagen. 2009. Recent insights into the biological roles of mucin-type O-glycosylation. *Glycoconj J* 26:325-334.

Yamada, K., S. Abe, T. Suzuki, K. Katayama, and T. Sato. 1986. A high-performance liquid chromatographic method for the determination of dolichyl phosphates in tissues. *Anal Biochem* 156:380-385.

Zufferey, R., R. Knauer, P. Burda, I. Stagljar, S. te Heesen, L. Lehle, and M. Aebi. 1995. STT3, a highly conserved protein required for yeast oligosaccharyl transferase activity in vivo. *EMBO J* 14:4949-4960.

Regulation of dolichol-linked glycosylation

Michael Welti

Institute of Physiology, University of Zürich, Zürich, Switzerland

Glycoconjugate Journal. 2013 Jan;30(1):51-6.

Corresponding author:

Michael Welti

Institute of Physiology

University of Zürich

Winterthurerstrasse 190

CH-8057 Zürich

Phone: +41-44-635-5072

Fax: +41-44-635-6814

E-mail: michael.welti@uzh.ch

Abstract

In the majority of congenital disorders of glycosylation, the assembly of the glycan precursor $GlcNAc_2Man_9Glc_3$ on the polyprenol carrier dolichyl-pyrophosphate is compromised. Because N-linked glycosylation is essential to life, most types of congenital disorders of glycosylation represent partial losses of enzymatic activity. Consequently, increased availability of substrates along the glycosylation pathway can be beneficial to increase product formation by the compromised enzymes. Recently, we showed that increased dolichol availability and improved N-linked glycosylation can be achieved by inhibition of squalene biosynthesis. This review summarizes the current knowledge on the biosynthesis of dolichol-linked glycans with respect to deficiencies in N-linked glycosylation. Additionally, perspectives on therapeutic treatments targeting dolichol and dolichol-linked glycan biosynthesis are examined.

Dolichol biosynthesis and its role in N-linked glycosylation

N-linked glycosylation occurs in all domains of life and the same basic molecular principles underlie this post-translational modification (Larkin and Imperiali, 2011; Schwarz and Aebi, 2011). Briefly, an oligosaccharide precursor is assembled on a lipid carrier before the oligosaccharide is transferred to a target protein. In eukaryotes, N-linked protein glycosylation requires the assembly of the oligosaccharide precursor at both the outer and inner leaflet of the ER membrane (Veneselli et al., 1998). The precursor is assembled on Dol-PP starting at the cytoplasmic side. The intermediate Dol-PP-$GlcNAc_2Man_5$ is then flipped to the luminal side of the ER where the assembly proceeds to Dol-PP-$GlcNAc_2Man_9Glc_3$. Note worthily, Dol serves as lipid carrier in eukaryotes and archaea whereas another isoprenoid alcohol, bactoprenol, is used in bacteria. Apart from its role as carrier of the oligosaccharide $GlcNAc_2Man_9Glc_3$, Dol is used to form the activated monosaccharides Dol-P-Man and Dol-P-Glc, which are substrates for glycosyltransferases involved in N-glycosylation, O-mannosylation, C-mannosylation and GPI-anchor biosynthesis.

Dol biosynthesis begins at the mevalonate pathway (Fig. 1) (Armstrong et al., 1993; Raucy et al., 1991), which produces essential isoprenoids. Isoprenoids are divided into two classes: sterol isoprenoids, such as cholesterol and steroid hormones, and non-sterol isoprenoids, encompassing polyprenols, ubiquinone, and Dol. Starting from acetyl-CoA via acetoacetyl-CoA, 3-hydroxy-3-methylglutaryl-CoA (HMG-CoA) is first produced. The reduction from HMG-CoA to mevalonate is catalyzed by the rate-limiting HMG-CoA reductase (HMGCR) enzyme. Mevalonate is then phosphorylated to mevalonate-P by mevalonate kinase (MVK). A second phosphorylation step and subsequent decarboxylation leads to isopentenyl-5-pyrophosphate (IPP), which represents an important building block for isoprenoids. IPP is an activated isoprene unit of five carbon atoms and is used to form farnesyl-pyrophosphate. At this point, the pathway diverges to feed on the one hand the biosynthesis of cholesterol and on the other hand the biosynthesis of non-sterol isoprenoids. To obtain Dol, dehydrodolichyl diphosphate synthase (DHDDS) catalyzes the stepwise head-to-tail *cis* addition of IPP to farnesyl-pyrophosphate, thus giving rise to polyprenyl-pyrophosphates of 15 to 19 isoprene units. These polyprenyl-pyrophosphates are then dephosphorylated by pyro- or monophosphatases. The resulting polyprenols are reduced at the α1 position to become Dol of different lengths. Dol is then phosphorylated by Dol kinase (DOLK). Dol-P

can then be utilized as the carrier for the oligosaccharide $GlcNAc_2Man_9Glc_3$ or as a carrier for Man and Glc. Dol-P-Man is produced by the Dol-P-Man synthase (DPM1-3) that transfers Man from GDP-Man to Dol-P while Dol-P-Glc is produced by the glucosyltransferase ALG5 that transfers Glc from UDP-Glc to Dol-P.

Importantly, Dol levels at the cytoplasmic leaflet of the ER are not only maintained by *de novo* synthesis but also depend on recycling of discharged Dol-PP and Dol-P. Once the oligosaccharide precursor is transferred to a target protein, Dol-PP is released and dephosphorylated to Dol-P by the luminal phosphatase DOLPP1 (Rush et al., 2002). Dol-P is then flipped across the membrane to the cytoplasmic leaflet by a yet unknown mechanism (Rush et al., 2008). Recycling of Dol-P and Dol-PP contributes significantly to the Dol pool available glycosylation in the ER. Consequently, a defect of the DOLPP1 orthologue in yeast leads to impaired N-linked glycosylation (van Berkel et al., 1999).

Deficiency of dolichol biosynthesis – a new family of CDG

Several forms of congenital disorders of glycosylation (CDG) caused by Dol biosynthesis defects have been characterized recently. The long sought polyprenol reductase has been identified though the description of SRD5A3-CDG (Cantagrel and Lefeber, 2011) and DHDDS deficiency was discovered in a subgroup of retinitis pigmentosa patients (Ghosh et al., 1993a). Moreover, the clinical picture of Dol kinase deficiency was extended through the description of new cases presenting with dilated cardiomyopathy (Jung et al., 1999).

Proximal to Dol, a defect along the mevalonate pathways has also been linked to diseases. Mutations in the mevalonate kinase gene (*MVK*) (Fig. 1) cause of two different forms: mevalonic aciduria (MVA) (Barone et al., 1999) and hyperimmunoglobulinemia D syndrome (HIDS) (Valnot et al., 1999). In MVA, MVK activity is reduced to 0-4% of the normal values. Patients die in early childhood. Typcial symptoms (Table 1) are psychomotor retardation, failure to thrive, progressive cerebellar ataxia, dysmorphic features, progressive visual impairment and frequent febrile attacks (Raucy et al., 1991; Sturla et al., 2003; Valliere-Douglass et al., 2009). Psychomotor retardation, failure to thrive, dysmorphic features, and visual impairment are also frequently found in CDG, thus suggesting possible glycosylation problems in MVA. HIDS is a milder form of the disease correlating with the residual MVK activity of 5-15% of normal values. In HIDS,

febrile attacks and skin rashes start in early childhood and can be triggered by diverse events, such as vaccinations or minor infections. The febrile disposition is believed to be linked to insufficient levels of anti-inflammatory isoprenylated proteins. Low geranylgeranyl-PP in HIDS leads to caspase-1 activation and IL-1β secretion (Parfait et al., 1999; van der Knaap et al., 1999). Other symptoms found in HIDS (Table 1) are mental retardation, ataxia, ocular symptoms and epilepsy (Kim et al., 2008). Diagnosing HIDS involves the detection of increased mevalonic acid in urine and increased serum immunoglobulin D and A. Apart from febrile attacks, the clinical features of MVA and HIDS are reminiscent of CDG. Indeed, metabolic labelling experiments with [^{14}C]galactose in MVK deficient fibroblasts revealed lower secretion of the radio-labelled macromolecules indicating impaired glycosylation, which is possibly due to decreased formation of Dol and Dol-P (Gebauer et al., 2008). However, systematic analysis of glycosylation in HIDS has not been performed yet.

Recently, DHDDS deficiency (Fig. 1) has been linked to inherited retinitis pigmentosa (Ghosh et al., 1993a), a disorder causing retinal degeneration with an estimated incidence of 1 in 3,000-4,500. The single mutation identified was autosomal-recessive and present in a very small subgroup of retinitis pigmentosa patients (Haldar et al., 1993). Interestingly, DHDDS patients did not show typical CDG symptoms despite the central role of DHDDS in Dol production (Table 1). This fact suggests that DHDDS mutations associated with retinitis pigmentosa only partially impair polyprenol-PP formation and that only few photoreceptor-specific proteins may be sensitive to a reduced polyprenol-PP pool. Note worthily, inhibition of N-linked glycosylation by tunicamycin also leads to retinal degeneration in *Xenopus* (Jenisch et al., 1999; Wimmer-Greinecker et al., 1999). Retinitis pimentosa is also associated with MVK deficiency and with cases of phosphomannomutase 2 deficiency in PMM2-CDG (Grunewald, 2009).

The third disorder of Dol biosynthesis is a recently described type of CDG, in which the *SRD5A3* gene (Fig. 1) is affected (Fu and van Halbeek, 1992; Hart et al., 1988). *SRD5A3* encodes the steroid 5α reductase type 3 protein, which reduces the α-isoprene in polyprenol to form Dol. Symptoms of SRD5A3-CDG are typical for glycosylation disorders and encompass ocular malformations, cerebellar vermis hypoplasia, skin lesions, psychomotor retardation, and facial dysmorphism (Table 1). Strikingly, these multisystemic manifestations strongly differ from those found in DHDDS-CDG despite the proximity of the two enzymes in the Dol pathway. SRD5A3-CDG features loss of

whole N-glycan chains on proteins. Different mutations of the SRD5A3 gene lead to truncated forms resulting in loss of function. Residual levels of Dol in SRD5A3 deficient cells suggest an alternative pathway for Dol biosynthesis.

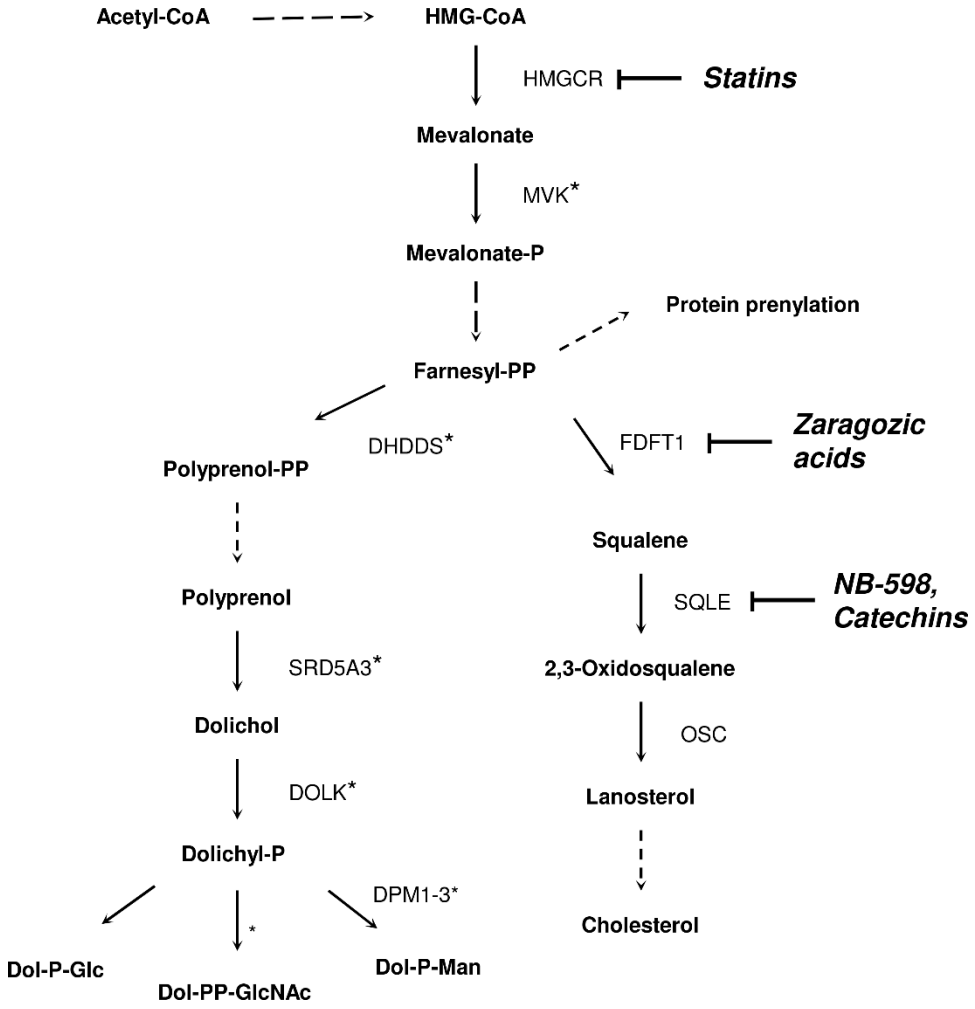

Figure 1: **Dolichol and cholesterol biosynthesis pathway.** Two acetyl building blocks are required for HMG-CoA formation. HMG-CoA reductase (HMGCR) catalyzes the rate limiting step, the formation of mevalonate. Mevalonate kinase (MVK) phosphorylates mevalonate in a CTP-dependent manner. Sequential action of dehydrodolichyl diphosphate synthase (DHDDS), pyro- or monophophatases, 5α steroid reductase type 3 (SRD5A3), and dolichol kinase (DOLK) produce Dol-P. Dol-P-Man synthase (DPM1-3) transfers a mannose to Dol-P. Squalene synthase (FDFT1) produces squalene from farnesyl-PP and subsequent action of squalene epoxidase (SQLE), and 2,3-oxidosqualene cyclase (OSC) leads to lanosterol. Dotted arrows indicate simplifications of the biosynthetic pathway and * point out known congenital defects in dolichol

biosynthesis of the respective enzymes.

Dol kinase deficiency, characterizing DOLK-CDG, impairs the phosphorylation of Dol to Dol-P (Fig. 1). DOLK-CDG presents with severe phenotypes including hypotonia, skin disorders, and the loss of hair (Schindler et al., 1987). Moreover, cardiomyopathy, seizures, hypoglycemia, microcephaly, and visual impairment can occur as well (Table 1). Due to the severity of the symptoms, most DOLK-CDG patients have died in early childhood. Reduced DOLK activity and the resulted low availability of Dol-P impair the assembly Dol-PP-$GlcNAc_2Man_9Glc_3$ and hence N-linked glycosylation. Recently, 11 children with dilated cardiomyopathy (DCM), a disease possibly linked to sudden cardiac death and heart failure, were found to have a novel mutation in DOLK (Jung et al., 1999). Besides DCM, only few of the patients exhibit additional symptoms like ichtyosis, failure to thrive, and mild neurological involvement. Biochemical analysis of Dol-P dependent glycosylation pathways of the DCM heart tissue indicated reduced O-mannosylation of α-dystroglycan (Ijland et al., 1999). Remarkably, abnormal N-glycosylation of serum transferrin was equally pronounced in both forms of DOLK-CDG. The phenotypes of DCM strongly contrast with the originally described features of DOLK-CDG, thus suggesting a possible tissue-specific regulation of Dol-P dependent glycosylation.

Human Dol-P-Man synthase (DPM1-3, Fig. 1) consists of 3 subunits. DPM1 is the catalytic subunit and DPM2/3 are regulatory and membrane anchoring proteins residing in the ER membrane (Maeda and Kinoshita, 2008). So far, two forms of Dol-P-Man synthase deficiency have been described featuring mutations in the *DPM1* and *DPM3* genes. DPM1-CDG is characterized by recurrent seizures, hypotonia, developmental delay, dysmorphic features, microcephaly, visual impairment, and in some cases ataxia and coagulopathy (Table 1) (Chen et al., 2005; Kreishman et al., 1972; Palamarczyk and Janczura, 1977; Tao et al., 2006). Lower Dol-P-Man levels lead to impaired Dol-PP-$GlcNAc_2Man_9Glc_3$ assembly, abnormal N-linked protein glycosylation, and decreased formation of GPI anchored proteins. DPM3-CDG appears to be a milder form of Dol-P-Man synthase deficiency, for which only one patient has been found so far (Zaia, 2013). The symptoms included mild myopathy, a dilated cardiomyopathy, moderate muscular dystrophy, and a single stroke-like episode. The adult patient is able to live a practically normal life. N-glycosylation of serum transferrin is only slightly abnormal. In DPM1-CDG and DPM3-CDG, the severity seems to reflect the molecular

functions of the affected subunits. So, a deficient catalytic subunit, DPM1, leads to a much more severe phenotype than a deficient tethering subunit, DPM3.

Table 1: Disorders of dolichol biosynthesis and their respective symptoms. Symptoms are distinguished between ** for typical/dominant symptoms and * for sporadic symptoms or symptoms of moderate severity.

	MVA	HIDS	DHDDS-CDG	SRD5A3-CDG	DOLK-CDG[a)]	DOLK-CDG[b)]	DPM1-CDG	DPM3-CDG
Cardiomyopathy				*	**	**		*
Cerebellar ataxia / malformation	**	**		**			**	
Coagulopathy				**			**	
Dysmorphic features	**			**	**			
Failure to thrive	**							
Febrile attacks	**	**						
Hypoglycemia					**			
Hypotonia					**		**	
Microcephaly	**	*			**		**	
Muscular dystrophy							**	*
Myopathy							**	*
Ocular malfunctions	**		**	**	**		**	
Psychomotor retardation	**	**		**	**	*	**	
Seizures	**	*			**		**	
Skin disorders	**	**		*	**	*		

a) Classical DOLK-CDG, b) DOLK defect in dilated cardiomyopathy.

In general, the clinical severity of Dol-related diseases does not correlate with the relative position of the deficient enzymes along the biosynthesis pathway. Defects of Dol biosynthesis are generally expected to be severe since not only the assembly of Dol-PP-

$GlcNAc_2Man_9Glc_3$ is impaired, but also GPI anchor formation and O-mannosylation are affected. This notion is confirmed in SRD5A3-CDG that present with severe multisystemic phenotypes. However, the discovery of DHDDS-CDG with a very specific phenotype and lack of the typical CDG symptoms suggests a complex regulation of Dol-dependent glycosylation. Future efforts addressing the regulation of Dol biosynthesis should provide a better understanding of the question and open the way to novel therapeutic perspectives.

Therapeutics targeting dolichol

To date, only two forms of CDG are treatable. MPI-CDG can be successfully treated with oral mannose supplementation (Liu et al., 2006; Tissot et al., 2007). In GFTP-CDG, GDP-fucose transporter deficiency can be compensated with nutritional fucose supplementation (Marquardt et al., 1999). The hypomorphic nature of most CDG mutations allows for a compensatory approach, for instance by providing more Dol to overcome the compromised assembly of Dol-PP-$GlcNAc_2Man_9Glc_3$. Along this line, inhibition of squalene synthase (FDFT1, Fig. 1) was shown to improve N-linked protein glycosylation and GPI-anchored protein expression in DPM1-CDG fibroblasts (Haeuptle et al., 2011). We tested potential drugs such as clofibrate for its ability to increase GPI anchor availability in DPM1-CDG fibroblasts. Clofibrate is a fibrate known to decrease cholesterol levels by targeting lipid metabolism via activation of peroxisome proliferator-activated receptors, especially PPARα (Abourbih et al., 2009; Forman et al., 1997). Indeed, GPI anchor availability was improved upon clofibrate treatment as observed by an increased surface expression of the GPI anchored protein CD59 (unpublished data). In another approach to increase the Dol pool, we attempted to increase DHDDS activity by treatment of DPM1-CDG fibroblasts with the AMP cyclase activator forskolin (Losfeld et al., 2012). DHDDS activity was previously shown to increase with higher cyclic AMP levels (Konrad and Merz, 1994; Konrad and Merz, 1996). Treatment of DPM1-CDG fibroblasts with forskolin led to higher levels of surface CD59 as well.

New therapeutic possibilities arise for CDG with the advance of non-statin cholesterol lowering drugs, which target the late pathway of cholesterol biosynthesis. Presently, statins are the prevalent medication to lower cholesterol and decrease cardiovascular

disease (Hoenger et al., 1993). Statins are inhibitors of the HMG-CoA reductase (Fig. 1), the rate limiting enzyme at the beginning of the mevalonate pathway. The effect of statins on Dol levels has not been investigated systematically. Hela cells treated with pravastatin showed a decrease in Dol-P by 65% (Kornfeld et al., 1985). However, rats treated with lovastatin did not show a change of total Dol-P levels but increase of Dol-P in the liver (Low et al., 1992). The potential of different statins to upregulate Dol could be investigated in a screen. For instance, CDG fibroblasts treated with an array of statins could be screened for changes of Dol levels.

Inhibition of the first committed enzyme of cholesterol biosynthesis, squalene synthase (FDFT1, Fig. 1), has proven effective in lowering cholesterol production (Dhar et al., 1993). Prominent among these inhibitors are zaragozic acids, which were identified in a screen of fungal compounds for cholesterol lowering activity (Bergstrom et al., 1995). Changes in Dol-P patterns were observed in human fibroblasts treated with zaragozic acid A. Also, DPM1-CDG fibroblasts showed improved N-linked glycosylation upon treatment with zaragozic acid A (Takahashi et al., 1993). Moreover, the expression of the GPI-anchored CD59 protein could be normalized in DPM1-CDG fibroblasts after treatment. Since zaragozic acid is well tolerated in animals (Baxter et al., 1992; Bergstrom et al., 1993), this class of FDFT1 inhibitors might be considered for clinical testing in some cases of CDG.

Squalene epoxidase (SQLE) catalyzes the next committed step of cholesterol biosynthesis after FDFT1 (Fig. 1). Therefore, inhibition of SQLE is considered to specifically lower cholesterol. Inhibition of SQLE by the compound NB-598 ((E)N-ethyl-N-(6,6-dimethyl-2-hepten-4-ynyl)-3-[(3,3'-bith iophen-5-yl)methoxy]benzene-methanamine) successfully reduced cholesterol levels (Ghosh et al., 1993c; Hope et al., 1993), although no changes in Dol levels were detected in treated HepG2 cells (Ghosh et al., 1993b). In spite of this early finding, newly developed SQLE inhibitors should be considered as promising candidates for an upregulation of Dol in CDG cells. Moreover, green tea has been attributed a cholesterol lowering effect, which is linked to SQLE inhibition (Abe et al., 2000). In a recent study, oral supplementation with the main green tea catechin epigallocatechin gallate was shown to lower LDL-cholesterol (Wu et al., 2012). The effects of epigallocatechin gallate on Dol have not been tested yet. Catechins might represent another option to upregulate Dol in CDG cells by inhibition of SQLE.

Oxidosqualene cyclase (OSC) inhibitors interfere with the conversion of 2,3-oxidosqualene to lanosterol (Fig. 1). Due to adverse effects, the development of such inhibitors has been stopped (Hope et al., 1993). Unless novel OSC inhibitors without adverse effects are discovered, the potential of such drugs to increase the Dol pool is not worth further investigation.

In conclusion, inhibitors of late cholesterol biosynthesis have a potential increasing effect on Dol levels and should be accordingly tested in CDG cells. Much effort is invested in the development of cholesterol lowering drugs in the context of cardiovascular diseases. Therefore, potential CDG therapies could profit from the discovery of novel cholesterol lowering drugs in the future.

Outlook

The recent identification of tissue-restricted symptoms in DHDDS-CDG and of a novel pathology associated to DOLK deficiency suggests a pronounced tissue specificity of Dol-related biology. Accordingly, additional diseases are likely to be associated with local alterations of Dol biosynthesis in the near future. The study of these tissue-restricted diseases represents valuable models to better understand the regulation of Dol biosynthesis and its impact on various types of glycosylation. Novel therapeutic approaches may be deduced from such insights. The treatment of CDG is still very limited and merits further attention. We believe that interference of cholesterol production and thus upregulation of Dol biosynthesis represents a valuable approach to improve glycosylation in CDG. High-throughput screenings of existing cholesterol lowering drugs that upregulate Dol are relatively straightforward and could open novel therapeutic opportunities.

References

Abe, I., T. Seki, K. Umehara, T. Miyase, H. Noguchi, J. Sakakibara, and T. Ono. 2000. Green tea polyphenols: novel and potent inhibitors of squalene epoxidase. *Biochem Biophys Res Commun* 268:767-771.

Abourbih, S., K.B. Filion, L. Joseph, E.L. Schiffrin, S. Rinfret, P. Poirier, L. Pilote, J. Genest, and M.J. Eisenberg. 2009. Effect of fibrates on lipid profiles and cardiovascular outcomes: a systematic review. *Am J Med* 122:962 e961-968.

Armstrong, S.J., R.A. Read, P. Ghosh, and D.M. Wilson. 1993. Moderate exercise exacerbates the osteoarthritic lesions produced in cartilage by meniscectomy: a morphological study. *Osteoarthritis Cartilage* 1:89-96.

Barone, R., L. Pavone, A. Fiumara, R. Bianchini, and J. Jaeken. 1999. Developmental patterns and neuropsychological assessment in patients with carbohydrate-deficient glycoconjugate syndrome type IA (phosphomannomutase deficiency). *Brain Dev* 21:260-263.

Baxter, A., B.J. Fitzgerald, J.L. Hutson, A.D. McCarthy, J.M. Motteram, B.C. Ross, M. Sapra, M.A. Snowden, N.S. Watson, R.J. Williams, and et al. 1992. Squalestatin 1, a potent inhibitor of squalene synthase, which lowers serum cholesterol in vivo. *J Biol Chem* 267:11705-11708.

Bergstrom, J.D., C. Dufresne, G.F. Bills, M. Nallin-Omstead, and K. Byrne. 1995. Discovery, biosynthesis, and mechanism of action of the zaragozic acids: potent inhibitors of squalene synthase. *Annu Rev Microbiol* 49:607-639.

Bergstrom, J.D., M.M. Kurtz, D.J. Rew, A.M. Amend, J.D. Karkas, R.G. Bostedor, V.S. Bansal, C. Dufresne, F.L. VanMiddlesworth, O.D. Hensens, and et al. 1993. Zaragozic acids: a family of fungal metabolites that are picomolar competitive inhibitors of squalene synthase. *Proc Natl Acad Sci U S A* 90:80-84.

Cantagrel, V., and D.J. Lefeber. 2011. From glycosylation disorders to dolichol biosynthesis defects: a new class of metabolic diseases. *J Inherit Metab Dis* 34:859-867.

Chen, B., B.G. Zhang, J. Zhang, Y.Q. Gu, J.X. Li, H.X. Yu, and Z.G. Wang. 2005. [Primary experimental study on the construction of tissue engineering blood vessel]. *Zhonghua Wai Ke Za Zhi* 43:1271-1274.

Dhar, S., A.J. Kanwar, and S. Ghosh. 1993. Leucotrichia in nevus depigmentosus. *Pediatr Dermatol* 10:198-199.

Forman, B.M., J. Chen, and R.M. Evans. 1997. Hypolipidemic drugs, polyunsaturated fatty acids, and eicosanoids are ligands for peroxisome proliferator-activated receptors alpha and delta. *Proc Natl Acad Sci U S A* 94:4312-4317.

Fu, D., and H. van Halbeek. 1992. N-glycosylation site mapping of human serotransferrin by serial lectin affinity chromatography, fast atom bombardment-mass spectrometry, and 1H nuclear magnetic resonance spectroscopy. *Anal Biochem* 206:53-63.

Gebauer, J.M., S. Muller, F.G. Hanisch, M. Paulsson, and R. Wagener. 2008. O-glucosylation and O-fucosylation occur together in close proximity on the first epidermal growth factor repeat of AMACO (VWA2 protein). *J Biol Chem* 283:17846-17854.

Ghosh, K., S. Ramakrishnan, and G. Chandra. 1993a. Resistivity and susceptibility studies on UPd2-xPtxAl3 (x=0, 0.1, 0.2, 0.3, and 0.5). *Phys Rev B Condens Matter* 47:8305-8307.

Ghosh, P., R. Read, S. Armstrong, D. Wilson, R. Marshall, and P. McNair. 1993b. The effects of intraarticular administration of hyaluronan in a model of early osteoarthritis in sheep. I. Gait analysis and radiological and morphological studies. *Semin Arthritis Rheum* 22:18-30.

Ghosh, P., R. Read, Y. Numata, S. Smith, S. Armstrong, and D. Wilson. 1993c. The effects of intraarticular administration of hyaluronan in a model of early osteoarthritis in sheep. II. Cartilage composition and proteoglycan metabolism. *Semin Arthritis Rheum* 22:31-42.

Grunewald, S. 2009. The clinical spectrum of phosphomannomutase 2 deficiency (CDG-Ia). *Biochimica et biophysica acta* 1792:827-834.

Haeuptle, M.A., M. Welti, H. Troxler, A.J. Hülsmeier, T. Imbach, and T. Hennet. 2011. Improvement of dolichol-linked oligosaccharide biosynthesis by the squalene synthase inhibitor zaragozic acid. *J Biol Chem* 286:6085-6091.

Haldar, K.K., B. Sahadalal, and E.L. Ghosh. 1993. Transferable drug resistance in Salmonella senftenberg. *Indian J Pathol Microbiol* 36:81-83.

Hart, G.W., G.D. Holt, and R.S. Haltiwanger. 1988. Nuclear and cytoplasmic glycosylation: novel saccharide linkages in unexpected places. *Trends Biochem Sci* 13:380-384.

Hoenger, A., R. Ghosh, C.A. Schoenenberger, U. Aebi, and A. Engel. 1993. Direct in situ structural analysis of recombinant outer membrane porins expressed in an OmpA-deficient mutant Escherichia coli strain. *J Struct Biol* 111:212-221.

Hope, N., P. Ghosh, T.K. Taylor, D. Sun, and R. Read. 1993. Effects of intraarticular hyaluronan on matrix changes induced in the lateral meniscus by total medial meniscectomy and exercise. *Semin Arthritis Rheum* 22:43-51.

Ijland, S.A., M.J. Jager, B.M. Heijdra, J.R. Westphal, and R. Peek. 1999. Expression of angiogenic and immunosuppressive factors by uveal melanoma cell lines. *Melanoma Res* 9:445-450.

Jenisch, S., S. Koch, T. Henseler, R.P. Nair, J.T. Elder, C.E. Watts, E. Westphal, J.J. Voorhees, E. Christophers, and M. Kronke. 1999. Corneodesmosin gene polymorphism demonstrates strong linkage disequilibrium with HLA and association with psoriasis vulgaris. *Tissue Antigens* 54:439-449.

Jung, H., P. Carmel, M.S. Schwartz, J.W. Witkin, K.H. Bentele, M. Westphal, J.H. Piatt, M.E. Costa, A. Cornea, Y.J. Ma, and S.R. Ojeda. 1999. Some hypothalamic hamartomas contain transforming growth factor alpha, a puberty-inducing growth factor, but not luteinizing hormone-releasing hormone neurons. *J Clin Endocrinol Metab* 84:4695-4701.

Kim, M.L., K. Chandrasekharan, M. Glass, S. Shi, M.C. Stahl, B. Kaspar, P. Stanley, and P.T. Martin. 2008. O-fucosylation of muscle agrin determines its ability to cluster acetylcholine receptors. *Mol Cell Neurosci* 39:452-464.

Konrad, M., and W.E. Merz. 1994. Regulation of N-glycosylation. Long term effect of cyclic AMP mediates enhanced synthesis of the dolichol pyrophosphate core oligosaccharide. *J Biol Chem* 269:8659-8666.

Konrad, M., and W.E. Merz. 1996. Long-term effect of cyclic AMP on N-glycosylation is caused by an increase in the activity of the cis-prenyltransferase. *Biochem J* 316 (Pt 2):575-581.

Kornfeld, P., E.P. Ambinder, R. Matta, A. Bender, A.E. Papatestas, H. Gross, and G. Genkins. 1985. Azathioprine experience in severe, generalized, recalcitrant myasthenia gravis. *Mt Sinai J Med* 52:347-352.

Kreishman, G.P., J.T. Witkowski, R.K. Robins, and M.P. Schweizer. 1972. The use of proton and carbon-13 nuclear magnetic resonance for assignment of the glycosylation site in 3- and 5-substituted 1- -D-ribofuranosyl-1,2,4-triazoles. *J Am Chem Soc* 94:5894-5896.

Larkin, A., and B. Imperiali. 2011. The expanding horizons of asparagine-linked glycosylation. *Biochemistry* 50:4411-4426.

Liu, X., D.J. McNally, H. Nothaft, C.M. Szymanski, J.R. Brisson, and J. Li. 2006. Mass spectrometry-based glycomics strategy for exploring N-linked glycosylation in eukaryotes and bacteria. *Anal Chem* 78:6081-6087.

Losfeld, M.E., F. Soncin, B.G. Ng, I. Singec, and H.H. Freeze. 2012. A sensitive green fluorescent protein biomarker of N-glycosylation site occupancy. *FASEB J* 26:4210-4217.

Low, P., M. Andersson, C. Edlund, and G. Dallner. 1992. Effects of mevinolin treatment on tissue dolichol and ubiquinone levels in the rat. *Biochimica et biophysica acta* 1165:102-109.

Maeda, Y., and T. Kinoshita. 2008. Dolichol-phosphate mannose synthase: structure, function and regulation. *Biochimica et biophysica acta* 1780:861-868.

Marquardt, T., K. Luhn, G. Srikrishna, H.H. Freeze, E. Harms, and D. Vestweber. 1999. Correction of leukocyte adhesion deficiency type II with oral fucose. *Blood* 94:3976-3985.

Palamarczyk, G., and E. Janczura. 1977. Lipid mediated glycosylation in yeast nuclear membranes. *FEBS Lett* 77:169-172.

Parfait, B., P. de Lonlay, J.C. von Kleist-Retzow, V. Cormier-Daire, D. Chretien, A. Rotig, D. Rabier, J.M. Saudubray, P. Rustin, and A. Munnich. 1999. The neurogenic weakness, ataxia and

retinitis pigmentosa (NARP) syndrome mtDNA mutation (T8993G) triggers muscle ATPase deficiency and hypocitrullinaemia. *Eur J Pediatr* 158:55-58.

Raucy, J.L., J.M. Lasker, J.C. Kraner, D.E. Salazar, C.S. Lieber, and G.B. Corcoran. 1991. Induction of cytochrome P450IIE1 in the obese overfed rat. *Molecular pharmacology* 39:275-280.

Rush, J.S., S.K. Cho, S. Jiang, S.L. Hofmann, and C.J. Waechter. 2002. Identification and characterization of a cDNA encoding a dolichyl pyrophosphate phosphatase located in the endoplasmic reticulum of mammalian cells. *J Biol Chem* 277:45226-45234.

Rush, J.S., N. Gao, M.A. Lehrman, and C.J. Waechter. 2008. Recycling of dolichyl monophosphate to the cytoplasmic leaflet of the endoplasmic reticulum after the cleavage of dolichyl pyrophosphate on the lumenal monolayer. *J Biol Chem* 283:4087-4093.

Schindler, M., M. Hogan, R. Miller, and D. DeGaetano. 1987. A nuclear specific glycoprotein representative of a unique pattern of glycosylation. *J Biol Chem* 262:1254-1260.

Schwarz, F., and M. Aebi. 2011. Mechanisms and principles of N-linked protein glycosylation. *Curr Opin Struct Biol* 21:576-582.

Sturla, L., R. Rampal, R.S. Haltiwanger, F. Fruscione, A. Etzioni, and M. Tonetti. 2003. Differential terminal fucosylation of N-linked glycans versus protein O-fucosylation in leukocyte adhesion deficiency type II (CDG IIc). *J Biol Chem* 278:26727-26733.

Takahashi, T., J.M. Lasker, A.S. Rosman, and C.S. Lieber. 1993. Induction of cytochrome P-4502E1 in the human liver by ethanol is caused by a corresponding increase in encoding messenger RNA. *Hepatology (Baltimore, Md* 17:236-245.

Tao, L., L.W. Wagner, P.E. Rouviere, and Q. Cheng. 2006. Metabolic engineering for synthesis of aryl carotenoids in Rhodococcus. *Appl Microbiol Biotechnol* 70:222-228.

Tissot, B., N. Gasiunas, A.K. Powell, Y. Ahmed, Z.L. Zhi, S.M. Haslam, H.R. Morris, J.E. Turnbull, J.T. Gallagher, and A. Dell. 2007. Towards GAG glycomics: analysis of highly sulfated heparins by MALDI-TOF mass spectrometry. *Glycobiology* 17:972-982.

Valliere-Douglass, J.F., L.J. Brady, C. Farnsworth, D. Pace, A. Balland, A. Wallace, W. Wang, M.J. Treuheit, and B. Yan. 2009. O-fucosylation of an antibody light chain: characterization of a modification occurring on an IgG1 molecule. *Glycobiology* 19:144-152.

Valnot, I., J. Kassis, D. Chretien, P. de Lonlay, B. Parfait, A. Munnich, J. Kachaner, P. Rustin, and A. Rotig. 1999. A mitochondrial cytochrome b mutation but no mutations of nuclearly encoded subunits in ubiquinol cytochrome c reductase (complex III) deficiency. *Hum Genet* 104:460-466.

van Berkel, M.A., M. Rieger, S. te Heesen, A.F. Ram, H. van den Ende, M. Aebi, and F.M. Klis. 1999. The Saccharomyces cerevisiae CWH8 gene is required for full levels of dolichol-linked oligosaccharides in the endoplasmic reticulum and for efficient N-glycosylation. *Glycobiology* 9:243-253.

van der Knaap, M.S., C. Jakobs, G.F. Hoffmann, M. Duran, A.C. Muntau, S. Schweitzer, R.I. Kelley, F. Parrot-Roulaud, J. Amiel, P. De Lonlay, D. Rabier, and O. Eeg-Olofsson. 1999. D-2-hydroxyglutaric aciduria: further clinical delineation. *J Inherit Metab Dis* 22:404-413.

Veneselli, E., R. Biancheri, M. Di Rocco, and S. Tortorelli. 1998. Neurophysiological findings in a case of carbohydrate-deficient glycoprotein (CDG) syndrome type I with phosphomannomutase deficiency. *Eur J Paediatr Neurol* 2:239-244.

Wimmer-Greinecker, G., G. Matheis, S. Dogan, T. Aybek, P. Kessler, K. Westphal, and A. Moritz. 1999. Complications of port-access cardiac surgery. *J Card Surg* 14:240-245.

Wu, A.H., D. Spicer, F.Z. Stanczyk, C. Tseng, C.S. Yang, and M.C. Pike. 2012. Effect of 2-month controlled green tea intervention on lipoprotein cholesterol, glucose, and hormonal levels in healthy postmenopausal women. *Cancer Prev Res (Phila)*

Zaia, J. 2013. Glycosaminoglycan glycomics using mass spectrometry. *Mol Cell Proteomics* 12:885-892.

Ethanol-induced impairment in the biosynthesis of N-linked glycosylation

Michael Welti and Andreas J. Hülsmeier

Institute of Physiology, University of Zürich, Zürich, Switzerland

Manuscript accepted in the Journal of Cellular Biochemistry 2013

Corresponding author:

Andreas J. Hülsmeier

Institute of Physiology

University of Zürich

Winterthurerstrasse 190

CH-8057 Zürich

Phone: +41-44-635-5104

Fax: +41-44-635-6814

E-mail: a.j.hulsmeier@access.uzh.ch

Abstract

Background

Deficiency in N-linked protein glycosylation is a long-known characteristic of alcoholic liver disease and congenital disorders of glycosylation. Previous investigations of ethanol-induced glycosylation deficiency demonstrated perturbations in the early steps of substrate synthesis and in the final steps of capping N-linked glycans in the Golgi. The significance of the biosynthesis of N-glycan precursors in the endoplasmic reticulum, however, has not yet been addressed in alcoholic liver disease.

Methods

Ethanol-metabolizing hepatoma cells were treated with increasing concentrations of ethanol. Transcript analysis of genes involved in the biosynthesis of N-glycans, activity assays of related enzymes, quantification of dolichol-phosphates, and analysis of dolichol-linked oligosaccharides were performed.

Results

Upon treatment of cells with ethanol, we found a decrease in the final N-glycan precursor Dol-PP-$GlcNAc_2Man_9Glc_3$ and in C95- and C100-dolichol-phosphate levels. Transcript analysis of genes involved in N-glycosylation showed a 17% decrease in expression levels of DPM1, a subunit of the dolichol-phosphate-mannose synthase, and a 8% increase in RPN2, a subunit of the oligosaccharyl transferase.

Conclusions

Ethanol treatment decreases the biosynthesis of dolichol-phosphate. Consequently, the formation of N-glycan precursors is affected, resulting in an aberrant precursor assembly. Messenger RNA levels of genes involved in N-glycan biosynthesis are not affected by ethanol treatment, indicating that the assembly of N-glycan precursors is not regulated at the transcriptional level.

General Significance

This study confirms that ethanol impairs N-linked glycosylation by affecting dolichol biosynthesis leading to impaired dolichol-linked oligosaccharide assembly. Together our data help to explain the underglycosylation phenotype observed in alcoholic liver disease and congenital disorders of glycosylation.

Highlights

- Dolichol-phosphate levels are reduced after ethanol treatment
- Assembly of the N-glycan precursor is impaired after ethanol treatment
- Transcript levels of genes involved in N-glycosylation are slightly affected after treatment

Keywords

N-linked glycosylation, alcoholic liver disease, dolichol, dolichol-linked oligosaccharides

Abbreviations

ALD, alcoholic liver disease; CDG, congenital disorder of glycosylation; CDT, carbohydrate-deficient transferrin; Dol-P, dolichol-phosphate; Dol-PP, dolichol-pyrophosphate; DPM1-3, dolichol-phosphate-mannose synthase subunits 1-3; RPN2, ribophorin 2; Glc, glucose; GlcNAc, N-acetylglucosamine; Man, mannose; ADH, alcohol dehydrogenase; CYP2E1; cytochrome P450 2E1

1. Introduction

Alcoholic liver disease (ALD) displays a broad spectrum of symptoms reflecting the diverse functions of the liver. Among the most prominent characteristics of ALD are fatty liver, hepatitis, and liver fibrosis. Hepatocytes are responsible for detoxification in the liver and thus for alcohol metabolism. Major metabolic changes in hepatocytes occur due to the constant need for ethanol oxidation. Ethanol conversion to acetate leads to a shift in the NAD/NADH ratio impairing glycolysis and lipolysis and initiating fatty acid synthesis. The inversion of glycolytic flux eventually results in alcoholic fatty liver (Purohit et al., 2009). Oxidative stress is evoked by reactive oxygen species from ethanol breakdown in hepatocytes and toll-like receptor 4 activation by LPS leaking from the gut into the blood stream (Wang et al., 2012; Zhu et al., 2012). This oxidative stress contributes to liver inflammation and can lead to liver fibrosis and eventually cirrhosis. Another clinical feature in ALD receiving less attention is alcohol-induced deficiency in N-linked protein glycosylation although it has been used as a marker for alcohol abuse (Stibler, 1991).

ALD and congenital disorders of glycosylation (CDG) share some symptoms. Typically, CDG display systemic deficiencies like psychomotor retardation with variable neuromuscular involvement and additional features like hormonal abnormalities and coagulopathies (Leroy, 2006). Importantly, fatty liver, hepatitis, and liver fibrosis are also found in CDG indicating a possible role of glycosylation in ALD pathology. Indeed, CDG was linked to a fibrotic response in fibroblasts involving the insulin-like growth factor-binding protein 5 (Lecca et al., 2011). As in CDG, blood serum proteins originating from the liver are not glycosylated properly in ALD. For instance, the distribution of carbohydrate-deficient transferrin (CDT) glycoforms found in ALD and CDG are similar (Bean and Peter, 1993; de Jong et al., 1992; Petren et al., 1987; Vigo and Adair, 1982). The two glycosylation sites of transferrin are normally occupied with carbohydrates adding up to four branches carrying terminal sialic acids. Besides tetrasialo-transferrin, disialo-transferrin is the most prevalent glycoform of transferrin in blood serum. In ALD and CDG, asialo- and disialo-transferrin become more apparent and tetrasialo-transferrin levels are reduced (Hülsmeier et al., 2007). In CDG, such a CDT pattern indicates a deficiency in the assembly of the N-linked glycan precursor in the ER (Filipovic and Menzel, 1981).

So far, glycosylation deficiency in ALD has been assessed at the levels of Golgi glycosylation and dolichol metabolism. However, N-linked glycosylation starts in the ER and requires the synthesis of an oligosaccharide precursor on dolichol-phosphate (Dol-P). On the outer leaflet of the ER, one phospho-GlcNAc, one GlcNAc, and five Man are sequentially transferred to Dol-P before flipping the resulting Dol-PP-$GlcNAc_2$-Man_5 into the ER lumen. After the addition of four Man and three Glc residues, the complete N-glycan precursor, Dol-PP-$GlcNAc_2$-Man_9-Glc_3 is transferred *en bloc* to target proteins. Microsomes isolated from rat livers of chronically ethanol-fed animals showed a decrease in total dolichol by 36% (Cottalasso et al., 1998; Cottalasso et al., 1996). Acute treatment with ethanol of rats resulted in a reduction of total dolichol in liver microsomes by up to 52%. In a cell culture model, HepG2 cells treated with 50-100 mM ethanol showed decreased transcription of the α2,6-sialyltransferase(Garige et al., 2006; Garige et al., 2005; Rao and Lakshman, 1997; Rao and Lakshman, 1999). This enzyme is responsible for terminal sialylation of sugar chains of transferrin in the Golgi apparatus. The same effect was observed in the liver from chronically ethanol-fed rats. Additionally, the α2,6-sialyltransferase mRNA is destabilized by a 3'-untranslated region-specific binding protein. Notably, besides downregulation of α2,6-sialyltransferase other effects could cause CDT. Several intermediates along the biosynthesis of the N-glycan precursor might be affected, potentially leading to an altered distribution of glycoforms. In one study the site occupancy of serum protein glycosylation in an alcohol abusing subject was reported to be reduced to levels observed in patients with mild forms of CDG (Hülsmeier et al., 2007). Another study reported the loss of one or both N-glycans as the cause for CDT in patients with severe alcohol abuse (Peter et al., 1998).

To understand the mechanisms underlying alcohol-induced glycosylation deficiency, we investigated the effects of ethanol exposure on the early steps of N-linked protein glycosylation in two cell models. Cultured hepatocytes usually lose the expression of drug metabolizing enzymes (Carter and Wands, 1988; Gapp et al., 2012; Luo et al., 2006; Utesch et al., 1992; Van Kaick et al., 1983). Therefore, we used two cell lines expressing ethanol metabolizing enzymes in our study. First, the HepaRG cell line derived from a human hepatocellular carcinoma with an inducible cytochrome p450 system which renders the cell line suitable as a model for metabolism of xenobiotics in the human liver (Crick and Carroll, 1987; Eggens et al., 1990; Eggens and Elmberger, 1990; Keller, 1986; Stoll et al., 1988; Yokoyama et al., 1989). Ethanol degradation via cytochrome p450 2E1

(CYP2E1) is a major pathway of ethanol metabolism and can be induced by DMSO treatment in HepaRG cells (Koop and Tierney, 1990; Lieber, 1999; Ohnishi and Lieber, 1977). The second cell line, VA-13, is derived from HepG2 cells, which expresses murine alcohol dehydrogenase 1 (ADH) (Clemens et al., 2002). Ethanol degradation via alcohol dehydrogenase is the second major pathway of ethanol metabolism in the liver. We tested the effect of ethanol metabolism in hepatocytes on the N-linked glycosylation pathway in the ER and found that N-linked glycosylation is affected at several stages along the biosynthetic pathway.

2. Materials and Methods

2.1 Cell lines and experimental conditions

HepaRG cells were kindly provided by Dr. N. Zitzmann (Department of Biochemistry, University of Oxford, UK). HepaRG cells were seeded at a density of 2.6 x 10^4 cells/cm^2 and cultured in Williams' Medium E (Sigma-Aldrich) supplemented with 10% FBS, 5 μg/ml insulin, 2 mM L-glutamine, and 50 μM hydrocortisone hemisuccinate for two weeks. To induce maximal induction of the P450 enzymes, HepaRG cells were cultured for two additional weeks in the same medium added with 2% DMSO (Sigma) (Gripon et al., 2002). On day 24 after seeding, ethanol was added to the medium and culture flasks were sealed with Parafilm to prevent evaporation of ethanol. HepaRG cells were harvested and analyzed after 28 days in culture. VA-13 cells were a kind gift from Dr. D.L. Clemens (Department of Internal Medicine, University of Nebraska Medical Center, USA). VA-13 cells are HepG2 cells stably transfected with an expression plasmid carrying the murine alcohol dehydrogenase gene, Adh-1 (Clemens et al., 2002). VA-13 cells were seeded at a density of 1.7 x 10^4 cells/cm^2 and ethanol treatment was started 6 h after seeding. VA-13 cells were harvested and analyzed 4 days after treatment start.

2.2 Isoelectric focusing gel electrophoresis and immunoblotting

Supernatant from cultured hepatoma cells was saturated with 0.4 mM ferric citrate in presence of 20 mM sodium hydrogen carbonate for 30 min. Samples were analyzed using pre-cast Novex pH 3-7 IEF gels (Invitrogen). Gels were run at 7 mA (500 V maximum voltage) for 4 h on ice. Proteins were transferred to a nitrocellulose membrane by Western blotting. Transferrin isoforms were visualized using polyclonal

rabbit anti-human transferrin primary antibody (DakoCytomation, Denmark) and peroxidase-coupled goat anti-rabbit secondary antibody (Vector Laboratories, USA).

2.3 Alcohol dehydrogenase activity assay

Alcohol dehydrogenase (ADH) activity was measured in cell lysates as previously described (Clemens et al., 1995). Activity was determined in an assay using ethanol and NAD as substrates. ADH activity was indirectly determined from the conversion of NAD by measuring NADH photometrically at 340 nm.

2.4 Cytochrome P450 2E1 activity assay

Cytochrome p450 2E1 activity was determined as described previously (Wu and Cederbaum, 2008). Microsomal fractions were prepared and assayed for CYP2E1 activity using *p*-nitrophenol and NADPH as substrates.

2.5 Quantitative PCR for transcript analysis

Transcript analysis of the glycosylation pathway were quantified with an adapted method for quantitative PCR in mice (Nairn et al., 2010). Mann-Whitney statistical analysis was done using the InStat software (GraphPad). Significance was accepted for $p < 0.05$.

2.6 Dolichol-phosphate-mannose synthase activity assay

Cells were grown on 300 cm^2 plates and collected by trypsinization. Prior to cell lysis, cells were washed twice in ice-cold PBS. The cells were lysed in 25 mM Tris-HCl, 150 mM KCl, 1% Triton X-100, and cell debris was removed by centrifugation. Protein concentration was determined by BCA (Pierce). Dolichol-phosphate-mannose (Dol-P-Man) synthase activity was assayed using 30 ml of cell lysate in 100 ml of reaction buffer, with the addition of 40 mg/ml Dol-P (Sigma-Aldrich Co.) and 17 mM GDP-[^{14}C] mannose (Amersham Pharmacia Biotech). The reaction buffer contained 50 mM HEPES (pH 7.4), 25 mM KCl, 5 mM $MgCl_2$, 5 mM $MnCl_2$, and 0.2% Triton X-100. Reaction mixtures were incubated for 5 min at 37°C. Dol-P-Man was isolated by organic

extraction with chloroform/methanol (2:1 vol/vol), and radioactivity was determined in a beta counter (Beckman Coulter Inc., Fullerton, California, USA) (McLachlan and Krag, 1994). Statistical significance was determined by paired student t-test. Significance was accepted for $p < 0.05$.

2.7 Fluorescent labeling and analysis of dolichol-phosphate

Extraction, labeling, and analysis of Dol-P were adapted from previous studies (Elmberger et al., 1989; Haeuptle et al., 2010). Briefly, approximately 3 x 10^8 cells were collected by trypsinization, counted, and washed once in PBS. For quantification, 10 µg C_{80}-polyprenol-phosphate (Larodan Fine Chemicals, Sweden) was added as internal standard. After addition of 6 ml methanol and 3 ml 15 M KOH, the sample was hydrolyzed for 1 h at 100 °C. Dolichol and Dol-P were extracted with chloroform/methanol (2:1 vol/vol) and the chloroform phase was dried under nitrogen. The sample was dissolved in methanol/water (98:2 vol/vol) supplemented with 20 mM phosphoric acid and applied to a C_{18} SepPak column (Waters, USA). Dolichol and Dol-P were eluted in chloroform/methanol (2:1 vol/vol) followed by separation on a Silica SepPak column (Waters, USA). Dol-P was eluted in chloroform/methanol/water (10:10:3 vol/vol/vol). Dol-P was fluorescently labeled with 9-anthryldiazomethane (Sigma-Aldrich) in a multi-step procedure described elsewhere (Haeuptle et al., 2010).

Samples were analyzed by using a LaChrom D-7000 HPLC system (Merck, Germany) equipped with an Inertsil ODS-3 column (5 µm, 4.6 x 250 mm; GL Sciences Inc., Japan). Fluorescence was detected using a LaChrom L-7485 fluorescence detector using 365 nm as excitation wavelength and 412 nm as emission wavelength. Separation was done by applying isocratic elution with acetonitrile/dichloromethane (3:2 vol/vol) supplemented with 0.01% diethylamine (Sigma–Aldrich). Flow was held constant at 1 ml/min at 30 °C. Statistical analysis was done by paired student t-test. Significance was accepted for $p < 0.05$.

2.8 Radioactive labeling and analysis of dolichol-linked oligosaccharides

After ethanol exposure, cells were washed with PBS and incubated in serum- and glucose-free DMEM (Invitrogen) for 45 min at 37°C. Metabolic labeling of dolichol-linked oligosaccharide was performed by addition of 150 µCi [^{3}H]mannose (Hartmann,

Germany) for 1 h at 37°C. Cells were washed twice with PBS and scraped in 11 ml methanol and 0.1 mM Tris, pH 7.4 (8:3 vol/vol). After the addition of 12 ml chloroform and vortexing, cells were pelleted by centrifugation at 5,000 x *g* for 5 min. Dolichol-linked oligosaccharides were extracted as described previously and were analyzed by HPLC (Burda et al., 1998; Zufferey et al., 1995). Data were subjected to paired t-test for statistical analysis. Significance was accepted for $p < 0.05$.

3. Results

3.1 VA-13 and HepaRG cell lines express ethanol-metabolizing enzymes

Initially, we assessed the CYP2E1 and ADH activities in the HepaRG and VA-13 cells to confirm their validity as ethanol metabolizing cell lines. Expression of murine ADH and induction of CYP2E1 were confirmed in VA-13 and HepaRG cells, respectively. ADH activity could not be detected in naïve HepG2 cells but was present in VA-13 cells (Figure 1 A). CYP2E1 activity could be induced with 2% DMSO treatment for two weeks in HepaRG cells (Figure 1 B). The activity of ADH and CYP2E1 was reflected in the cytotoxicity towards ethanol (Figure 1 C and D). After 4 d of ethanol treatment, viability of VA-13 cells was markedly decreased.

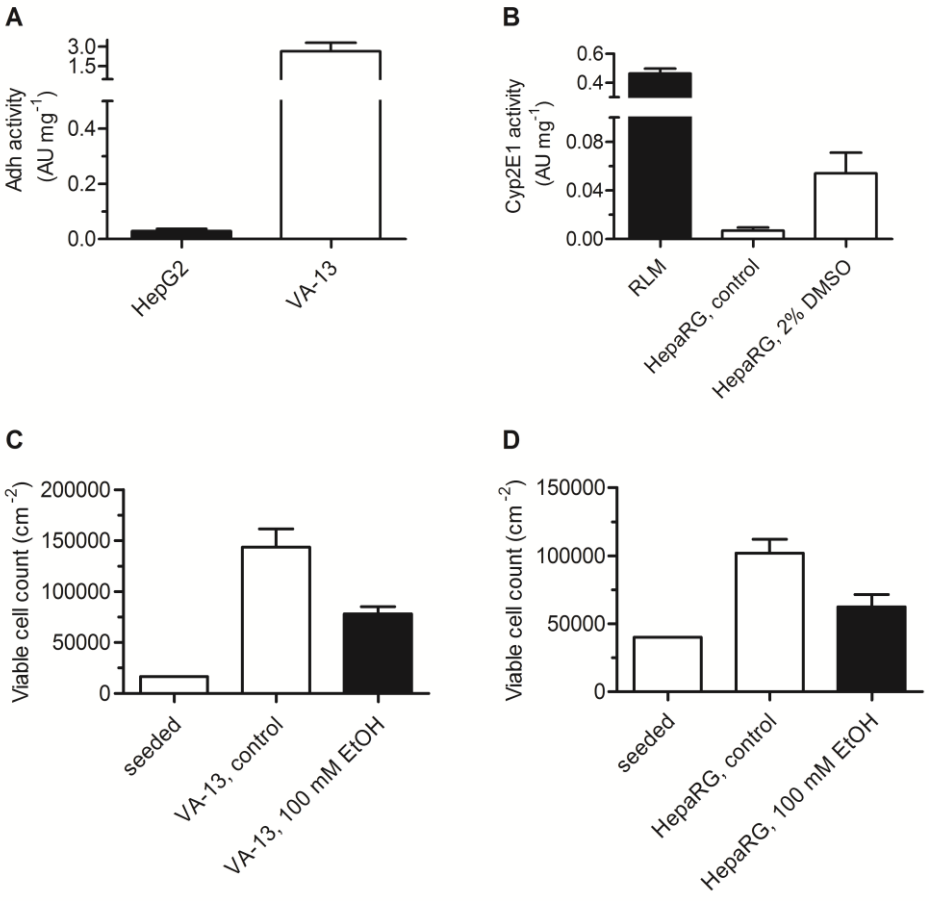

Figure 1. Ethanol-metabolizing enzyme activities and viability in VA-13 and HepaRG cell lines. VA-13 cells were seeded at 16.7 x 10^3 cells per cm^2 and cultured for 4 days previous to ADH activity measurement (A). HepaRG cells were treated as described in Materials and Methods and CYP2E1 activity was tested in microsomal proteins of induced and un-induced cells (B). Viable cell count was determined after treatment with 100 mM ethanol for 4 days (C and D).

VA-13 sensitivity towards ethanol has been previously described (Clemens et al., 2002). Compared to rat liver microsomes, the microsomal fractions of induced HepaRG cells showed a 8.6-fold reduced activity of CYP2E1. Induced HepaRG cells showed a similar sensitivity to ethanol as the VA-13 cells and viability was reduced by 39% upon ethanol treatment.

3.2 Transferrin glycosylation is unaffected by ethanol treatment

To investigate the production of CDT, hepatocytes were exposed to different concentrations of ethanol for 4 days and supernatants were analyzed. Supernatants were subjected to isoelectric focusing and immunoblotting against transferrin. Transferrin glycoform distribution was different in supernatants of cultured hepatocytes compared to blood serum (Figure 2). In contrast to blood serum, supernatants showed more prominent asialo- up to trisialo-transferrin bands instead of tetrasialo- and disialo-transferrin, which were prominent in healthy control serum. This pattern could be observed both cell lines and reflects the aberrant N-glycosylation found in hepatic carcinoma conditions (Kamiyama et al., 2013). Moreover, no effect on

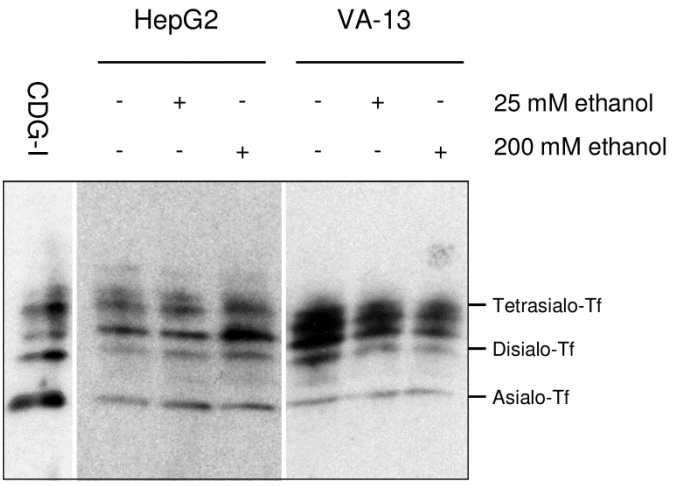

Figure 2. Carbohydrate-deficient transferrin as marker for glycosylation deficiency. Transferrin was analyzed 4 days after ethanol exposure using isoelectric focusing and subsequent immunoblotting. As a comparison, blood serum from a phosphomannomutase 2-CDG patient was analyzed by the same procedure.

glycoform distribution was visible using concentrations between 25 to 200 mM ethanol. With higher ethanol concentrations, less transferrin was detected. The decrease in

transferrin signal reflected low cell numbers due to ethanol toxicity or may indicate impaired protein secretion.

3.3 Transcript analysis reveals potential regulatory changes along the N-glycosylation pathway

To get more detailed information of changes occurring in the N-linked glycosylation pathway, we analyzed the transcripts of different glycosylation genes that are involved in key steps of the Dol-linked oligosaccharide assembly by quantitative PCR after 25 mM and 100 mM ethanol treatment for 4 days (Figure 3 A). No significant changes could be observed for the analyzed transcripts upon 25 mM ethanol treatment. After treatment with 100 mM ethanol, however, the mRNA levels of two genes were slightly changed. DPM1, a subunit of DPM synthase, was downregulated by 17%. DPM synthase works as a heterotrimer (DPM1-DPM3) transferring a Man-1-P from GDP-mannose to Dol-P. The resulting Dol-P-Man serves as a substrate for mannosyl transferases in the ER lumen. The second transcript RPN2 was upregulated by 8%. RPN2 is a ribophorin taking part in the recruitment of the oligosaccharyl transferase complex to the ER-coupled ribosomes. We observed a dose dependency on ethanol concentration as a trend in all the tested transcripts. For instance, DPM1 mRNA was decreased at 25 mM ethanol but only at 100 mM ethanol the change was significant between control and ethanol-treated cells.

DPM synthase activity was measured to determine whether the lower transcript level of DPM1 would affect DPM synthase activity. We found a marked increase in DPM synthase activity in cell lysates from ethanol treated VA-13 cells (Figure 3 B). The increase in DPM synthase activity stands in contrast with the minor decrease in DPM1 transcript levels. Notably, the catalytic subunit of DPM synthase was not affected at the transcriptional level. The moderate downregulation in DPM1 transcript together with the 36% increase in DPM synthase activity might point to a regulatory mechanism.

3.4 Dolichol-phosphate pool is decreased after ethanol treatment

Next, we assessed the most prevalent Dol-P species consisting of 90, 95, and 100 carbon atoms in hepatoma cells. Treatment of HepaRG cells with ethanol resulted in a decrease of Dol-P levels (Figure 4). The strongest decrease was detected for the C95-Dol-P, which

was reduced by 80% whereas C100-Dol-P was decreased by 64% in comparison to untreated cells (Figure 4 C).

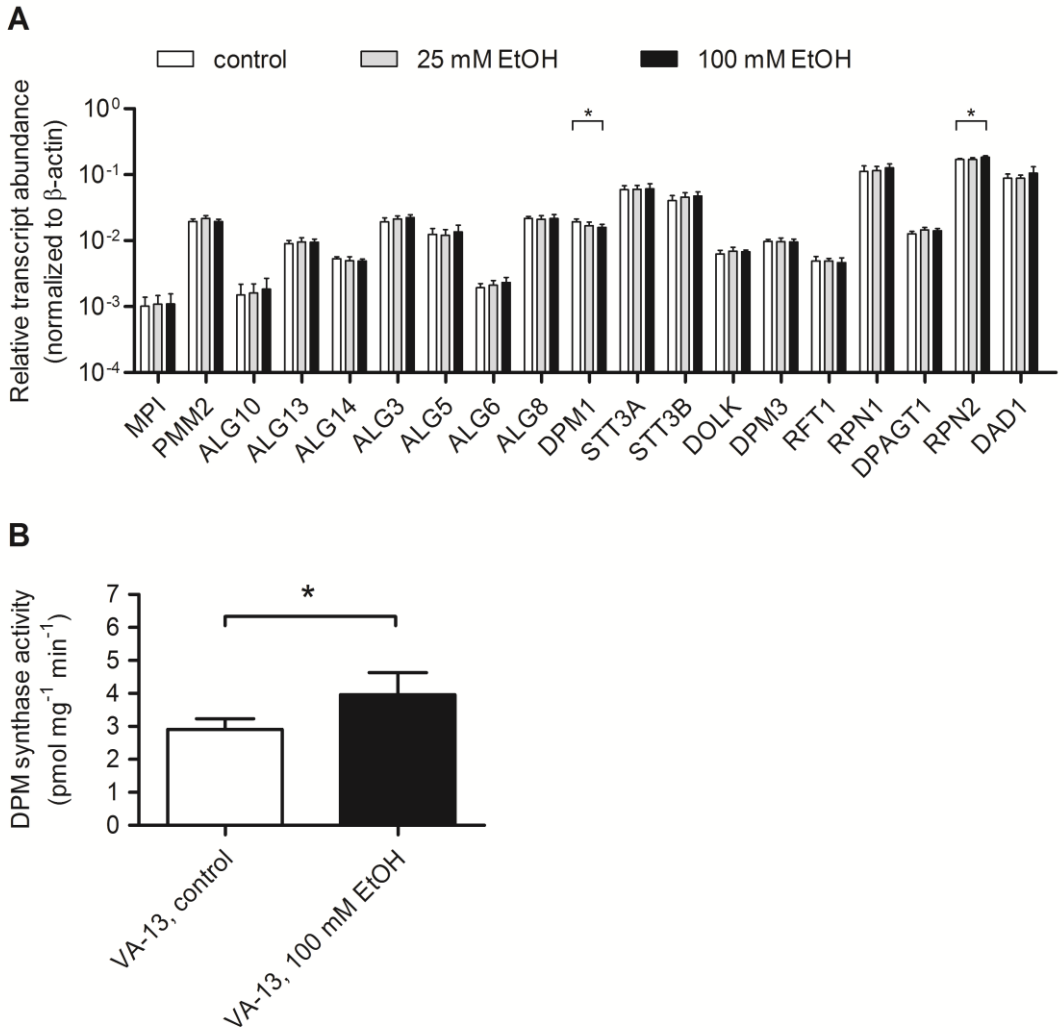

Figure 3. Transcript analysis of the glycosylation pathway in the ER and DPM synthase activity after 100 mM ethanol treatment. Transcript analysis was performed from RNA of VA-13 cells treated with 25 or 100 mM ethanol for 4 days (A). Results are shown as mean ± SEM of four independent samples. *, $p < 0.05$. Enzyme activity was determined using cell lysates from treated or untreated VA-13 cells in an assay using C95-Dol-P as acceptor and radioactive GDP-[^{3}H]mannose as donor substrate (B). The radioactivity of labeled C95-Dol-P-Man was quantified by liquid scintillation counting. Activities shown as mean ± SEM of six independent experiments. *, $p < 0.05$.

3.5 N-glycan precursor assembly is impaired after ethanol treatment

In CDG types that affect the biosynthesis of the N-glycan precursor, different intermediate dolichol-linked oligosaccharides can accumulate. To address ethanol-

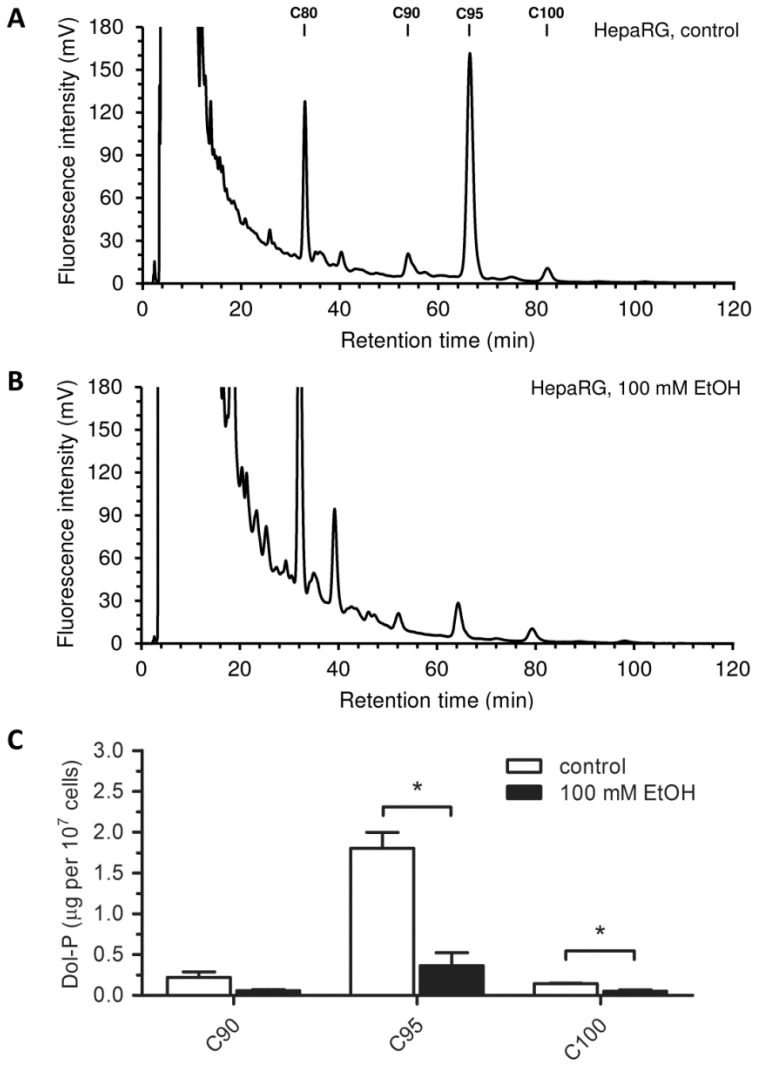

Figure 4. Dolichol-phosphate levels after 100 mM ethanol treatment. Dol-P levels were determined in HepaRG cells after 4 d of ethanol treatment. C90, C95, and C100 peaks were identified using Dol-P standards and quantitative determination was done with using C80-Dol-P as internal standard. Representative HPLC profiles are shown (A, B). Peak areas were determined and analyzed (C). Data represent mean values ±SEM of three independent experiments. *, $p < 0.05$.

induced changes in N-glycan precursor assembly, we metabolically labeled dolichol-linked oligosaccharides with [^{3}H]mannose and subsequently separated them by HPLC coupled to a flow scintillation analyzer. The dolichol-linked oligosaccharide profile underwent a shift, displaying a smaller fraction of the final oligosaccharide precursor when cells were treated with 100 mM ethanol (Figure 5 A , B). A reduction of the $GlcNAc_2$-Man_9-Glc_3 peak by 27% was observed in HepaRG cells indicating either a lower availability of dolichol leading to a general decrease is dolichol-linked oligosaccharide or a defect in a later stage of the N-glycan biosynthesis in the ER. Typically, defects more

early in the biosynthesis lead to an accumulation or a uniform decrease of dolichol-linked oligosaccharide precursors (Figure 5 C). The same trend of a reduced $GlcNAc_2$-Man_9-Glc_3 peak could be observed in VA-13 cells (Figure 5 D).

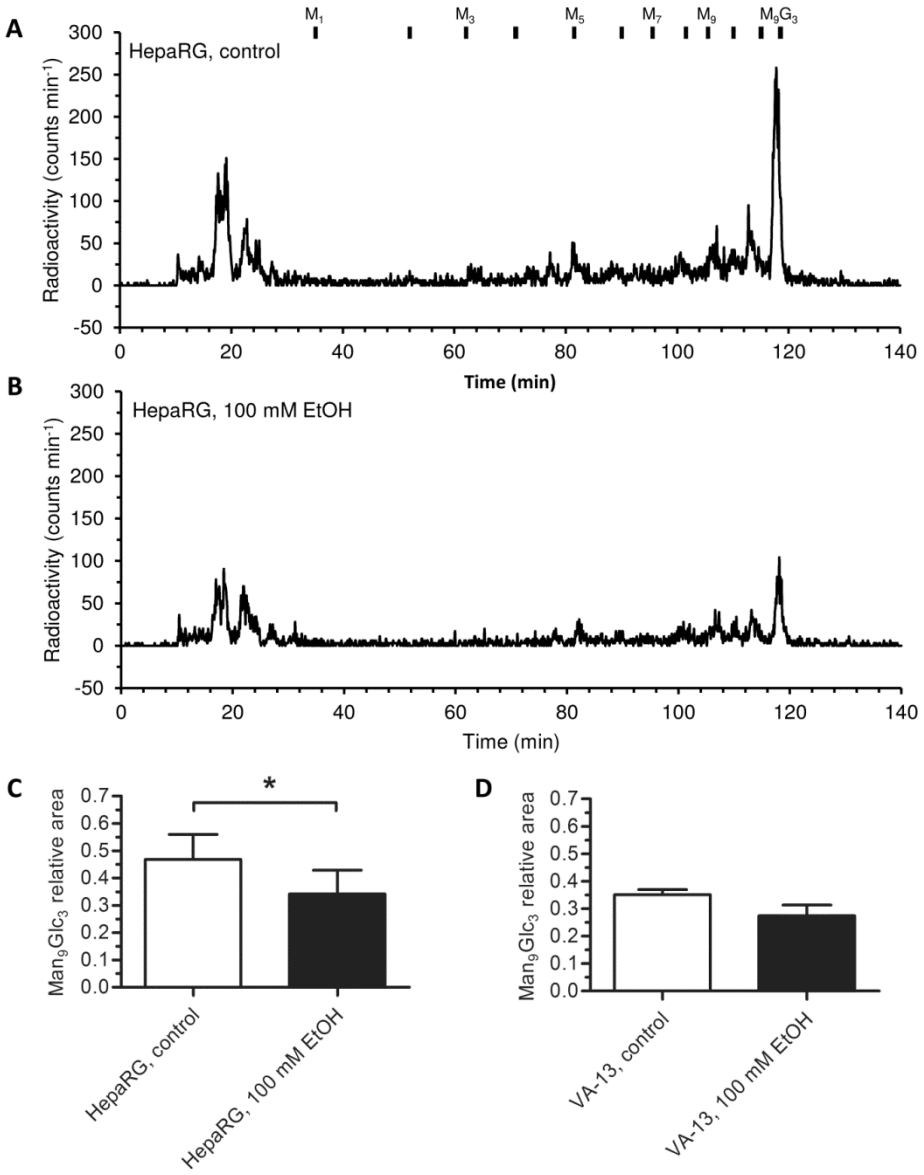

Figure 5. Dolichol-linked oligosaccharide analysis. VA-13 and HepaRG cells were metabolically labeled with [^{3}H]mannose to analyze dolichol-linked oligosaccharide precursors. Representative control and 100 mM ethanol treated sample profiles are shown (A and B). Relative peak areas of the $GlcNAc_2Man_9Glc_3$ to total area were calculated (C and D). Data represent mean values ±SEM of three independent experiments. *, $p < 0.05$.

4. Discussion

We investigated the effect of ethanol exposure on N-linked protein glycosylation and observed lower Dol-P levels, in particular C95-Dol-P in our HepaRG model. Lower dolichol levels have been reported previously in murine model systems upon ethanol treatment (Cottalasso et al., 1998; Cottalasso et al., 1996). Dol-P is critical for N-glycosylation in two ways. First, it serves as a carrier for the N-glycan precursor. Second, Dol-P coupled to Man or Glc is essential for glycosyltransferases located in the ER lumen. Accordingly, low availability of Dol-P-Man in DPM1-CDG was previously demonstrated to be attenuated by increasing Dol-P thereby compensating the low activity of DPM synthase with better substrate availability (Haeuptle et al., 2011). The strategy of increasing dolichol levels to attenuate glycosylation deficiency in ALD would be interesting but might not be sufficient due to the complexity of ethanol-induced N-glycosylation deficiency.

This is the first study showing ethanol-induced effects on the biosynthesis of the N-glycan precursors, namely a reduction of Dol-PP-$GlcNAc_2Man_9Glc_3$ compared to untreated cells. Interestingly, while general decrease in dolichol-linked oligosaccharide is well defined in CDG, such a reduction of the final dolichol-linked precursor has not been observed yet, neither in inherited nor in acquired glycosylation deficiencies. The dolichol-linked oligosaccharide pattern suggests a deficiency in the ER luminal assembly of the N-glycan precursor or could be a consequence of lower dolichol levels. CDG research has shown that deficient enzymes of the early, cytosolic steps of N-glycan precursor biosynthesis preferentially lead to an accumulation of Dol-P precursors, such as Dol-PP-$GlcNAc_2$-Man_5 in DPM1-CDG (Imbach et al., 2000). The shortage in dolichol could also explain the lower Dol-PP-$GlcNAc_2Man_9Glc_3$ levels with decreased availability of the N-glycan precursors, leading to drainage of the dolichol-linked oligosaccharide pool. CDG with deficient dolichol or Dol-P biosynthesis typically result in reduced dolichol-linked oligosaccharide but do not alter the distribution of the dolichol-linked precursors as observed in DOLK-CDG (Kranz et al., 2007). In SRD5A3-CDG, the polyprenol reductase along the dolichol biosynthetic pathway is non-functional but does not lead to decreased dolichol levels and fibroblasts show a healthy dolichol-linked oligosaccharide distribution (Grundahl et al., 2012). Symptoms on the systemic level are not shared by CDG affecting dolichol biosynthesis and ALD. The tendency of CDG for liver malformation or disease is apparent in other forms of CDG with defects in later

steps of the N-linked glycosylation pointing towards a more complex mechanism in N-glycosylation deficiency in ALD.

Transcriptional regulation of N-glycosylation genes could explain ethanol-induced N-glycosylation deficiency. We found a trend for transcript alteration upon ethanol treatment but only to a marginal extent. DPM1, a subunit of the DPM synthase, was transcriptionally downregulated by 17% indicating a regulatory mechanism. This notion is supported by our observation that DPM synthase activity was increased by 36%. More work is needed to elucidate possible regulatory mechanisms for the N-glycosylation pathway in ALD. Since reduced Dol-PP-$GlcNAc_2Man_9Glc_3$ might be due to dysfunction of the later, luminal steps of the N-glycan precursor assembly, a deregulation of the oligosaccharyl transferase (OST) offers an explanation. Indeed, we found an indication for potential OST deregulation. RPN2, a part of the OST complex, was slightly upregulated. RPN2 was shown to promote glycosylation of P-glycoprotein, an ABC transporter of the multidrug resistance family (Honma et al., 2008; Kerb et al., 2001). Knock-down of RPN2 resulted in reduced glycosylation as well as reduced membrane localization of P-glycoprotein. We speculate that RPN2 upregulation upon ethanol-treatment induces changes in N-linked glycosylation of RPN2 target proteins contributing to an aberrant dolichol-linked oligosaccharide pattern. It would be interesting to further investigate the expression and function of OST subunits in order to get a notion of the impact of ethanol on OST activity.

5. Conclusion

In conclusion, we found that decreased Dol-P and altered dolichol-linked oligosaccharide profiles contribute to ethanol-induced N-linked glycosylation deficiency. Furthermore, altered transcription of genes along the N-linked glycosylation pathway was found indicating a deregulation in N-glycosylation. Together with previous findings of lower sialyltransferase and higher sialidase activities, ethanol-induced glycosylation deficiency proves to be a result of metabolic interferences along the N-glycosylation biosynthetic pathway starting from the early steps of dolichol synthesis, continuing with the biosynthesis of the N-linked glycan precursor, and concluding with the final steps of glycan capping in the Golgi apparatus.

References

Bean, P., and J.B. Peter. 1993. A new approach to quantitate carbohydrate-deficient transferrin isoforms in alcohol abusers: partial iron saturation in isoelectric focusing/immunoblotting and laser densitometry. *Alcohol Clin Exp Res* 17:1163-1170.

Burda, P., L. Borsig, J. de Rijk-van Andel, R. Wevers, J. Jaeken, H. Carchon, E.G. Berger, and M. Aebi. 1998. A novel carbohydrate-deficient glycoprotein syndrome characterized by a deficiency in glucosylation of the dolichol-linked oligosaccharide. *J Clin Invest* 102:647-652.

Carter, E.A., and J.R. Wands. 1988. Ethanol-induced inhibition of liver cell function: I. Effect of ethanol on hormone stimulated hepatocyte DNA synthesis and the role of ethanol metabolism. *Alcohol Clin Exp Res* 12:555-562.

Clemens, D.L., A. Forman, T.R. Jerrells, M.F. Sorrell, and D.J. Tuma. 2002. Relationship between acetaldehyde levels and cell survival in ethanol-metabolizing hepatoma cells. *Hepatology* 35:1196-1204.

Clemens, D.L., C.M. Halgard, R.R. Miles, M.F. Sorrell, and D.J. Tuma. 1995. Establishment of a recombinant hepatic cell line stably expressing alcohol dehydrogenase. *Arch Biochem Biophys* 321:311-318.

Cottalasso, D., A. Bellocchio, M.A. Pronzato, C. Domenicotti, N. Traverso, M.V. Gianelli, U.M. Marinari, and G. Nanni. 1998. Effect of ethanol administration on the level of dolichol in rat liver microsomes and Golgi apparatus. *Alcoholism, clinical and experimental research* 22:730-737.

Cottalasso, D., P. Gazzo, D. Dapino, C. Domenicotti, M.A. Pronzato, N. Traverso, A. Bellocchio, G. Nanni, and U.M. Marinari. 1996. Effect of chronic ethanol consumption on glycosylation processes in rat liver microsomes and Golgi apparatus. *Alcohol and alcoholism (Oxford, Oxfordshire)* 31:51-59.

Crick, D.C., and K.K. Carroll. 1987. Extraction and quantitation of total cholesterol, dolichol and dolichyl phosphate from mammalian liver. *Lipids* 22:1045-1048.

de Jong, G., W.L. van Noort, and H.G. van Eijk. 1992. Carbohydrate analysis of transferrin subfractions isolated by preparative isoelectric focusing in immobilized pH gradients. *Electrophoresis* 13:225-228.

Eggens, I., T.J. Ekstrom, and F. Aberg. 1990. Studies on the biosynthesis of polyisoprenols, cholesterol and ubiquinone in highly differentiated human hepatomas. *J Exp Pathol (Oxford)* 71:219-232.

Eggens, I., and P.G. Elmberger. 1990. Studies on the polyisoprenoid composition in hepatocellular carcinomas and its correlation with their differentiation. *APMIS* 98:535-542.

Elmberger, P.G., I. Eggens, and G. Dallner. 1989. Conditions for quantitation of dolichyl phosphate, dolichol, ubiquinone and cholesterol by HPLC. *Biomed Chromatogr* 3:20-28.

Filipovic, I., and B. Menzel. 1981. Action of low-density lipoprotein and compactin, a competitive inhibitor of 3-hydroxy-3-methylglutaryl-CoA reductase, on the synthesis of dolichol-linked oligosaccharides and low-density-lipoprotein receptor in human skin fibroblasts. *Biochem J* 196:625-628.

Gapp, I.W., C.R. Congreve, and B.S. Lieberman. 2012. Unraveling the phylogenetic relationships of the Eccoptochilinae, an enigmatic array of ordovician cheirurid trilobites. *PLoS One* 7:e49115.

Garige, M., M. Gong, and M.R. Lakshman. 2006. Ethanol destabilizes liver Gal beta l, 4GlcNAc alpha2,6-sialyltransferase, mRNA by depleting a 3'-untranslated region-specific binding protein. *The Journal of pharmacology and experimental therapeutics* 318:1076-1082.

Garige, M., M. Gong, M.N. Rao, Y. Zhang, and M.R. Lakshman. 2005. Mechanism of action of ethanol in the down-regulation of Gal(beta)1, 4GlcNAc alpha2,6-sialyltransferase messenger RNA in human liver cell lines. *Metabolism* 54:729-734.

Gripon, P., S. Rumin, S. Urban, J. Le Seyec, D. Glaise, I. Cannie, C. Guyomard, J. Lucas, C. Trepo, and C. Guguen-Guillouzo. 2002. Infection of a human hepatoma cell line by hepatitis B virus. *Proc Natl Acad Sci U S A* 99:15655-15660.

Grundahl, J.E., Z. Guan, S. Rust, J. Reunert, B. Muller, I. Du Chesne, K. Zerres, S. Rudnik-Schoneborn, N. Ortiz-Bruchle, M.G. Hausler, J. Siedlecka, E. Swiezewska, C.R. Raetz, and T. Marquardt. 2012. Life with too much polyprenol: polyprenol reductase deficiency. *Mol Genet Metab* 105:642-651.

Haeuptle, M.A., A.J. Hülsmeier, and T. Hennet. 2010. HPLC and mass spectrometry analysis of dolichol-phosphates at the cell culture scale. *Anal Biochem* 396:133-138.

Haeuptle, M.A., M. Welti, H. Troxler, A.J. Hülsmeier, T. Imbach, and T. Hennet. 2011. Improvement of dolichol-linked oligosaccharide biosynthesis by the squalene synthase inhibitor zaragozic acid. *J Biol Chem* 286:6085-6091.

Honma, K., K. Iwao-Koizumi, F. Takeshita, Y. Yamamoto, T. Yoshida, K. Nishio, S. Nagahara, K. Kato, and T. Ochiya. 2008. RPN2 gene confers docetaxel resistance in breast cancer. *Nat Med* 14:939-948.

Hülsmeier, A.J., P. Paesold-Burda, and T. Hennet. 2007. N-glycosylation site occupancy in serum glycoproteins using multiple reaction monitoring liquid chromatography-mass spectrometry. *Mol Cell Proteomics* 6:2132-2138.

Imbach, T., B. Schenk, E. Schollen, P. Burda, A. Stutz, S. Grunewald, N.M. Bailie, M.D. King, J. Jaeken, G. Matthijs, E.G. Berger, M. Aebi, and T. Hennet. 2000. Deficiency of dolichol-phosphate-mannose synthase-1 causes congenital disorder of glycosylation type Ie. *J Clin Invest* 105:233-239.

Kamiyama, T., H. Yokoo, J. Furukawa, M. Kurogochi, T. Togashi, N. Miura, K. Nakanishi, H. Kamachi, T. Kakisaka, Y. Tsuruga, M. Fujiyoshi, A. Taketomi, S. Nishimura, and S. Todo. 2013. Identification of novel serum biomarkers of hepatocellular carcinoma using glycomic analysis. *Hepatology* 57:2314-2325.

Keller, R.K. 1986. The mechanism and regulation of dolichyl phosphate biosynthesis in rat liver. *J Biol Chem* 261:12053-12059.

Kerb, R., S. Hoffmeyer, and U. Brinkmann. 2001. ABC drug transporters: hereditary polymorphisms and pharmacological impact in MDR1, MRP1 and MRP2. *Pharmacogenomics* 2:51-64.

Koop, D.R., and D.J. Tierney. 1990. Multiple mechanisms in the regulation of ethanol-inducible cytochrome P450IIE1. *Bioessays* 12:429-435.

Kranz, C., C. Jungeblut, J. Denecke, A. Erlekotte, C. Sohlbach, V. Debus, H.G. Kehl, E. Harms, A. Reith, S. Reichel, H. Grobe, G. Hammersen, U. Schwarzer, and T. Marquardt. 2007. A defect in dolichol phosphate biosynthesis causes a new inherited disorder with death in early infancy. *Am J Hum Genet* 80:433-440.

Lecca, M.R., C. Maag, E.G. Berger, and T. Hennet. 2011. Fibrotic response in fibroblasts from congenital disorders of glycosylation. *J Cell Mol Med* 15:1788-1796.

Leroy, J.G. 2006. Congenital disorders of N-glycosylation including diseases associated with O- as well as N-glycosylation defects. *Pediatr Res* 60:643-656.

Lieber, C.S. 1999. Microsomal ethanol-oxidizing system (MEOS): the first 30 years (1968-1998)--a review. *Alcoholism, clinical and experimental research* 23:991-1007.

Luo, Y., A. Nita-Lazar, and R.S. Haltiwanger. 2006. Two distinct pathways for O-fucosylation of epidermal growth factor-like or thrombospondin type 1 repeats. *J Biol Chem* 281:9385-9392.

McLachlan, K.R., and S.S. Krag. 1994. Three enzymes involved in oligosaccharide-lipid assembly in Chinese hamster ovary cells differ in lipid substrate preference. *J Lipid Res* 35:1861-1868.

Nairn, A.V., M. dela Rosa, and K.W. Moremen. 2010. Transcript analysis of stem cells. *Methods Enzymol* 479:73-91.

Ohnishi, K., and C.S. Lieber. 1977. Reconstitution of the microsomal ethanol-oxidizing system. Qualitative and quantitative changes of cytochrome P-450 after chronic ethanol consumption. *J Biol Chem* 252:7124-7131.

Peter, J., C. Unverzagt, W.D. Engel, D. Renauer, C. Seidel, and W. Hosel. 1998. Identification of carbohydrate deficient transferrin forms by MALDI-TOF mass spectrometry and lectin ELISABiochim Biophys Acta 1998 Aug 24;1381(3):356. *Biochimica et biophysica acta* 1380:93-101.

Petren, S., O. Vesterberg, and H. Jornvall. 1987. Differences among five main forms of serum transferrin. *Alcohol Clin Exp Res* 11:453-456.

Purohit, V., B. Gao, and B.J. Song. 2009. Molecular mechanisms of alcoholic fatty liver. *Alcohol Clin Exp Res* 33:191-205.

Rao, M.N., and M.R. Lakshman. 1997. Chronic ethanol downregulates Gal-beta-1,4GlcNAc alpha 2,6-sialyltransferase and Gal-beta-1,3GlcNAc alpha 2,3-sialyltransferase mRNAs in rat liver. *Alcoholism, clinical and experimental research* 21:348-351.

Rao, M.N., and M.R. Lakshman. 1999. Chronic ethanol consumption leads to destabilization of rat liver beta-galactoside alpha2,6-sialyltransferase mRNA. *Metabolism: clinical and experimental* 48:797-803.

Stibler, H. 1991. Carbohydrate-deficient transferrin in serum: a new marker of potentially harmful alcohol consumption reviewed. *Clinical chemistry* 37:2029-2037.

Stoll, J., A.G. Rosenwald, and S.S. Krag. 1988. A Chinese hamster ovary cell mutant F2A8 utilizes polyprenol rather than dolichol for its lipid-dependent asparagine-linked glycosylation reactions. *J Biol Chem* 263:10774-10782.

Utesch, D., B. Diener, E. Molitor, F. Oesch, and K.L. Platt. 1992. Characterization of cryopreserved rat liver parenchymal cells by metabolism of diagnostic substrates and activities of related enzymes. *Biochem Pharmacol* 44:309-315.

Van Kaick, G., D. Lieberman, D. Lorenz, W.J. Lorenz, H. Luhrs, K.E. Scheer, H. Wesch, H. Muth, A. Kaul, H. Immich, G. Wagner, and K. Wegener. 1983. Recent results of the German Thorotrast study--epidemiological results and dose effect relationships in Thorotrast patients. *Health Phys* 44 Suppl 1:299-306.

Vigo, C., and W.L. Adair, Jr. 1982. In vivo biosynthesis of the saturated isoprene unit of dolichyl phosphate. *Biosci Rep* 2:835-840.

Wang, H.J., B. Gao, S. Zakhari, and L.E. Nagy. 2012. Inflammation in alcoholic liver disease. *Annu Rev Nutr* 32:343-368.

Wu, D., and A.I. Cederbaum. 2008. Development and properties of HepG2 cells that constitutively express CYP2E1. *Methods Mol Biol* 447:137-150.

Yokoyama, K., H. Mizuguchi, Y. Araki, S. Kaya, and E. Ito. 1989. Biosynthesis of linkage units for teichoic acids in gram-positive bacteria: distribution of related enzymes and their specificities for UDP-sugars and lipid-linked intermediates. *J Bacteriol* 171:940-946.

Zhu, H., Z. Jia, H. Misra, and Y.R. Li. 2012. Oxidative stress and redox signaling mechanisms of alcoholic liver disease: updated experimental and clinical evidence. *J Dig Dis* 13:133-142.

Zufferey, R., R. Knauer, P. Burda, I. Stagljar, S. te Heesen, L. Lehle, and M. Aebi. 1995. STT3, a highly conserved protein required for yeast oligosaccharyl transferase activity in vivo. *EMBO J* 14:4949-4960.

GENERAL DISCUSSION

Considering the immense abundance of glycans on cell surfaces and secreted proteins, countless essential biological functions depend on glycosylation. However, glycobiology has been a comparatively small field of research so far. Although glycobiologists are very active in promoting their field, glycobiology has received relatively little attention in other areas of biological sciences. In part, this was due to the gap of knowledge about the significance of glycosylation but also due to restricted possibilities regarding efficient methods to analyze the almost unmanageable complexity of sugar structures. With the advent of advanced technologies such as high-throughput mass spectrometry in conjunction with powerful computational software, glycans have moved within reach of researchers other than glycobiologists (Kolarich et al., 2013; Mechref et al., 2012; Zaia, 2010; Zaia, 2013). Additionally, progress in glycobiology prompted other scientists to consider glycobiological aspects in their field of research. Consequently, the significance of glycosylation is being discovered in many fields including cancer research, immunology, virology, and developmental biology. This development is highly beneficial for the understanding of glycans and their functions.

Initially, glycans were merely considered decorating structures on cell surfaces of all kind of cell types in all the domains of life. The significance of these "decorations" for humans was first realized with the discovery of the ABO blood groups in 1900 (Landsteiner, 1900). At the time, the nature of the determinants was totally elusive but the consequences for blood transfusion were immense. Nearly 60 years later, Morgan and Watkins defined sugars to be the blood group determinants (Morgan and Watkins, 1959; Watkins and Morgan, 1959). Later, the first carbohydrate-deficient glycoprotein syndrome was discovered (Jaeken et al., 1980). The patients suffered from mental retardation, muscular hypotonia, failure to thrive, inverted nipples, and abnormal fat deposits. Carbohydrate-deficient transferrin (CDT) was defined as a marker for CDG using isoelectric focusing of blood serum. Only fifteen years after its discovery, a phosphomannomutase deficiency was defined as the molecular basis of this CDG (Van Schaftingen and Jaeken, 1995). In the meantime, a CDG with a different CDT profile was discovered with a defect in GnT-II. It was termed CDG-II (Jaeken et al., 1994; Ramaekers et al., 1991). The discovery rate of novel forms of CDG was rapidly increasing and greatly contributed to the understanding of the glycosylation pathways. Yeast models have been

instrumental by comparison of DLO profiles of yeast mutants with DLO profiles of CDG patients thereby identifying genes of the glycosylation machinery in yeast and subsequently confirmation of the mutation in CDG patients by gene sequencing (Aebi and Hennet, 2001). Considering the 2% fraction of the genome that is involved in glycosylation, it can be speculated that the majority of CDG types is yet to be discovered. Recently discovered forms of CDG surprisingly do not have the typical symptomatic picture but show tissue- or organ-specific impact. In DHDDS-CDG, for instance, retinal degeneration is the single apparent symptom (Zelinger et al., 2011). DHDDS is the dehydrodolichyl diphosphate synthase which catalyzes the synthesis of polyprenol-PP from two molecules of farnesyl-PP. Thus, DHDDS is crucial for Dol biosynthesis and the implications of a defective DHDDS would seem to cause a much broader spectrum of symptoms. Either the discovered DHDDS-CDG cases have enough residual polyprenol-PP production from mutated DHDDS or another enzyme can compensate for the loss in DHDDS activity. Retinis pigmentosa is a manifestation well known in CDG as it occurs also in mevalonate kinase deficiency and PMM2-CDG (Goldfinger, 2009; Grunewald, 2009).

The challenge of uncovering regulatory mechanisms

The pathways of glycosylation in humans are well defined and all the N-linked glycosylation steps are assigned to enzymes (Haeuptle and Hennet, 2009; Jaeken, 2010b). However, parallel pathways to the ones already discovered are more difficult to identify partly because of the more complex human genome compared to model systems like yeast. Some of the pathways are specific to vertebrates or even restricted to mammals (Dell et al., 2010). Moreover, deficient enzymes involved in more peripheral functions such as regulatory enzymes or tissue specific glycosylation-associated genes render a characterization more difficult because of the difficulty to detect such defects unlike the strong phenotype of classical CDG. Generally, the regulation of the glycosylation machinery is elusive. Importantly, pathways with global contributions to an organism are highly regulated as can be seen in metabolic pathways but also signal transduction or gene regulation (Alberts, 2008). Regulation of glycosylation seems likely to be tightly regulated especially during development of the embryo since CDG patients have severe, multisystemic defects in early childhood (Haltiwanger and Lowe, 2004;

Jaeken, 2010a). Additionally, mechanisms of development of CDG have not been defined yet. Investigations in this direction are difficult, though. An promising approach is a switch system in which genes can be turned on and off at certain points in development using mouse models.

We encountered a possible regulatory mechanism for N-linked glycosylation in liver cells exposed to ethanol. ALD is unique due a non-systemic ethanol-induced N-glycosylation deficiency of liver proteins. We tested the effect of ethanol on N-linked glycosylation in a cell culture model using two hepatic carcinoma cell models to define N-linked glycosylation deficiency in ALD. Ethanol exposure led to decreased Dol-P levels supporting previous experiments with ethanol-fed rats and particularly the C95 species was dramatically decreased (Cottalasso et al., 1998; Cottalasso et al., 1996). As a possible consequence, we found a decreased amount of the N-glycan precursor. This was the first characterization of Dol-linked oligossacharide profiles in ethanol-induced N-glycosylation deficiency. To investigate gene regulation at the transcriptional level, we tested the glycosylation genes taking part in ER glycosylation steps. Interestingly, we found a dose dependency of transcription on ethanol concentration as a trend. Transcription of two genes was significantly changed. DPM1, a component of the trimeric DPM synthase, was downregulated whereas RPN2, a regulatory subunit of the OST, was upregulated. To obtain a hint whether the transcriptional changes might be of regulatory nature, we tested the activity of DPM synthase and found a strong upregulation of enzymatic activity. How this potential regulatory mechanism is governed has yet to be investigated for instance by determination of the dose-dependency of DPM synthase activity and DPM1 transcriptional downregulation on ethanol concentration and by looking at the correlation of activity and transcript level. In case of RPN2, we can only speculate about the effect of this upregulation due to the complexity of the OST which can consist of different subunits possibly targeting different sets of proteins or even individual proteins (Vleugels et al., 2009). Identification of RPN2-specific N-glycosylation targets could provide a readout for our findings.

Therapeutics for glycosylation disorders

While novel forms of CDG are being discovered, efforts to treat the known forms of CDG have been undertaken. However, treatment for CDG is principally limited to post-natal patients because of the lack of pre-natal tests for CDG (Funke et al., 2013). Glycosylation is crucial for development and proper functioning of a variety of organ systems, particularly for the nervous system evident from the neurological component of most CDG. Unfortunately, neurological deficits in CDG are not treatable with present-day medicine. In order to find therapeutic targets, identifying mutations in the genome is not enough. High-throughput sequencing methods like whole-exome sequencing enable screening of patients with inherited diseases to pinpoint mutations (Freeze, 2013). However, biochemical read-outs are required to confirm candidate genes and potential treatments need to be validated for improvements of biochemical parameters.

MPI-CDG is a special case of CDG due to the usual lack of neurological symptoms (Westphal et al., 2001). This lack indicates that the defect does not manifest already during development but is important for maintaining the function of developed organs. However, the liver and gastrointestinal tract are affected. Symptoms include vomiting, diarrhea, gastrointestinal bleeding, protein-losing enteropathy, hepatomegaly, and liver fibrosis during childhood and they improve in adulthood. Severe cases show coagulopathy, hypoglycemia, and thrombosis. Nutritional mannose supplementation has been successful in relieving many of the symptoms (Babovic-Vuksanovic et al., 1999; de Lonlay et al., 1999; Niehues et al., 1998; Penel-Capelle et al., 2003; Westphal et al., 2001). Besides MPI-CDG, only two other CDG were reported to respond to treatment (Jaeken, 2010a). In SLC35C1-CDG, the deficiency in the GDP-Fuc transporter in the Golgi network can be compensated with fucose supplementation in some cases (Hellbusch et al., 2007). In PIGM-CDG, histone histone acetylation at the PIGM promotor is impaired and thus lowers PIGM-dependent mannosyltransferase transcription (Almeida et al., 2006). Using butyrate to inhibit histone deacetylase increased PIGM transcription and stopped seizures. Considering yet undiscovered CDG with non-developmental symptoms, medical treatment could help to attenuate manifestations caused by impaired glycosylation. Delivery of the medication is critical of course and in case of mannose supplementation an easy task. Recently, prenatal mannose treatment of mice with an engineered PMM2 defect has proven successful. Embryonic lethality of the hypomorphic PMM2 mutation could be overcome by mannose administration to the mother

(Schneider et al., 2011). The mannose-treated PMM2-defective embryos showed no manifestations of CDG. These examples demonstrate the main difficulties when it comes to CDG treatment. First, CDG affecting development, which include most CDG, require pre-natal treatment and need to be identified by methods that are not yet available. Second, pre-natal treatment is more difficult because treatment usually is applied on the mother and is restricted by the placenta barrier (Giaginis et al., 2012; Vahakangas and Myllynen, 2009). In case of non-developmental effects, the efficiency of medication greatly depends on sufficient residual activity of the affected enzyme. Importantly, development of medication for rare diseases is financially unattractive and therefore mannose treatment for MPI-CDG treatment has been a lucky exception due to its low cost and easy application.

In this work, we tested a therapeutic approach to treat DPM1-CDG. We exploited the action of Zaragozic acid, a cholesterol-lowering drug that differs from the classical statins. Zaragozic acid was discovered in a screen for cholesterol-lowering compounds in the context of cardiovascular disease treatment (Bergstrom et al., 1995). It inhibits squalene synthase which is active at a bifurcation in the mevalonate pathway. The bifurcation divides into cholesterol biosynthesis – through the action of squalene synthase – and into Dol biosynthesis (Welti, 2013). We could show that supplying fibroblasts with the squalene synthase inhibitor Zaragozic acid improved N-linked protein glycosylation and GPI-anchor formation in DPM1-CDG (Haeuptle et al., 2011). As expected, inhibition of squalene synthase resulted in lower cholesterol and higher Dol-P levels. We speculated that higher Dol-P levels could compensate for the insufficient DPM synthase activity. Indeed, Dol-P-Man levels could be restored. Moreover, Dol-linked oligosaccharide and N-linked oligosaccharide profiles were partly normalized and were reminiscent of healthy oligosaccharide profiles. Moreover, GPI anchor availability was improved as assessed by the expression of the GPI-anchored membrane surface protein CD59. With this work, we provided a first step in DPM1-CDG therapy. We used an available drug that was shown to be well tolerated at least in rats and confirmed the treatment success by measuring biochemical readouts (Baxter et al., 1992; Bergstrom et al., 1993). Whether such a treatment could attenuate DPM1-CDG manifestations at the level of an entire organism, needs further confirmation for instance using an animal model.

Future directions

Considering the 2% of genes that are predicted to be involved in glycosylation processes, it is safe to speculate that glycobiology plays an important – even if not yet fully recognized and defined – part in other diseases like cancer, immune disorders, or infectious diseases (Freeze et al., 2012). We showed, for instance, that glycosylation is perturbed at the level of Dol-linked oligosaccharide assembly in ethanol-treated hepatoma cells. This is likely to be associated with lower Dol levels. The specific consequences of underglycosylation of blood proteins as found in ALD are difficult to estimate due to the impact of chronic alcohol consumption on multiple organ systems (Wang et al., 2010). Future studies might assess the contribution of glycosylation deficiency to the clinical picture of ALD and other consequences of alcoholism.

Importantly, connecting glycobiology to other fields of research is beneficial in many ways. Awareness of glycan functions can be raised, more knowledge about mechanisms in regulation of glycosylation can be gained, and possibly novel therapeutic targets in CDG could be identified. In this way, glycobiologists can profit from the attention and knowledge of other fields as we demonstrated by using cholesterol-lowering Zaragozic acid found in the fight against cardiovascular disease to improve glycosylation in DPM1-CDG. In ALD, liver fibrosis is a well-known characteristic as it is in certain forms of CDG (Jaeken et al., 1998; Pelletier et al., 1986). Efforts to uncover mechanisms how liver fibrosis develops in CDG might help to understand liver fibrosis in ALD given the common deficiency in N-glycosylation. Vice versa, understanding the development of ethanol-induced glycosylation deficiency might reveal regulatory mechanisms for N-linked glycosylation.

References

Aebi, M., and T. Hennet. 2001. Congenital disorders of glycosylation: genetic model systems lead the way. *Trends Cell Biol* 11:136-141.

Alberts, B. 2008. Molecular biology of the cell. Garland Science, New York. 1268 pp.

Almeida, A.M., Y. Murakami, D.M. Layton, P. Hillmen, G.S. Sellick, Y. Maeda, S. Richards, S. Patterson, I. Kotsianidis, L. Mollica, D.H. Crawford, A. Baker, M. Ferguson, I. Roberts, R. Houlston, T. Kinoshita, and A. Karadimitris. 2006. Hypomorphic promoter mutation in PIGM causes inherited glycosylphosphatidylinositol deficiency. *Nat Med* 12:846-851.

Babovic-Vuksanovic, D., M.C. Patterson, W.F. Schwenk, J.F. O'Brien, J. Vockley, H.H. Freeze, D.P. Mehta, and V.V. Michels. 1999. Severe hypoglycemia as a presenting symptom of carbohydrate-deficient glycoprotein syndrome. *J Pediatr* 135:775-781.

Baxter, A., B.J. Fitzgerald, J.L. Hutson, A.D. McCarthy, J.M. Motteram, B.C. Ross, M. Sapra, M.A. Snowden, N.S. Watson, R.J. Williams, and et al. 1992. Squalestatin 1, a potent inhibitor of squalene synthase, which lowers serum cholesterol in vivo. *J Biol Chem* 267:11705-11708.

Bergstrom, J.D., C. Dufresne, G.F. Bills, M. Nallin-Omstead, and K. Byrne. 1995. Discovery, biosynthesis, and mechanism of action of the zaragozic acids: potent inhibitors of squalene synthase. *Annu Rev Microbiol* 49:607-639.

Bergstrom, J.D., M.M. Kurtz, D.J. Rew, A.M. Amend, J.D. Karkas, R.G. Bostedor, V.S. Bansal, C. Dufresne, F.L. VanMiddlesworth, O.D. Hensens, and et al. 1993. Zaragozic acids: a family of fungal metabolites that are picomolar competitive inhibitors of squalene synthase. *Proc Natl Acad Sci U S A* 90:80-84.

Cottalasso, D., A. Bellocchio, M.A. Pronzato, C. Domenicotti, N. Traverso, M.V. Gianelli, U.M. Marinari, and G. Nanni. 1998. Effect of ethanol administration on the level of dolichol in rat liver microsomes and Golgi apparatus. *Alcoholism, clinical and experimental research* 22:730-737.

Cottalasso, D., P. Gazzo, D. Dapino, C. Domenicotti, M.A. Pronzato, N. Traverso, A. Bellocchio, G. Nanni, and U.M. Marinari. 1996. Effect of chronic ethanol consumption on glycosylation processes in rat liver microsomes and Golgi apparatus. *Alcohol and alcoholism (Oxford, Oxfordshire)* 31:51-59.

de Lonlay, P., M. Cuer, S. Vuillaumier-Barrot, G. Beaune, P. Castelnau, M. Kretz, G. Durand, J.M. Saudubray, and N. Seta. 1999. Hyperinsulinemic hypoglycemia as a presenting sign in phosphomannose isomerase deficiency: A new manifestation of carbohydrate-deficient glycoprotein syndrome treatable with mannose. *J Pediatr* 135:379-383.

Dell, A., A. Galadari, F. Sastre, and P. Hitchen. 2010. Similarities and differences in the glycosylation mechanisms in prokaryotes and eukaryotes. *Int J Microbiol* 148178:27.

Freeze, H.H. 2013. Understanding human glycosylation disorders: biochemistry leads the charge. *J Biol Chem* 288:6936-6945.

Freeze, H.H., E.A. Eklund, B.G. Ng, and M.C. Patterson. 2012. Neurology of inherited glycosylation disorders. *Lancet Neurol* 11:453-466.

Funke, S., T. Gardeitchik, D. Kouwenberg, M. Mohamed, S.B. Wortmann, E. Korsch, M. Adamowicz, L. Al-Gazali, R.A. Wevers, A. Horvath, D.J. Lefeber, and E. Morava. 2013. Perinatal and early infantile symptoms in congenital disorders of glycosylation. *Am J Med Genet A* 3:578-584.

Giaginis, C., S. Theocharis, and A. Tsantili-Kakoulidou. 2012. Current toxicological aspects on drug and chemical transport and metabolism across the human placental barrier. *Expert Opin Drug Metab Toxicol* 8:1263-1275.

Goldfinger, S. 2009. The inherited autoinflammatory syndrome: a decade of discovery. *Trans Am Clin Climatol Assoc* 120:413-418.

Grunewald, S. 2009. The clinical spectrum of phosphomannomutase 2 deficiency (CDG-Ia). *Biochimica et biophysica acta* 1792:827-834.

Haeuptle, M.A., and T. Hennet. 2009. Congenital disorders of glycosylation: an update on defects affecting the biosynthesis of dolichol-linked oligosaccharides. *Hum Mutat* 30:1628-1641.

Haeuptle, M.A., M. Welti, H. Troxler, A.J. Hülsmeier, T. Imbach, and T. Hennet. 2011. Improvement of dolichol-linked oligosaccharide biosynthesis by the squalene synthase inhibitor zaragozic acid. *J Biol Chem* 286:6085-6091.

Haltiwanger, R.S., and J.B. Lowe. 2004. Role of glycosylation in development. *Annual review of biochemistry* 73:491-537.

Hellbusch, C.C., M. Sperandio, D. Frommhold, S. Yakubenia, M.K. Wild, D. Popovici, D. Vestweber, H.J. Grone, K. von Figura, T. Lubke, and C. Korner. 2007. Golgi GDP-fucose transporter-deficient mice mimic congenital disorder of glycosylation IIc/leukocyte adhesion deficiency II. *J Biol Chem* 282:10762-10772.

Jaeken, J. 2010a. Congenital disorders of glycosylation. *Ann N Y Acad Sci*

Jaeken, J. 2010b. Congenital disorders of glycosylation. *Ann N Y Acad Sci* 1214:190-198.

Jaeken, J., G. Matthijs, J.M. Saudubray, C. Dionisi-Vici, E. Bertini, P. de Lonlay, H. Henri, H. Carchon, E. Schollen, and E. Van Schaftingen. 1998. Phosphomannose isomerase deficiency: a carbohydrate-deficient glycoprotein syndrome with hepatic-intestinal presentation. *Am J Hum Genet* 62:1535-1539.

Jaeken, J., H. Schachter, H. Carchon, P. De Cock, B. Coddeville, and G. Spik. 1994. Carbohydrate deficient glycoprotein syndrome type II: a deficiency in Golgi localised N-acetyl-glucosaminyltransferase II. *Arch Dis Child* 71:123-127.

Jaeken, J., M. Vanderschueren-Lodeweyckx, P. Casaer, L. Snoeck, L. Corbeel, E. Eggermont, and R. Eeckels. 1980. Familial psychomotor retardation with markedly fluctuating serum prolactin, FSH and GH levels, partial TBG-deficiency, increased serum arylsulphatase A and increased CSF protein: a new syndrome[quest]: 90. *Pediatr Res* 14:179-179.

Kolarich, D., E. Rapp, W.B. Struwe, S.M. Haslam, J. Zaia, R. McBride, S. Agravat, M.P. Campbell, M. Kato, R. Ranzinger, C. Kettner, and W.S. York. 2013. The minimum information required for a glycomics experiment (MIRAGE) project: improving the standards for reporting mass-spectrometry-based glycoanalytic data. *Mol Cell Proteomics* 12:991-995.

Landsteiner, K. 1900. Zur Kenntnis der antifermentativen, lytischen und agglutinierenden Wirkungen des Blutserums und der Lymphe. *Zentralbl Bak* 27:357-362.

Mechref, Y., Y. Hu, A. Garcia, and A. Hussein. 2012. Identifying cancer biomarkers by mass spectrometry-based glycomics. *Electrophoresis* 33:1755-1767.

Morgan, W.T., and W.M. Watkins. 1959. Some aspects of the biochemistry of the human blood-group substances. *Br Med Bull* 15:109-113.

Niehues, R., M. Hasilik, G. Alton, C. Korner, M. Schiebe-Sukumar, H.G. Koch, K.P. Zimmer, R. Wu, E. Harms, K. Reiter, K. von Figura, H.H. Freeze, H.K. Harms, and T. Marquardt. 1998. Carbohydrate-deficient glycoprotein syndrome type Ib. Phosphomannose isomerase deficiency and mannose therapy. *J Clin Invest* 101:1414-1420.

Pelletier, V.A., N. Galeano, P. Brochu, C.L. Morin, A.M. Weber, and C.C. Roy. 1986. Secretory diarrhea with protein-losing enteropathy, enterocolitis cystica superficialis, intestinal lymphangiectasia, and congenital hepatic fibrosis: a new syndrome. *J Pediatr* 108:61-65.

Penel-Capelle, D., D. Dobbelaere, J. Jaeken, A. Klein, M. Cartigny, and J. Weill. 2003. Congenital disorder of glycosylation Ib (CDG-Ib) without gastrointestinal symptoms. *J Inherit Metab Dis* 26:83-85.

Ramaekers, V.T., H. Stibler, J. Kint, and J. Jaeken. 1991. A new variant of the carbohydrate deficient glycoproteins syndrome. *J Inherit Metab Dis* 14:385-388.

Schneider, A., C. Thiel, J. Rindermann, C. DeRossi, D. Popovici, G.F. Hoffmann, H.J. Grone, and C. Korner. 2011. Successful prenatal mannose treatment for congenital disorder of glycosylation-Ia in mice. *Nat Med* 18:71-73.

Vahakangas, K., and P. Myllynen. 2009. Drug transporters in the human blood-placental barrier. *Br J Pharmacol* 158:665-678.

Van Schaftingen, E., and J. Jaeken. 1995. Phosphomannomutase deficiency is a cause of carbohydrate-deficient glycoprotein syndrome type I. *FEBS Lett* 377:318-320.

Vleugels, W., E. Schollen, F. Foulquier, and G. Matthijs. 2009. Screening for OST deficiencies in unsolved CDG-I patients. *Biochem Biophys Res Commun* 390:769-774.

Wang, H.J., S. Zakhari, and M.K. Jung. 2010. Alcohol, inflammation, and gut-liver-brain interactions in tissue damage and disease development. *World J Gastroenterol* 16:1304-1313.

Watkins, W.M., and W.T. Morgan. 1959. Possible genetical pathways for the biosynthesis of blood group mucopolysaccharides. *Vox Sang* 4:97-119.

Welti, M. 2013. Regulation of dolichol-linked glycosylation. *Glycoconjugate journal* 30:51-56.

Westphal, V., S. Kjaergaard, J.A. Davis, S.M. Peterson, F. Skovby, and H.H. Freeze. 2001. Genetic and metabolic analysis of the first adult with congenital disorder of glycosylation type Ib: long-term outcome and effects of mannose supplementation. *Mol Genet Metab* 73:77-85.

Zaia, J. 2010. Mass spectrometry and glycomics. *OMICS* 14:401-418.

Zaia, J. 2013. Glycosaminoglycan glycomics using mass spectrometry. *Mol Cell Proteomics* 12:885-892.

Zelinger, L., E. Banin, A. Obolensky, L. Mizrahi-Meissonnier, A. Beryozkin, D. Bandah-Rozenfeld, S. Frenkel, T. Ben-Yosef, S. Merin, S.B. Schwartz, A.V. Cideciyan, S.G. Jacobson, and D. Sharon. 2011. A missense mutation in DHDDS, encoding dehydrodolichyl diphosphate synthase, is associated with autosomal-recessive retinitis pigmentosa in Ashkenazi Jews. *Am J Hum Genet* 88:207-215.

ACKNOWLEDGEMENTS

I anticipated the excitement of discovering new things but also the struggles of going through PhD studies before starting my project. However, I did not anticipate how much I would rely on people to support me in various ways. Many thanks to all of you!

First, I would like to thank Prof. Dr. Thierry Hennet for giving me the opportunity to work in his lab on an exciting project. His guidance and support through the project were crucial and taught me a lot not only about hard-core glycobiology but also about project management, publishing, and funding. Many thanks to Dr. Andreas Hülsmeier for his supervision and constant support in science, methods, writing, and other problems. Further, I would like to thank my PhD committee members PD Dr. Lubor Borsig and Prof. Dr. Matthias Baumgartner for their scientific support and guidance through my PhD studies.

One other thing I also failed to anticipate when I started my PhD studies was that I would find so many dear friends and colleagues. I thank Dr. Nikunj Shah (my fellow Asian no. 1 for keeping the lab socialized), Dr. Adrienne Weiss (our very kind dancing queen for being my personal baker), Jürg Cabalzar (our interim dancing king and Sola manager for many scientific and other discussions), Eddie "The Dragon" Huang (my fellow Asian no. 2 for his perfect sense of timing to drop his dry humor), Stephan Baumann (our 1000% guy for starting our trip habit and for inspirational discussions), Anna Rommel (our cupcake and style expert for new fitness excercises), Nina Hochhold (the in many ways promising start of a new generation of PhD students), Dr. Kelvin Luther (for his never-failing grumpiness), Christoph Rutschmann (for always being willing to help), Sacha Schneeberger (my fellow Asian no. 3 for expanding my martial art experience), and Giovanna Roth (our supersecretary for taking good care of all of us). Further, many thanks to the former members of the group: Micha Häuptle (for our joint project and introducing me to lab methods), Andrea Fuhrer (for motivational discussions), Charlotte Maag, Adriano Guetg, Cinzia Bernardi (my only and dearest bench neighbor).

I would also like to thank the people from the L-floor and the whole Institute of Physiology for providing a good work atmosphere and non-work-related activities. I thank Dr. Katya Kurakevich, Dr. Alexandra Hoos, Carole Oertli, Irina Häuselmann, Jesus Glaus (for the most manly hugs), Marko Roblek, Darya Protsyuk, Sonia Youhanna, Jenny

Kürth, Alkaly Gassama, Dr. Bob Claudemans, Dr. Aurelia Lelli (the most disciplined of my favourite Ju-jitsu students), Melroy Miranda (the least disciplined of my favourite Ju-Jitsu students), Dr. Sara Santambrogio (the most kind of my favourite Ju-Jitsu students), Elisa Randi (clearly the strongest of my favourite Ju-Jitsu students), and Heidi Preisig.

Special thanks to Hung Nguyen who ensured that I could take my mind off work in the many Ju-Jitsu trainings during my PhD studies.

I want to express my profound gratitude to my parents, Brenda and Hans Welti, for their unfailing support without which none of this would have been possible. I am deeply grateful to Manuela Gloor for constantly supporting me, pushing me if needed, and believing in me.

CURRICULUM VITAE

Name:	Michael Andreas WELTI
Date of birth:	April 12, 1983
Place of birth:	Schlieren ZH
Place of citizenship:	Berikon AG

Education

2009 - 2013	PhD thesis at the Institute of Physiology, University of Zürich, in the group of Prof. Dr. Thierry Hennet "Congenital and Ethanol-induced Disorder of N-linked Protein Glycosylation"
2004-2009	Bachelor and master studies at the Swiss Federal Institute of Technology (ETH) Zürich, graduation as Master of Science ETH in Biology Master thesis at the Institute of Biochemistry in the group of PD Dr. Hemmo Meyer "Interaction of p97 with a protein complex of Inh-3, PP1, and Sds22 and implications for nuclear envelope formation"
1999-2003	Matura at Kantonsschule Baden AG Schwerpunktfach Biologie und Chemie Ergänzungsfach Wirtschaft und Recht Akzentfach Moderne Sprachen
1995 – 1999	Secondary School in Berikon AG
1990 – 1995	Primary School in Berikon AG

Publications

M. Welti and A.J. Hülsmeier
"Ethanol-induced impairment in the biosynthesis of N-linked glycosylation"
Manuscript accepted in J Cell Biochem (2013)

M. Welti
"Regulation of dolichol-linked glycosylation"
Glycoconjugate journal, 30 (2013) 51-56.

A.J. Hülsmeier, M. Welti, T. Hennet
"Glycoprotein maturation and the UPR"
Methods Enzymol, 491 (2011) 163-182.

M.A. Häuptle, M. Welti, H. Troxler, A.J. Hülsmeier, T. Imbach, T. Hennet
"Improvement of dolichol-linked oligosaccharide biosynthesis by the squalene synthase inhibitor zaragozic acid"
J Biol Chem, 286 (2011) 6085-6091.